AD_____

Award Number: DAMD17-01-1-0450

TITLE: MCAK and Stathmin Upregulationin Breast Cancer Cells: Etiology and Response to Pharmacologic Reagents

PRINCIPAL INVESTIGATOR: Linda G. Wordeman, Ph.D.

CONTRACTING ORGANIZATION: University of Washington
Seattle, Washington 98105-6692

REPORT DATE: July 2003

TYPE OF REPORT: Annual

PREPARED FOR: U.S. Army Medical Research and Materiel Command
Fort Detrick, Maryland 21702-5012

REPORT DOCUMENTATION PAGE

Form Approved
OMB No. 074-0188

1. AGENCY USE ONLY (Leave blank)	2. REPORT DATE	3. REPORT TYPE AND DATES COVERED
	July 2003	Annual (1 Jul 2002 - 30 Jun 2003)

4. TITLE AND SUBTITLE
MCAK and Stathmin Upregulation in Breast Cancer Cells: Etiology and Response to Pharmacologic Reagents

5. FUNDING NUMBERS
DAMD17-01-1-0450

6. AUTHOR(S)
Linda G. Wordeman, Ph.D.

7. PERFORMING ORGANIZATION NAME(S) AND ADDRESS(ES)
University of Washington
Seattle, Washington 98105-6692

E-Mail: worde@u.washington.edu

8. PERFORMING ORGANIZATION REPORT NUMBER

9. SPONSORING / MONITORING AGENCY NAME(S) AND ADDRESS(ES)
U.S. Army Medical Research and Materiel Command
Fort Detrick, Maryland 21702-5012

10. SPONSORING / MONITORING AGENCY REPORT NUMBER

11. SUPPLEMENTARY NOTES
Original contains color plates: All DTIC reproductions will be in black and white.

12a. DISTRIBUTION / AVAILABILITY STATEMENT
Approved for Public Release; Distribution Unlimited

12b. DISTRIBUTION CODE

13. ABSTRACT (Maximum 200 Words)

The goal of this study is to assay the role that two modulators of microtubule dynamics, Mitotic centromere-associated Kinesin (MCAK) and Op18/stathmin (stathmin) play in the development of cancer. These proteins are elevated in aggressive breast cancer tumors and changes in the levels and activity of these proteins have been correlated with alterations in chromosome number and cell motility and invasiveness. In addition to our previously discovered C-terminal regulation, we have uncovered another major regulatory mechanism to control microtubule dynamics through MCAK activity. Phosphorylation of conserved serine residue in the neck and N-terminus of MCAK by Aurora B kinase inhibits its activity. It is likely that phosphorylatin and dephosphorylatin controls MCAK's activity diruing mitosis and also, via other kinases, during interphase. We have also identified two other Kin I kinesisns which regulate microtubule dynamics in cultured cells and are likely to be regulated by kinases and phosphatases. These regulatory kinases also control stathmin activity in cells. Regulation of these proteins via cascades of kinase and phosphatase activities opens up a major new area for the application of therapeutics to control microtubule dynamics and augment existing cancer therapies that target microtubules.

14. SUBJECT TERMS
Mitosis, centromere, microtubule, mitotic spindle, stathmin, cancer MCAK, immortalization, transformation, aneuploidy

15. NUMBER OF PAGES
102

16. PRICE CODE

17. SECURITY CLASSIFICATION OF REPORT	18. SECURITY CLASSIFICATION OF THIS PAGE	19. SECURITY CLASSIFICATION OF ABSTRACT	20. LIMITATION OF ABSTRACT
Unclassified	Unclassified	Unclassified	Unlimited

Table of Contents

INTRODUCTION:

The long-term objective of this study is to determine the role that regulators of cellular microtubules such as Mitotic Centromere-associated Kinesin (MCAK) and Op18/stathmin (stathmin) play in the development of breast cancer. Elevated levels of MCAK and stathmin have been detected in proliferative breast cancers (1). Alterations in the levels of these modulators of microtubule dynamics can lead to aneuploidy (chromosome gain or loss) and also to changes in the metastatic potential of cancer cells (2,3,4,5). Specifically, we plan to correlate elevated levels or decreased levels of MCAK or Stathmin with immortalization, aneuploidy and proliferative potential. It is likely that changes in the expression levels or activity of MCAK and/or stathmin are involved in the escape from cell cycle checkpoint control (which is exquisitely sensitive to microtubule polymer dynamics) and the acquisition of unrestrained growth potential. Additionally, we have uncovered a regulatory pathway (see sections 1 and 2) that has to potential to regulate the activity of these proteins without changing protein levels. MCAK, Op18/stathmin and their modulators may serve as diagnostic indicators of tumor potential or as targets for therapeutic drug intervention.

RESEARCH ACCOMPLISHMENTS:

1. MCAK's activity is regulated by Aurora B kinase.

Aurora B kinase is an important regulator of microtubule attachment to the kinetochore (6) and Aurora kinases are also implicated in many cancers including breast cancer (7). We have discovered that Aurora B is able to phosphorylate MCAK at three locations within the primary sequence. Importantly for this project, Op18/Stathmin is also regulated by Aurora B (R. Heald, Univ. of California, personal communication). Thus we have uncovered an essential second messenger for the regulation of microtubule dynamics in normal and transformed cells. Furthermore, this represents the first report that phosphorylation of a kinesin can modulate it's ATP-dependent activity. The details of this study are included in the manuscript by Andrews et al included in the APPENDIX. This manuscript has been favorably received by Developmental Cell and is now in final revision.

This key discovery opens up a new area to study the regulation of microtubule dynamics via phosphorylation. Because we have vast experience in studying modulation of microtubules by MCAK and Op18/stathmin we were able to quickly establish a link between Aurora activity and microtubule regulation. We have previously shown that the positive electrostatic potential of the MCAK neck is essential for depolymerizing activity (8, reprint included in Appendix). One of the sites that we have identified in collaboration with Paul Andrews and Jason Swedlow (University of Dundee) is in the neck of MCAK. We hypothesize that a negatively charged phosphate group on the neck would inactivate MCAK. We mutated the known phosphorylation sites to A (unphosphorylatable) and E (mimic phosphorylated state) and used our in vivo depolymerization assay (described in DOD Annual Report number 1) to measure the extent of depolymerization. We found that phosphorylation does indeed inactivate MCAK. This study indicates that a balance of kinase and phosphatase activity are required to regulate MCAK's activity at the kinetochore and also globally (see Section 2).

2. Increasing the level of cytoplasmic phosphatase activity increases microtubule turnover.

The most likely phosphatases that would activate MCAK activity are those that oppose Aurora kinases. Two classes of these phosphatases are Protein Phosphatase 1 gamma (PP1γ) and also Protein Phosphatase 2c (PP2c). Because PP1γ is associated with the kinetochore (9) we prepared a CFP-PP1γ construct for expression in CHO cells. Overexpression of this construct decreases the amount of microtubule polymer in CHO cells. This effect is not seen when a CFP-PP1γHA (phosphatase-dead) version of PP1γ is overexpressed. We will use 2-D gel electrophoresis in order to determine whether this is due to dephosphorylation of MCAK, Op18/stathmin or both and also measure the effect of this response on the tubulin autoregulatory system (see Annual Report number 1 and Statement of Work, III). Inclusion of the kinase/phosphatase pathways that regulate MCAK and Op18/stathmin into our long-term goals is essential because many useful anti-cancer pharmaceuticals may be designed to target these regulators and thus affect microtubule dynamics (10). Furthermore, alterations in kinase and phosphatase activity may affect microtubule dynamics and lead to anti-cancer drug resistance (11).

3. The C-terminus of MCAK negatively regulates MCAK activity.

In addition to regulation by phosphorylation we previously reported that deletion of 5 amino acids from the C-terminus of MCAK significantly increases its microtubule depolymerization activity (manuscript by Moore and Wordeman included in APPENDIX). We have determined, mechanistically, that this occurs by increasing the efficiency with which MCAK targets microtubule ends. This is an important result because it defines an alternate regulatory domain of MCAK. Mutations affecting this domain could increase MCAK activity within cells leading to aneuploidy and facilitating cancer progression. This manuscript is ready for submission to J. Cell Biology.

4. Preparation of an inducible cell line for MCAK expression.

Previously, we reported that we were changing to a proteomic approach to facilitate our Correlative Study (Statement of Work, I). This entails assaying genes pre-determined to be important for cancer progression for response to changes in MCAK expression. This does not change the original purpose of Statement of Work (I) which is to correlate changes in MCAK and stathmin levels with the transformed phenotype and will provide more information in that we will know exactly which cancer-related genes are affected by changes in levels of the microtubule depolymerizing enzymes. As described in Annual Report number 1, we used the pTRE-2 inducible expression vector to produce a cell line that expresses MCAK to controlled levels in response to doxycycline withdrawal. We have completed the first stage of this project, which is the successful production of an inducible CHO AA8 cell line (**Figure 1**). We are presently constructing the inducible GFP-stathmin cell line now. These cell lines will be used to prepare biotin-labeled cDNA to screen GEArray™ membranes. Control cDNA will be prepared from untransfected cells although transfected cells cultured for 48 hours in doxycycline can also be used. This cDNA will be used to probe three gene expression profiles using GEArray Q Series membranes (SuperArray). Mouse genes will be used with the hamster cDNA. The screen and cancer arrays to be used were described in detail in Annual Report 1. We have no plans to

deviate from this described screen. We will also duplicate the studies in human cells and the HMEC cell model as previously outlined.

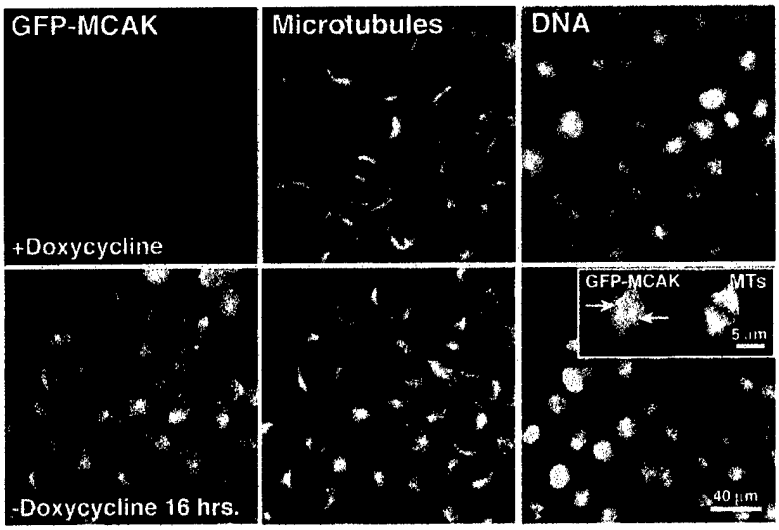

Figure 1. *Inducible stable CHO AA8 cells expressing modest levels of GFP-MCAK in response to doxycycline withdrawal. GFP-MCAK associates with centromeres in mitotic cells (inset). L. Wordeman, unpublished.*

5. Application of RNAi to control MCAK and Op18/stathmin levels.

We have begun to use RNAi to reduce MCAK levels in cultured cells. We report preliminary success with some of our selected regions of the gene. This technique is considerably less toxic than lowering MCAK levels with antisense oligos. Once we have decided which region is most efficacious in depleting MCAK protein we will prepare an expression construct which will allow us to bombard our cells with high levels of RNAi over time. We also plan to prepare co-expressing RNAi constructs for the simultaneous down regulation of both MCAK and Op18/stathmin. This gentler technique will be much more amenable to delicate cell lines such as the HMEC cells. This represents a slight technical deviation from our Statement of Work (II. Experimental Analysis) but represents technological improvements that have occurred since this study was proposed. We have previously shown that MCAK responds to changes in Op18/stathmin levels (Annual Report 1). The use of RNAi to modulate the levels of these proteins will be a key technique to confirm and extend those data.

KEY RESEARCH ACCOMPLISHMENTS:

- Determination that phosphorylation of MCAK by Aurora B inactivates MCAK activity. This important kinase is implicated in cancer progression.
- Confirmation that MCAK is a major substrate of Aurora B in vivo. These two major discoveries are described in the manuscript (Andrews et al.) included in the APPENDIX.
- Mathematical modeling and assays in vitro indicate that five amino acids at the C-terminus of MCAK reduce the efficiency of microtubule depolymerization by inhibiting ATP-dependent biased diffusional motility. This could contribute to the regulation of MCAK activity in vivo. Moore and Wordeman, APPENDIX.
- Determination that the electrostatic potential of the neck of MCAK is essential for depolymerization activity. These data serve as the basis for the inactivation of MCAK by kinases and the reactivation by phosphatase activity. Published in the Journal of Cell Biology and cited by Faculty of 1000. Reprint included in APPENDIX (Ovechkina et al.).
- Modulation of MCAK activity by RNAi.

- Preparation of cell line for a biomolecular screen which will identify cancer-related genes that respond to changes in MCAK and Op18/stathmin protein levels.
- Discovery that increased phosphatase activity results in a decrease in microtubule polymer in interphase cells.

REPORTABLE OUTCOMES:

- Abstract: Era of Hope Meeting: Regulation of Mitotic Centromere-associated Kinesin (MCAK). A. T. Moore and L. Wordeman.
- Abstract: American Association for Cell Biology Annual Meeting. K-loop insertion restores microtubule depolymerizing activity of a "neckless" MCAK mutant. Mol. Biol. Cell 2002 13:322a.
- Science in Medicine Lecture: Order from Chaos: Microtubule dynamics and Chromosome Segregation.
- Publication: K-loop insertion rescues depolymerizing activity of a "neckless" MCAK mutant. 2002. Y. Ovechkina, M. Wagenbach and L. Wordeman. J. Cell Biol. 159:557-562.
- Publication: Unconventional Motoring: An overview of the Kin C and Kin I kinesins. 2003. Traffic 4:367-375.

CONCLUSIONS:

We have shown that MCAK activity is regulated by the important mitotic kinase Aurora B. This represents a groundbreaking discovery within the kinesin field. This discovery also has immense implications within the cancer field. Changes in Aurora kinase levels had already been reported in the literature to be diagnostic for certain proliferative tumors and Aurora kinases are a key target for anti-cancer therapeutics. Because we have shown that Aurora negatively regulates MCAK activity drugs that inactivate Aurora might antagonize the effect of drugs such as paclitaxel. This is because active MCAK can antagonize the effect of paclitaxel (Annual Report 1). The regulation of MCAK activity by Aurora B kinase represents part of our genomic analysis of genes that control MCAK, was facilitated by a productive collaboration. However, we have also made significant progress toward correlating MCAK and Op18/stathmin levels with microtubule response and immortalization (Statement of Work II, III). In this year we have spent time refining techniques (RNAi) and building reagents (inducible cell lines) in order to confirm and extend our initial results on the interplay between MCAK and Op18/stathmin and the role that this has in immortalization and tumor progression.

REFERENCES:

1-Perou, C.M., S. Jeffrey, M. van de Rijn, C. Rees, M. Eisen, D. Ross, A. Pergamenschikov, C. Williams, S. Zhu, J. Lee, D. Lashkari, D. Shalon, P. Brown and D. Botstein. 1999. Distinctive gene expression patterns in human mammary epithelial cells and breast cancers. P.N.A.S. 96:9212-9217.

2- Curmi, P., C. Nogues, S. Lachkar, N. Carelle, M.-P. Gonthier, A. Sobel, R. Lidereau and I. Bieche. 2000. Overexpression of stathmin in breast carcinomas points out to highly proliferative tumors. Br. J. Cancer 82:142-150.

3-Lakshmi, M.S., C. Parker, and G.V.Sherbet. 1993. Metastasis associated MTS1 and NM23 genes affect tubulin polymerisation in B16 Melanomas: A possible mechanism of their regulation of metastatic behaviour of tumours. Anticancer Res. 13:299-304.

4-Takenaga, K., Y. Nakamura, and S. Sakiyama. 1997. Expression of antisense RNA to S100A4 gene encoding an S100-related calcium-binding protein suppressses metastatic potential of high-metastatic Lewis lung carcinoma cells. Oncogene 14:331-337.

5- Maney, T., A. W. Hunter, M. Wagenbach, and L. Wordeman. 1998. Mitotic centromere-associated kinesin is important for anaphase. J. Cell Biol. 142:787-801.

6- Cheeseman IM, Anderson S, Jwa M, Green EM, Kang J, Yates JR 3rd, Chan CS, Drubin DG, Barnes G. 2002 Phospho-regulation of kinetochore-microtubule attachments by the Aurora kinase Ipl1p. Cell. 111(2):163-72.

7- Tanaka T, Kimura M, Matsunaga K, Fukada D, Mori H, Okano Y. 1999. Centrosomal kinase AIK1 is overexpressed in invasive ductal carcinoma of the breast. Cancer Res. 59(9):2041-4.

8- Ovechkina Y, Wagenbach M, Wordeman L. 2002 K-loop insertion restores microtubule depolymerizing activity of a "neckless" MCAK mutant. J Cell Biol. 159(4):557-62.

9-Trinkle-Mulcahy L, Andrews PD, Wickramasinghe S, Sleeman J, Prescott A, Lam YW, Lyon C, Swedlow JR, Lamond AI. 2003. Time-lapse Imaging Reveals Dynamic Relocalization of PP1gamma throughout the Mammalian Cell Cycle. Mol Biol Cell. 14(1):107-17.

10- Mahadevan D, Bearss DJ, Vankayalapati H. 2003. Structure-based design of novel anti-cancer agents targeting aurora kinases. Curr Med Chem Anti-Canc Agents. 3(1):25-34.

11- Anand S, Penrhyn-Lowe S, Venkitaraman AR. 2003. AURORA-A amplification overrides the mitotic spindle assembly checkpoint, inducing resistance to Taxol. Cancer Cell. 2003 Jan;3(1):51-62.

APPENDIX:

1-Era of Hope Abstract 2002 (Moore and Wordeman). C-term. regulation of MCAK.
2-ASCB Abstract 2002 (Ovechkina, Wagenbach and Wordeman) Contribution of Neck domain to MCAK depolymerization activity reported here.
3-Reprint (Ovechkina, Wagenbach and Wordeman) Forms basis for regulation by phosphorylation of the Neck domain of MCAK.
4-Reprint (Ovechkina and Wordeman). Review of Kin I kinesins.
5-Seminar notice (Wordeman) Discusses the biology underlying microtubule dynamics aneuploidy and the regulation by phosphorylation.
6-Manuscript (Moore and Wordeman). C-terminal regulation of MCAK function.
7-Manuscript (Andrews et al.) Regulation of MCAK function by Aurora B kinase.

REGULATION OF THE ACTIVITY OF MITOTIC CENTROMERE-ASSOCIATED KINESIN (MCAK)

Ayana T. Moore and Linda Wordeman, Ph.D.

Department of Physiology and Biophysics, University of Washington, Seattle, WA 98195

worde@u.washington.edu

Mitotic centromere-associated kinesin (MCAK) is a protein which is required for the proper segregation of chromosomes during cell division. Overexpression of MCAK disrupts microtubules and leads to aberrant mitotic spindle assembly. Depletion of MCAK protein levels leads to lagging chromosomes during anaphase and aneuploidy. MCAK has been identified as a protein which shows high levels of expression in proliferative breast cancer tumors.

Rather than transporting cargo along assembled microtubule polymer like most kinesin family proteins, MCAK depolymerizes microtubules. In this way MCAK influences the dynamic behavior of microtubules in the cell. Some chemotherapeutic drugs may also function, in part, to alter the dynamic properties of microtubules. Because MCAK is required to ensure the correct ploidy in daughter cells during cell division and also because MCAK influences the dynamic behavior of microtubules it is essential to determine how MCAK activity in the cell is regulated.

We have identified three types of MCAK regulation that occurs in mammalian cells; (i) structural regulation, (ii) posttranslational regulation and (iii) tubulin-linked regulation. In the first case we have determined that the final five amino acids at the extreme C-terminus of the protein inhibits the microtubule depolymerizing activity of MCAK. Premature truncation or other alterations in C-term. structure could produce overactive MCAK protein which would adversely affect cellular microtubules. In the second case, we have linked MCAK to the ubiquitin conjugating enzyme system. Posttranslational modification of MCAK by ubiquitin may target the protein for degradation or for localization to specific regions of the cell. Finally, we have found that the tubulin autoregulatory system responds to the level of MCAK protein in the cell. The level of tubulin polymer in the cell determines how much tubulin dimer is synthesized by that cell so that the ratio of polymer to dimer remains constant. We have found that when the level of MCAK changes within the cell, the tubulin autoregulatory system responds accordingly. This suggests that MCAK levels are critical for microtubule function and incates that MCAK may be a suitable marker for early stages of cancer or as a target for cancer therapy.

The U.S. Army Medical Research and Materiel Command under DAMD17-01-1-0450 supported this work.

1811

K-loop insertion restores microtubule depolymerizing activity of a "neckless" MCAK mutant

Y. Y. Ovechkina, M. Wagenbach, L. Wordeman; Department of Physiology and Biophysics, University of Washington, Seattle, WA

While most kinesins use ATP energy to translocate along the surface of microtubules, Mitotic Centromere-Associated Kinesin (MCAK) and its homologs depolymerize microtubules from either end (Maney et al. 2001, JBC, 276: 34753, Niederstrasser et al. 2002, J Mol Biol 316:817, Moores et all. 2002, Mol Cell. 9:903). MCAK has a unique ability to directly target microtubule ends while motile kinesins have a high affinity for the microtubule lattice. MCAK has a catalytic motor domain that is conserved throughout the kinesin superfamily. The motor domain is preceded by the "neck' domain which is highly conserved within the KIN I subfamily but very divergent from the rest of the kinesin-related proteins. The neck domain of the motile kinesins is important for directionality and processivity of the ATP-hydrolyzing motor domain. Using an *in vivo* microtubule depolymerization assay, we found that deletions and alanine substitutions of highly conserved positively charged residues in the MCAK "neck' domain significantly reduced microtubule depolymerization activity. Furthermore, when we substituted the neck domain with the positively charged KIF1A K-loop (known for its ability to interact with the negatively charged C-terminus of tubulin and promote diffusion along microtubules), we found that the resulting chimera displayed fully restored depolymerization activity. We propose that the neck, analogously to the K-loop, may interact electrostatically with the negatively charged microtubule lattice to diffuse MCAK along the microtubules toward their ends where MCAK-mediated depolymerization occurs.

JCB Report

K-loop insertion restores microtubule depolymerizing activity of a "neckless" MCAK mutant

Yulia Ovechkina, Michael Wagenbach, and Linda Wordeman

Department of Physiology and Biophysics, University of Washington School of Medicine, Seattle, WA 98195

Unlike most kinesins, mitotic centromere–associated kinesin (MCAK) does not translocate along the surface of microtubules (MTs), but instead depolymerizes them. Among the motile kinesins, refinements that are unique for specific cellular functions, such as directionality and processivity, are under the control of a "neck" domain adjacent to the ATP-hydrolyzing motor domain. Despite its apparent lack of motility, MCAK also contains a neck domain. We found that deletions and alanine substitutions of highly conserved positively charged residues in the MCAK neck domain significantly reduced MT depolymerization activity. Furthermore, substitution of MCAK's neck domain with either the positively charged KIF1A K-loop or poly-lysine rescues the loss of MT-depolymerizing activity observed in the neckless MCAK mutant. We propose that the neck, analogously to the K-loop, interacts electrostatically with the tubulin COOH terminus to permit diffusional translocation of MCAK along the surface of MTs. This weak-binding interaction may also play an important role in processivity of MCAK-induced MT depolymerization.

Introduction

Members of the kinesin superfamily transport cargo along the surface of microtubules (MTs)* using the power of an ATP-hydrolyzing motor domain (Goldstein and Philp, 1999; Woehlke and Schliwa, 2000). Mitotic centromere–associated kinesin (MCAK) is a member of the Kin I subfamily of kinesin-related proteins that shares high homology within the motor domain with other members of the kinesin superfamily (Wordeman and Mitchison, 1995; Vale and Fletterick, 1997). However, although most kinesins translocate along the surface of MTs, MCAK and its homologues depolymerize MTs from either end (Walczak et al., 1996; Desai et al., 1999; Hunter and Wordeman, 2000; Kinoshita et al., 2001; Maney et al., 2001). Kinetic analysis suggests that processivity and diffusional motility may contribute to MCAK's rapid rate of MT depolymerization (unpublished data). The novel ability to modulate MT dynamics suggests that these kinesins may be important contributors to cell cycle progression (Zhai et al., 1996) and tumorgenesis (Lakshmi et al., 1993).

The direction of transport and the affinity for MTs are molecular refinements that adapt motile kinesins for specific cellular functions within the realm of intracellular transport, cell division, and MT dynamics (Goldstein and Philp, 1999; Woehlke and Schliwa, 2000). The "neck" domain, a region adjacent to the motor domain (head), is responsible for conferring directionality and processivity to the core motor domain (Case et al., 1997; Henningsen and Schliwa, 1997; Endow and Waligora, 1998; Romberg et al., 1998). MCAK's neck domain is highly conserved within the Kin I subfamily, but is very divergent from other kinesin-related proteins (Vale and Fletterick, 1997; Maney et al., 2001). A truncated MCAK protein, consisting of the neck domain (A182-D246) plus the core motor domain (P247-E581), shows MT depolymerization activity similar to that of the full-length (FL) MCAK (Maney et al., 2001). However, the neck itself does not possess depolymerizing activity (Maney et al., 1998), nor does it confer depolymerization activity to a motile kinesin because a chimera consisting of the MCAK neck fused to the motor domain of a conventional kinesin (KIF5B) exhibits no MT depolymerization activity when expressed in cultured cells (Maney et al., 2001). Finally, the neck domain is not involved in dimerization because the A182-E581 fragment of MCAK, which includes the neck, is a monomer (Maney et al., 2001). What, then, is the role of the neck domain in the MT depolymerization activity of MCAK?

The electrostatic interactions between a positively charged neck domain and the negatively charged COOH terminus of tubulin have been shown to be important for the processivity of conventional kinesins. The addition of positive charges to the neck of a conventional kinesin increases its processivity by perhaps tethering the kinesin near the MT surface

Address correspondence to Linda Wordeman, Dept. of Physiology and Biophysics, University of Washington, 1959 NE Pacific St., Box 357290, Seattle, WA 98195-7290. Tel.: (206) 543-4135. Fax: (206) 685-0619. E-mail: worde@u.washington.edu

*Abbreviations used in this paper: FL, full-length; MCAK, mitotic centromere–associated kinesin; MT, microtubule.

Key words: Kin I; XKCM1; kinesins; processivity; diffusional motility

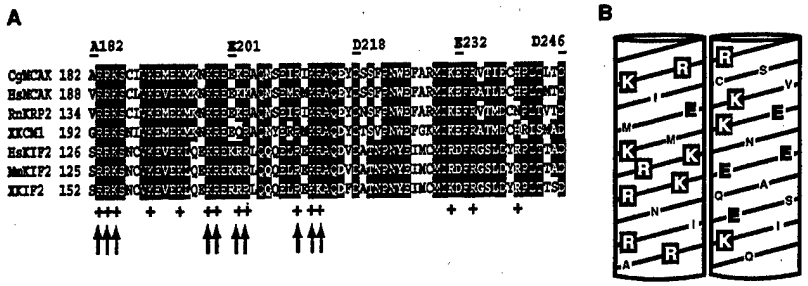

Figure 1. **The structural analysis of the MCAK neck.** (A) Sequence alignment of the neck domain of seven Kin I kinesins: CgMCAK, *C. griseus* (residues A182-D246; GenBank/EMBL/DDBJ accession no. U11790); HsMCAK, *Homo sapiens* (GenBank/EMBL/DDBJ accession no. U63743); RnKRP2, *Rattus norvegicus* (GenBank/EMBL/DDBJ accession no. U44979); XKCM1, *Xenopus laevis* (GenBank/EMBL/DDBJ accession no. U36485); HsKIF2, *Homo sapiens* (GenBank/EMBL/DDBJ accession no. CAA69621); MmKIF2, *Mus musculus* (GenBank/EMBL/DDBJ accession no. D12644); XKIF2, *X. laevis* (GenBank/EMBL/DDBJ accession no. U36486). Identical residues are shaded in black, similar ones are shaded in gray. The 64-amino acid neck domain sequences are 50% identical and 75% similar. The + symbols indicate highly conserved positively charged amino acids in the neck domain. The arrows show residues that were substituted for alanine. The borders of deletions in the neck domain are indicated by flanking residue numbers above the neck alignment. (B) Two sides of a helical diagram of a highly charged hydrophilic helix (residues R183–Q215) found in the CgMCAK neck. Positively charged amino acids are white, negatively charged residues are black, and the other residues are gray.

(Thorn et al., 2000). Similarly, the positively charged K-loop in the motor domain of the KIF1 single-headed kinesin provides a flexible attachment site for binding to MTs in the weakly bound state (Okada and Hirokawa, 2000; Rogers et al., 2001). Given the high percentage of positively charged amino acids in the MCAK neck region and their strong conservation among Kin I kinesins (Fig. 1 A), it is reasonable to suggest that the neck might be anchoring MCAK to MTs. Here, we used mutational analysis and chimeras to test whether the MCAK neck functions as an electrostatic tether. We found that although the removal of positive charges from the neck region significantly diminished the MT depolymerization activity of MCAK, the insertion of the positively charged K-loop into "neckless" MCAK completely restored its MT depolymerization activity. We propose that the neck, analogous to the K-loop, may interact electrostatically with the negatively charged MT lattice. This interaction may serve to target MCAK to MT ends by diffusional motility. The weak electrostatic interaction between MCAK's neck and MT ends may also play an important role in processivity of MCAK-induced MT depolymerization.

Results and discussion

Quantitation of MT depolymerization activity in vivo

To estimate the effect of the deletions in the MCAK neck domain on the MT depolymerization activity, we devised a quantitative in vivo MT depolymerization assay. In brief, EGFP–MCAK fusion constructs were transfected into cultured cells, fixed, and stained for tubulin (Fig. 2). Digital images were acquired using a cooled CCD camera. The transfected cells chosen for quantitation displayed similar EGFP–MCAK fusion protein expression levels (Figs. 3 and 4). The average pixel intensity (the mean gray value) over the entire cellular area was measured and corrected for noncellular background. Cells transfected with a control EGFP construct showed normal levels of MT polymer and were assigned an MT polymer value of 100%. EGFP-transfected cells displayed a mean tubulin fluorescence value of 1,902 gray-scale units, which represented the sum of free tubulin and MT polymer fluorescence (Fig. 3 A). Expression of FL MCAK resulted in the loss of all MTs at the analyzed level of expression with only a lightly stained background of unpolymerized tubulin remaining (Fig. 2 D, arrow). Such cells showed a mean tubulin fluorescence value of 734 gray-scale units, which was designated as 0% of the MT polymer (Fig. 3 A). Consequently, the mean intensity of tubulin fluorescence in the FL MCAK–transfected cells was less than half of that in the EGFP-transfected cells.

The low level of free (unpolymerized) tubulin seen in cells transfected with FL MCAK might be a result of a tubulin autoregulation mechanism. Increasing the concentration of free tubulin by depolymerizing MTs with MT-destabilizing drugs, e.g., nocodazole, leads to a rapid decrease in the level of tubulin mRNAs and an eventual decrease in the unassembled tubulin level (Cleveland et al., 1981; Gonzalez-Garay and Cabral, 1996). Similar to MCAK-mediated MT depolymerization, we found that treatment with a low concentration of nocodazole (1 μM) for 12 h produced cells with a low

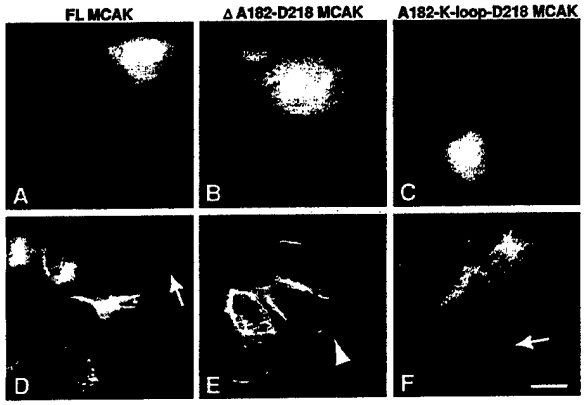

Figure 2. **Depolymerization of MTs by MCAK and MCAK mutants.** (A–C) EGFP fluorescence, (D–F) tubulin staining of the same cells. A cell transfected with full-length (FL) MCAK (A and D) displays a loss of MT polymer and low intensity unpolymerized tubulin staining (arrow). A cell transfected with the neckless MCAK mutant (B and E; Δ A182-D218 MCAK) exhibits a normal network of cytoplasmic MTs (arrowhead) as a consequence of the significantly decreased MT depolymerization activity of neckless MCAK. (C and F) Cells transfected with the A182-K-loop-D218 MCAK construct, the K-loop insertion into the neckless Δ A182-D218 MCAK mutant. The insertion of the KIF1A K-loop (NKNKKKKK) into the neckless MCAK restores the MT depolymerization activity to the level of FL MCAK. Arrow in F illustrates a cell with MT polymer loss similar to that in FL MCAK–transfected cells (D, arrow). All panels are the same magnification. Bar, 10 μm.

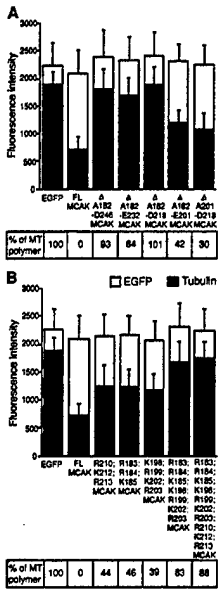

Figure 3. **Removal of positive charges in the neck domain significantly reduced MT depolymerization activity of MCAK.** (A) The effect of deletions in the neck region. Each Δ symbol represents a deletion of the MCAK neck region with borders indicated by flanking amino acid numbers. (B) The effect of alanine substitutions in the neck region. The residues changed to alanine are shown for each MCAK mutant. The average pixel intensity over the cell area is plotted on the y axis in gray-scale units. White bars show the mean EGFP fluorescence. Black bars represent the mean tubulin fluorescence. Error bars are SDs. EGFP indicates cells transfected with the EGFP control; FL MCAK designates cells transfected with FL wild-type MCAK. The percentage of MT polymer left in the transfected cells is shown.

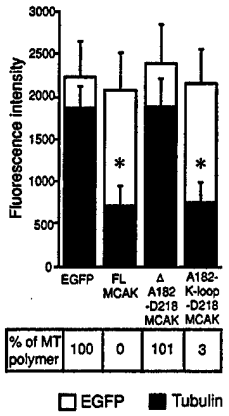

Figure 4. **Insertion of KIF1A K-loop into the neckless MCAK fully restores MT depolymerization activity.** y and x axis categories are the same as described in Fig. 3 legend. Error bars are SDs. A182-K-loop-D218 MCAK represents cells transfected with the KIF1A K-loop insertion into the neckless MCAK mutant, A182-NKNKKKKK-D218 MCAK. Asterisks label two samples, FL MCAK and A182-K-loop-D218 MCAK, whose means are statistically similar ($P = 0.92$) to each other as determined using the *t* test. The percentage of MT polymer left in the transfected cells is indicated.

intensity free-tubulin background and no MTs. The mean tubulin fluorescence intensity of these cells was 798 ± 169 gray-scale units ($n = 88$) as determined by the in vivo depolymerization assay described in this report. The mean tubulin intensity of cells treated with 1 μM nocodazole for 15 min was 1,645 ± 189 ($n = 41$). These cells displayed almost no MT polymer and bright free-tubulin staining due to the fact that 15 min was not long enough for autoregulation to take place and decrease the level of free tubulin. Nontreated cells with a normal network of cytoplasmic MTs showed the mean tubulin intensity equal to 1,870 ± 301 ($n = 77$).

The removal of positive charges from the neck domain dramatically reduced MT depolymerization activity of MCAK

As expected from previous studies (Maney et al., 2001), cells transfected with neckless MCAK (Δ A182-D246) displayed a normal MT network. The mean tubulin fluorescence of the Δ A182-D246 MCAK mutant was similar to that of the EGFP control and equaled 1,825 gray-scale units (Fig. 3 A). Cells transfected with MCAK mutants containing progressively smaller deletions in the neck domain, Δ A182-E232 and Δ A182-D218 (Fig. 2 E, arrowhead), also showed normal levels of MT polymer that were similar to that of the EGFP-transfected cells (Fig. 3 A). Hence, these neckless MCAK mutants exhibited severely impaired MT depolymerization activity. Smaller deletions in the neck region (Δ A182-E201 and Δ E201-D218) diminished MT depolymerization activity to a lesser degree. (Fig. 3 A). Next, we performed alanine substitutions of the highly conserved positively charged residues in the neck domain (Fig. 1, arrows) to test whether the loss of positive charges in this region affects the depolymerization activity of MCAK. Alanine substitutions of 3–4 positively charged amino acids resulted in some reduction of MT depolymerization activity (more than 50% of MTs were depolymerized in the transfected cells). Substitutions of 7 to 10 amino acids resulted in much greater inhibition of the depolymerization activity (<20% of MTs were depolymerized; Fig. 3 B). Therefore, the total sum of removed positive charges was of greater importance than the positions of the substituted residues.

In summary, we identified Δ A182-D218 as the smallest neck deletion that would reduce MT depolymerizing activity to the level of the EGFP control (Fig. 3 A). This region contains 13 (36%) positively charged residues and 7 (19%) negatively charged residues (Fig. 1). The net charge of A182-D218 region is positive and equals +6. Alanine substitutions of only 7 positive residues rendered the net charge of A182-D218 segment negative and resulted in greatly diminished MT depolymerization activity (Fig. 3 B). The A182-D218 region contains a highly charged hydrophilic helix (residues R183-Q215) as predicted by SSpro2 server (http://promoter.ics.uci.edu/BRNN-PRED [Baldi et al., 1999]). The helical wheel representation of this helix shows that the positively charged residues lie mostly on one side of the helix, whereas the opposite side contains most of the negatively charged residues found in this neck region (Fig. 1 B).

KIF1A K-loop insertion into neckless MCAK rescues MT depolymerization activity

We have shown that elimination of the positive charges in the MCAK neck region, A182-D218, either by deletions or alanine substitutions inhibits MT depolymerization activity of MCAK. Conversely, Niederstrasser et al. (2002) showed that the interaction between the COOH terminus of tubulin (C-hook) and MCAK is required for MT depolymerization because subtilisin cleavage of the C-hook abolishes depolymerization of MTs by the MCAK homologue, XKCM1. Furthermore, Okada and Hirokawa (2000) have shown that the positively charged K-loop of KIF1A interacts with the negatively charged C-hook and serves as an electrostatic tether to support the diffusion of KIF1A along MT protofilament. The positively charged neck of MCAK might interact with the negatively charged C-hook of tubulin analogously to the KIF1A K-loop. We tested this hypothesis by inserting the K-loop of KIF1A into the MT depolymerization deficient neckless MCAK. We found that MCAK with the A182-D218 neck segment replaced by the KIF1A K-loop, NKNKKKKK, (abbreviated as A182-K-loop-D218 MCAK) depolymerized MTs with the same efficiency as FL MCAK (Figs. 2 F and 4). Moreover, mitotic cells transfected with the A182-NKNKKKKK-D218 MCAK mutant displayed the same mitotic defects (unpublished data) described for overexpression of FL MCAK, namely bundling

and depolymerization of spindle MTs, which in turn resulted in prometaphase arrest and an elevated mitotic index in transfected cells (Maney et al., 1998).

None of the MCAK mutations described in this report interfered with centromere or centrosome binding. The nuclear/cytoplasmic localization of the mutants was identical to that of wild-type FL MCAK (unpublished data). All MCAK mutants showed the ability to bind MTs in vivo when cells were extracted before fixation in the absence of nucleotide (unpublished data) in a manner identical to FL MCAK (Maney et al., 1998). This implies that all mutated MCAKs were functional proteins with motor domains able to bind MT lattice in the nucleotide-free state, similar to conventional kinesins.

In vitro MT depolymerization activity of MCAK neck mutants

The rescue of the MT depolymerization–deficient neckless MCAK by K-loop insertion suggests that the MCAK neck is affecting the interactions between motor and MTs rather than regulating the depolymerization activity. To test this hypothesis further, we replicated our depolymerization assays in vitro. We expressed and purified the following proteins: core motor plus neck (A182-S583); core motor plus alanine-substituted neck (A182-Ala-S583 with substituted residues indicated by arrows in Fig. 1 A); core motor plus truncated neck (D218-S583); core motor plus K-loop in substitution for the neck (A182-K-loop-D218-S583); core motor plus poly-lysine (5K) in substitution for the neck (A182–5K-D218-S583); and core motor domain of MCAK (I253-S583; Fig. 5 A). The purified proteins were added to the taxol-stabilized MTs and were incubated at 24 ± 1°C for 10 min in the presence of 1 mM ATP. The depolymerization of tubulin polymer was measured as the percentage of tubulin released in the supernatant after subtraction of tubulin in supernatant of the no-motor control reaction and normalizing the supernatant and pellet fractions. Fig. 5 B shows the supernatants and pellets of the in vitro depolymerization reactions containing 100 nM active motor proteins and 1,500 nM taxol MTs. Although the core motor plus neck (A182-S583) depolymerizes 92 ± 4% of tubulin polymer, the core motor plus alanine-substituted neck, A182-Ala-S583 depolymerized only 10 ± 4% of tubulin polymer (Fig. 5 B). The truncated neck plus core motor (D218-S583) lacks the positively charged helix found in the FL neck (Fig. 1 B). This protein depolymerized only 13 ± 5% of tubulin polymer. Therefore, removal of positive charges from the neck either by alanine substitutions or deletions dramatically suppresses the MT depolymerization activity of this kinesin, but does not eliminate it completely in vitro. Although analogous neckless MCAK mutants (Δ A182-D246, Δ A182-E232, and Δ A182-D218) expressed to high levels in vivo displayed no detectable depolymerization activity (Fig. 2 E, 3A), in corroboration with our in vitro data, extremely high levels of expression showed a slightly disassembled MT network (unpublished data).

Also, we substituted the positively charged helix found in the A182-D218 region of CgMCAK neck (Fig. 1 B) with the positively charged K-loop of KIF1A by linking the K-loop to the NH_2 terminus of truncated neck plus core motor construct, D218-S583. This construct exhibited five-fold-increased depolymerization activity over D218-S583 (Fig. 5 B). However, although the K-loop rescues the depolymerization activity of the neckless mutant 100% in vivo

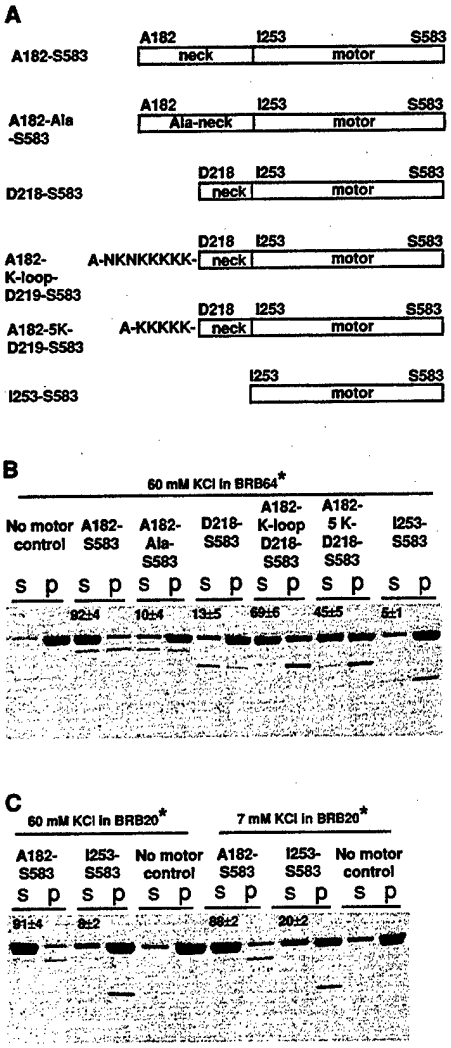

Figure 5. **Depolymerization activity of MCAK mutants in vitro.** (A) Diagram illustrating the truncated MCAK mutants used for in vitro depolymerization assays: core motor plus neck (A182-S583); core motor plus alanine-substituted neck (A182-Ala-S583 with R183, R184, K185, K198, R199, K202, R203, R210, K212, and R213 substituted to alanine); core motor plus truncated neck (D218-S583); core motor plus K-loop (NKNKKKKK) in substitution for the neck (A182-K-loop-D218-S583); core motor plus poly-L-lysine (KKKKK) in substitution for the neck (A182–5K-D218-S583); and core motor (I253-S583). B compares the depolymerization activity of the truncated MCAK mutants described above. C compares the depolymerization activity of the core motor plus neck (A182-S583) and the core motor domain of MCAK (I253-S583) in 60 mM KCl, BRB20 versus 7 mM KCl, BRB20. For both B and C, the percentage of tubulin in the supernatant of no-motor control reactions was subtracted from the percentage of tubulin in supernatant of the motor-containing reactions. The numbers are percentages of tubulin released in supernatant of the motor-containing reactions. The average of at least three experiments ± SD is shown for each supernatant fraction. In each case, the top band on the gel is tubulin and the bottom band is the added motor. In all assays, 100 nM of active motor protein was added to 1,500 nM taxol-stabilized MTs in the presence of 1 mM ATP. *Refer to Materials and methods for exact buffer composition.

(Fig. 4), it rescues only 75% of the depolymerization activity of D218-A182 construct in vitro (Fig. 5 B). Therefore, the MCAK neck plus motor (A182-S583) is still the most optimal construct for MT depolymerization, which might be one of the reasons why it is so highly conserved. It is likely that the K-loop rescues the depolymerization activity because it contains positively charged residues. We have further confirmed that charge is an important functional property of the neck by constructing the poly-lysine mutant, A182-KKKKK-D218-S583 (abbreviated as A182–5K-D218-S583), which contains poly-lysine peptide instead of K-loop in place of A182-D218 neck region. Fig. 5 B shows that the poly-lysine peptide substitution rescues the depolymerization activity of D218-S583, but to a lesser degree than the K-loop substitution, perhaps due to fewer positive charges found in the poly-lysine peptide (+5) than in K-loop (+6).

The rescue of the MT depolymerization–deficient neckless MCAK by K-loop insertion suggests that the MCAK neck might function analogously to the K-loop. The K-loop of KIF1A mediates diffusional motility (Okada and Hirokawa, 2000; Rogers et al., 2001). Similarly, we propose that the neck of MCAK may support diffusional motility to transport MCAK along the MT protofilament toward MT ends where Kin I–mediated MT depolymerization occurs (Desai et al., 1999). The neck of MCAK may also use diffusional motility to confer accelerated kinetics or processivity to the core motor domain (unpublished data).

Moores et al. (2002) have clearly shown that a conserved core motor domain of a *Plasmodium falciparum* Kin I kinesin (pKinI) can disassemble MTs. However, the assay conditions (extremely low ionic strength) were chosen to maximize electrostatic interactions. Maximizing the electrostatic interactions and raising the stoichiometry of Kin I/tubulin (≥1:10) obviates the need for processivity or diffusional motility despite the fact that it is essential for depolymerization under physiological conditions. We have duplicated the low ionic strength conditions used by Moores et al. (2002). The decrease in salt concentration from 60 to 7 mM KCl in BRB20 buffer produced a twofold increase of tubulin polymer depolymerized by the core motor (Fig. 5 C). This shows that the core motor of MCAK (I253-S583) is also a definite but enfeebled depolymerizer. Direct comparison of the neck plus motor (A182-S583) with the conserved core motor (I253-S583) shows that the neck plus motor is a tremendously more effective depolymerizer than the core motor (Fig. 5, B and C).

In summary, we demonstrated that deletions or alanine substitutions of positively charged residues of A182-D218 neck region drastically reduced the MT depolymerization activity. Insertion of the positively charged KIF1A K-loop or poly-lysine rescued the neckless MCAK mutants. We propose that the neck acts as an electrostatic tether. This electrostatic tether may increase the rate of MT depolymerization by either increasing the on-rate of MCAK to MT ends (perhaps by mediating diffusional motility) or decreasing the off-rate of MCAK from MTs (perhaps by conferring processivity to the core motor domain; unpublished data). The data presented here do not allow us to distinguish between diffusional targeting and processivity. Mediation of diffusional targeting and processivity are two distinct and not mutually exclusive hypotheses for the contribution of the neck to the MT depolymerization activity of MCAK.

Materials and methods

Constructs

pTRE2-EGFP-CgMCAK was made by the subcloning of NheI-BspEI EGFP cDNA fragment (from pEGFP-C1; CLONTECH Laboratories, Inc.) and the BspEI-NotI *Cricetulus griseus* MCAK cDNA fragment (from pOPRSVICAT-GFP-MCAK; Maney et al., 1998) into the pTRE2 vector (CLONTECH Laboratories, Inc.) digested with NheI and NotI. The gene expression level controlled by TRE promoter is similar to the high expression levels in the traditional CMV promoter–driven systems (Yin et al., 1996). The deletion, alanine substitution, and K-loop insertion constructs were prepared by overlap PCR using specially designed mutagenic primers and PfuTurbo® DNA polymerase (Stratagene). The mutations were confirmed by DNA sequencing. Constructs for bacterially expressed proteins were made by amplifying the coding sequences of MCAK mutants from the constructs in pTRE2 vector with PfuTurbo® DNA polymerase (Stratagene), and then subcloning the resulting fragments into pET-28a+ (Novagen) digested with Nco1 and Not1.

Cell transfection and immunofluorescence

CHO AA8 Tet-Off™ cells (CLONTECH Laboratories, Inc.) were grown in 90% αMEM, 10% FBS, and 100 μg/ml G418 at 37°C, 5% CO_2. 1 d before transfection, cells were plated onto 12-mm coverslips at low density (2×10^4 cells/cm^2). Transfections were done with ExGen 500 transfection reagent (MBI Fermentas). Cells were cultured for 24 h after transfection and fixed with 1% PFA in precooled methanol for 10 min. The cells were then incubated with mouse anti–tubulin DM1α (Sigma-Aldrich) at 1:50 dilution for 1 h and Texas red anti–mouse antibodies (Jackson ImmunoResearch Laboratories) at 1:100 dilution in PBS plus 0.1% Triton X-100 and 1% BSA for 1 h. Cells were washed with PBS, stained with DAPI, and mounted in Vectashield® mounting medium (Vector Laboratories). Analysis was done with a microscope (model FX-A; Nikon) equipped with 60×/1.4 NA Plan Apo oil objective. The digital images were acquired with a cooled CCD camera (SenSys; Photometrics) controlled by QED camera software (QED Imaging, Inc.).

Quantitation of MT depolymerization activity in vivo

To quantify the microtubule (MT) depolymerization activity, we collected digital images of the transfected cells at the same exposure for each set of GFP and MT images and below saturation level of the camera (the 4,096 gray-value maximum). All images were saved as 12-bit TIFF images for quantification by NIH Image 1.62 software and Microsoft Excel. Mean EGFP or tubulin fluorescence intensities over the entire cellular area were measured as the average gray value within the area. Mean fluorescence over the cell-free area in each image was subtracted from mean fluorescence over the cellular area to correct for background fluorescence. All analyzed cells were in interphase and were free of aggregates of overexpressed protein. 20–90 transfected cells were measured for each construct with >500 cells quantified overall. To quantify the MT polymer left in the transfected cells, we assigned an MT polymer value of 0% to the cells transfected with full-length (FL) MCAK, which displayed no MTs and a mean tubulin fluorescence intensity equal to 734 gray-scale units. Similar to nontransfected cells, EGFP-transfected cells showed normal levels of MT polymer, which was given a 100% value. The mean tubulin fluorescence of EGFP-transfected cells was equal to 1,902 gray-scale units. To quantify the percentage of MT polymer left in the cells transfected with mutant MCAK constructs, we used the following formula: {[(the mean tubulin fluorescence intensity of mutant-transfected cells − 734)/1,168] × 100%} where 1168 is the difference between EGFP control and FL MCAK mean gray values.

In vitro MT depolymerization assays

The bacterially expressed COOH-terminally 6his-tagged proteins were purified as described in Maney et al. (2001). The active motor concentration was determined as the concentration of nucleotide-binding sites because there is one ATP-binding site per each monomeric motor protein analyzed in this study in vitro. The concentration of nucleotide-binding sites was measured radiometrically as described by Coy et al. (1999). The depolymerization of taxol-stabilized MTs, polymerized from bovine tubulin (Cytoskeleton, Inc.), was performed as described in Maney et al. (2001). In brief, for the assay shown in Fig. 5 A, 100 nM of the active motor proteins in 20 μl of the elution buffer (250 mM imidazole, pH 7.0, 300 mM KCl,

0.2 mM $MgCl_2$, 0.01 mM Mg-ATP, 1 mM DTT, and 20% glycerol) was mixed with 1,500 nM taxol-stabilized MTs in 80 μl of BRB80 (80 mM Pipes, pH 6.8, 1 mM EGTA, and 1 mM $MgCl_2$), 12.5 μM taxol, 1 mM DTT, and 1.25 mM Mg-ATP incubated at 24 ± 1°C for 10 min, and then centrifuged at 30 psi for 10 min. For the assay shown in Fig. 5 B, 100 nM of the active motor proteins in 2.3 μl of the elution buffer was mixed with 1,500 nM taxol-stabilized MTs in 97.7 μl of BRB20 (20 mM Pipes, pH 6.8, 1 mM EGTA, and 1mM $MgCl_2$), 10.2 μM taxol, 1 mM DTT, 10 μg/ml BSA, and 1.02 mM Mg-ATP with or without addition of KCl up to 60 mM, incubated at 24 ± 1°C for 10 min, and then centrifuged at 30 psi for 10 min. Supernatants and pellets were assayed for the presence of tubulin on Coomassie-stained SDS-polyacrylamide gels (Novex). Gels were calibrated and quantified using NIH Image 1.62 software. The percentage of tubulin in the supernatant of no-motor control reactions was subtracted from the percentage of tubulin in supernatant of the motor-containing reactions. The percentages of tubulin released in supernatant of the motor-containing reactions were then normalized with the percentages of tubulin in the corresponding pellet fractions.

We thank Andy Hunter, Ayana Moore, and Kathleen Rankin for many discussions and comments on the manuscript. We also thank Ayana Moore (University of Washington School of Medicine, Seattle, WA) for the pTRE2-GreenLantern-CgMCAK plasmid.

This work was supported by the National Institutes of Health grant (GM53654A) and the Department of Defense grant (DAMD17-01-1-0450) to L. Wordeman.

Submitted: 17 May 2002
Revised: 16 October 2002
Accepted: 17 October 2002

References

Baldi, P., S. Brunak, P. Frasconi, G. Soda, and G. Pollastri. 1999. Exploiting the past and the future in protein secondary structure prediction. *Bioinformatics.* 15:937–946.

Case, R.B., D.W. Pierce, N. Hom-Booher, C.L. Hart, and R.D. Vale. 1997. The directional preference of kinesin motors is specified by an element outside of the motor catalytic domain. *Cell.* 90:959–966.

Cleveland, D.W., M.A. Lopata, P. Sherline, and M.W. Kirschner. 1981. Unpolymerized tubulin modulates the level of tubulin mRNAs. *Cell.* 25:537–546.

Coy, D.L., M. Wagenbach, and J. Howard. 1999. Kinesin takes one 8-nm step for each ATP that it hydrolyzes. *J. Biol. Chem.* 274:3667–3671.

Desai, A., S. Verma, T.J. Mitchison, and C.E. Walczak. 1999. Kin I kinesins are microtubule-destabilizing enzymes. *Cell.* 96:69–78.

Endow, S.A., and K.W. Waligora. 1998. Determinants of kinesin motor polarity. *Science.* 281:1200–1202.

Goldstein, L.S., and A.V. Philp. 1999. The road less traveled: emerging principles of kinesin motor utilization. *Annu. Rev. Cell Dev. Biol.* 15:141–183.

Gonzalez-Garay, M.L., and F. Cabral. 1996. alpha-Tubulin limits its own synthesis: evidence for a mechanism involving translational repression. *J. Cell Biol.* 135:1525–1534.

Henningsen, U., and M. Schliwa. 1997. Reversal in the direction of movement of a molecular motor. *Nature.* 389:93–96.

Hunter, A.W., and L. Wordeman. 2000. How motor proteins influence microtubule polymerization dynamics. *J. Cell Sci.* 113:4379–4389.

Kinoshita, K., I. Arnal, A. Desai, D.N. Drechsel, and A.A. Hyman. 2001. Reconstitution of physiological microtubule dynamics using purified components. *Science.* 294:1340–1343.

Lakshmi, M.S., C. Parker, and G.V. Sherbet. 1993. Metastasis associated MTS1 and NM23 genes affect tubulin polymerisation in B16 melanomas: a possible mechanism of their regulation of metastatic behaviour of tumours. *Anticancer Res.* 13:299–303.

Maney, T., A.W. Hunter, M. Wagenbach, and L. Wordeman. 1998. Mitotic centromere-associated kinesin is important for anaphase chromosome segregation. *J. Cell Biol.* 142:787–801.

Maney, T., M. Wagenbach, and L. Wordeman. 2001. Molecular dissection of the microtubule depolymerizing activity of mitotic centromere-associated kinesin. *J. Biol. Chem.* 276:34753–34758.

Moores, C.A., M. Yu, J. Guo, C. Beraud, R. Sakowicz, and R.A. Milligan. 2002. A mechanism for microtubule depolymerization by KinI kinesins. *Mol. Cell.* 9:903–909.

Niederstrasser, H., H. Salehi-Had, E.C. Gan, C. Walczak, and E. Nogales. 2002. XKCM1 acts on a single protofilament and requires the C terminus of tubulin. *J. Mol. Biol.* 316:817–828.

Okada, Y., and N. Hirokawa. 2000. Mechanism of the single-headed processivity: diffusional anchoring between the K-loop of kinesin and the C terminus of tubulin. *Proc. Natl. Acad. Sci. USA.* 97:640–645.

Rogers, K.R., S. Weiss, I. Crevel, P.J. Brophy, M. Geeves, and R. Cross. 2001. KIF1D is a fast non-processive kinesin that demonstrates novel K-loop-dependent mechanochemistry. *EMBO J.* 20:5101–5113.

Romberg, L., D.W. Pierce, and R.D. Vale. 1998. Role of the kinesin neck region in processive microtubule-based motility. *J. Cell Biol.* 140:1407–1416.

Thorn, K.S., J.A. Ubersax, and R.D. Vale. 2000. Engineering the processive run length of the kinesin motor. *J. Cell Biol.* 151:1093–1100.

Vale, R.D., and R.J. Fletterick. 1997. The design plan of kinesin motors. *Annu. Rev. Cell Dev. Biol.* 13:745–777.

Walczak, C.E., T.J. Mitchison, and A. Desai. 1996. XKCM1: a *Xenopus* kinesin-related protein that regulates microtubule dynamics during mitotic spindle assembly. *Cell.* 84:37–47.

Woehlke, G., and M. Schliwa. 2000. Walking on two heads: the many talents of kinesin. *Nat. Rev. Mol. Cell Biol.* 1:50–58.

Wordeman, L., and T.J. Mitchison. 1995. Identification and partial characterization of mitotic centromere-associated kinesin, a kinesin-related protein that associates with centromeres during mitosis. *J. Cell Biol.* 128:95–104.

Yin, D.X., L. Zhu, and R.T. Schimke. 1996. Tetracycline-controlled gene expression system achieves high-level and quantitative control of gene expression. *Anal. Biochem.* 235:195–201.

Zhai, Y., P.J. Kronebusch, P.M. Simon, and G.G. Borisy. 1996. Microtubule dynamics at the G2/M transition: abrupt breakdown of cytoplasmic microtubules at nuclear envelope breakdown and implications for spindle morphogenesis. *J. Cell Biol.* 135:201–214.

Traffic 2003; 4: 367–375
Blackwell Munksgaard

ISSN 1398-9219

Review

Unconventional Motoring: An Overview of the Kin C and Kin I Kinesins

Yulia Ovechkina and Linda Wordeman*

University of Washington School of Medicine, Department of Physiology and Biophysics, Seattle, WA 98195, USA
** Corresponding author: Linda Wordeman, worde@u.washington.edu*

All kinesins share a conserved core motor domain implying a common mechanism for generating force from ATP hydrolysis. How is it then that kinesins exhibit such divergent activities: motility, microtubule cross-linking and microtubule depolymerization? Although conventional motile kinesins have served as the paradigm for understanding kinesin function, the unconventional kinesins exploit variations on the motile theme to perform unexpected tasks. This review summarizes the biological functions and examines the possible molecular mechanisms of Kin C and Kin I unconventional kinesins. We also discuss the possible differences between the microtubule destabilization models proposed for Kar3 and Kin I kinesins.

Key words: depolymerization, Kar3, KIF2, kinesin, Kip3, Klp5/6, MCAK, microtubule dynamics, motor, XKCM1

Received 2 March 2003, revised and accepted for publication 26 March 2003

Kinesins are a large superfamily of microtubule motor proteins that use the energy of ATP hydrolysis to produce force. They are defined by the presence of a catalytic core motor domain (historically known as the 'head' domain), which hydrolyzes ATP and binds to microtubules (MTs). Kinesins are classified into three subfamilies based on the position of their motor domain within the primary sequence of the protein. The Kin C subfamily comprises kinesins with a C-terminally located core motor domain; Kin N kinesins have an N-terminally located core motor domain; and Kin I kinesins possess an internally located core motor domain (Figure 1). All kinesins share a high degree of sequence identity within the core motor domain. The crystal structures of the Kin N and Kin C core motor domains are clearly similar to each other (1,2). The first kinesin to be identified was purified from the giant axon of the squid (3). This extensively studied member of the Kin N family of kinesins serves as the prototype for all other kinesin-related proteins by virtue of its relative abundance and ubiquitous tissue distribution. As a result, Kin N kinesins that are structurally related to squid axonal kinesin have earned the designation 'conventional kinesins'. By default, the Kin C and Kin I kinesins have been labeled 'unconventional kinesins'.

Functionally, the position of a kinesin's motor domain within the polypeptide chain usually predicts its directionality. Kin N kinesins walk toward the plus ends of MTs, whereas Kin C kinesins translocate toward the minus ends of MTs. Unexpectedly, the Kin I kinesins are not able to translocate along MTs in the conventional sense but, instead, depolymerize MT filaments from both ends (4,5). It is important to note, however, that the directionality of motile kinesins is not directly controlled by the position of the motor domain in the polypeptide chain but rather by the conserved region immediately outside the motor core domain, called the 'neck' domain [reviewed in (6,7)]. Vale and Fletterick (8) have defined the neck domain as 'the most class-specific region' within the kinesin primary sequence. This region is highly conserved within each respective kinesin subfamily but extremely variable across subfamilies (8). It is thought that the conserved core motor domains of both Kin N and Kin C subfamilies possess intrinsic slow plus-end directed motile activity. The Kin N-type neck may act to amplify this activity, while the presence of a Kin C-type neck is sufficient to direct the motor toward MT minus-ends [reviewed in (6,9)]. The neck domains of the Kin C and Kin I kinesins are located N-terminally to the core motor domain, while the neck of the Kin N kinesins is C-terminal to the core motor (Figure 1). Many kinesins contain an α-helical coiled-coil stalk domain through which they dimerize (Figure 1). In addition, kinesins typically have a globular tail domain capable of carrying out a wide variety of functions, such as interacting with cargo or kinesin-associated proteins (10); regulating the core motor ATPase activity (11); providing non-ATP dependent MT binding sites (12); and targeting kinesins to different locations in cells (13).

All conventional kinesins (Kin N subfamily members) characterized so far are processive, meaning they are able to take hundreds of steps before dissociating from an MT filament [reviewed in (14,15)]. Processivity requires that the motor be continuously attached to the MT during successive steps in the cycle of translocation. In the case of conventional kinesin, conformational changes in the dimerized heads are coupled intermolecularly to the ATP hydrolysis cycle, so that one head is always strongly bound

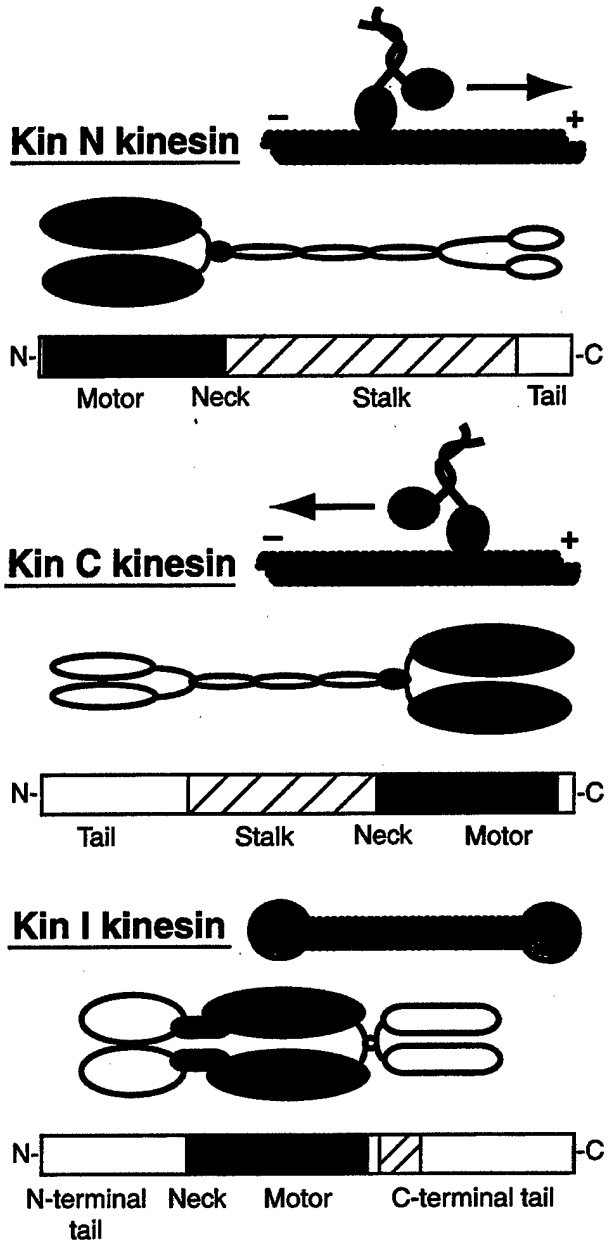

Figure 1: Schematic representations of kinesin structure. Members of Kin N, Kin C, and Kin I kinesin subfamilies are shown. Kin N kinesins move toward the plus ends of MTs, Kin C kinesins translocate toward the minus ends of MTs, whereas the Kin I kinesins depolymerize MTs from both ends. The conserved core motor domain is shaded in black; the neck is in gray; tail domains are in white; and coiled-coil regions are striped.

to MTs while the motor domains translocate in a hand-over-hand manner along the surface of the microtubule lattice. In contrast, the Kin C dimeric kinesins are nonprocessive motors. They lack the ability to take even a few successive steps along a MT filament [reviewed in (6,15)]. However, when multiple nonprocessive motors work together, for example by attaching to a surface of a vesicle, they can processively transport it along MTs. A recent study by Hunter et al. (4) has demonstrated that the Kin I kinesin, CgMCAK, is a processive depolymerase. A single CgMCAK dimer will remove multiple tubulin dimers while maintaining an attachment to MT ends (4).

All in all, the unconventional kinesins are important for numerous biological processes and their malfunctions have been implicated in human diseases [reviewed in (16,17)]. Mutations in the Kin C kinesin, DmNCD, cause chromosome nondisjunction during female meiosis in *Drosophila* (18). Related Kin C kinesins also operate during vertebrate meiosis and mitosis to insure accurate chromosome segregation (19,20). Chromosome nondisjunction during meiosis is the most common cause of mental retardation and conceptus wastage in humans (21), making this class of kinesins of fundamental importance for genomic stability and human health.

In addition, the ability of Kin I kinesins to modulate microtubule dynamics has major implications for both chromosome segregation and malignancy. A member of the Kin I subfamily, HsMCAK (KNSL6), is overexpressed in human cancers (22,23). The hamster homolog of HsMCAK can depolymerize paclitaxel-stabilized MTs in cells (24). Significantly, the other major MT depolymerizing nonmotor protein, stathmin, is incapable of destabilizing cellular MTs in the presence of comparable levels of paclitaxel (24,25). Therefore, HsMCAK overexpression, in particular, may be responsible for decreased sensitivity to the microtubule-stabilizing anticancer drug paclitaxel (Taxol, registered trademark of Bristol Myers Squibb) in some cancers (26). HsMCAK may antagonize the effect of paclitaxel by promoting MT dynamics. Targeting cancer cells with MCAK inhibitors alone or together with paclitaxel may present a potential strategy in treatment of paclitaxel-resistant tumors.

The functional contribution of the unconventional kinesins to cell division and other cellular processes is mechanistically linked with their activities at a molecular level. Here, we will review the molecular mechanisms and cellular functions of the Kin C and Kin I unconventional kinesins.

Kin C Kinesins are Minus-End Directed Motor Proteins

Kin C kinesins are minus-end directed motor proteins that have been implicated in the organization of bipolar spindles, retrograde transport, and Golgi apparatus positioning (summarized in Table 1). Kin Cs contain ATP-independent MT binding sites outside of the core motor domain (12). The ability of these kinesins to bundle MTs suggests that they possess MT cross-linking activity (12,19). Combining MT cross-linking activity with motile activity would enable these molecules to slide one MT with respect to another. Hence, it was proposed that Kin C kinesins cross-link spindle MTs and move toward the minus ends to promote

Table 1: Diverse functions of Kin C kinesins. Representative members of Kin C subfamily are shown. The first two letters of the motor name refer to the species name: Dm, *Drosophila melanogaster*; Xl, *Xenopus laevus*; Hs, *Homo sapiens*; Sc, *Saccharomyces cerevisiae*; Mm, *Mus musculus*

Kin C kinesins	Subcellular localization	Mutant (deficient) phenotype	Functions
DmNCD	spindles and spindle poles (18)	spindles with splayed poles and chromosome nondisjunction during female meiosis (18)	organizing ends of oocyte spindle MTs into poles; and spindle integrity (18,27,28)
XlCTK2	spindles and spindle poles (19)	inhibition of bipolar spindle assembly in *Xenopus* egg extracts (19)	promoting bipolar spindle assembly in *Xenopus* egg extracts (19)
HsHSET	spindles and spindle poles (20)	splayed spindle poles and loss of spindle bipolarity in murine oocytes (20)	establishing spindle poles during meiosis (20)
ScKAR3	spindles and spindle pole bodies (39,42)	failure in nuclear fusion during mating (35); aberrant MT arrays and prophase arrest during meiosis (75); short mitotic spindles and increased number and length of cytoplasmic MTs (35,39)	cross-bridging MTs between fusing nuclei to draw them together during mating (35); nuclear and spindle positioning (76); and spindle integrity (39,76)
MmKIFC2	neural cell bodies, dendrites, and axons (77)	Homozygous KifC2 mouse mutants were viable and reproduced normally (78)	retrograde transport (77)
MmKIFC3	perinuclear regions in the adrenocortical cells (79); apical plasma membrane in epithelial cells (80)	fragmentation of the Golgi apparatus under the cholesterol-depleted condition (79)	Golgi positioning and integration (79); apical transport in epithelial cells (80)

focused association of the MT minus ends at the spindle poles (18,27,28). The minus-end directed activity of Kin C kinesins appears to act antagonistically to the plus-end directed activity of BimC kinesins (Kin N type) (20,28–30). Kin C kinesins produce forces which pull spindle poles together, while BimC kinesins produce forces which separate spindle poles. Deficiency in BimC activity results in centrosome separation defects and failure of bipolar spindle formation, whereas removal of Kin C activity in BimC mutants rescues these defects (20,29,30). Thus, opposing motors generate counteracting forces to establish and maintain bipolar spindle structure [reviewed in (31)]. The contribution of Kin C kinesin activity to the establishment of spindle poles is most essential during meiosis or in the absence of centrosomes (18,27,28). Kin C function is thought to be supplemented to a greater degree by centrosomes and also the minus-end directed motor, dynein, in somatic cells (20,28).

Interestingly, ScKar3 stands out from the Kin C subfamily because of its ability to destabilize MTs *in vitro* specifically from minus ends (32). MT destabilizing activity has not yet been reported for any other Kin C kinesin tested *in vitro* (33,34). As expected, a truncated ScKar3 protein [lacking N-terminal nonmotor MT binding domain (35), 1–276 residues] fused to GST tag exhibited minus-end directed motility *in vitro* (32). However, while observing minus-end directed motility of GST-ScKar3, Endow et al. noted that MT lengths were reducing, giving the appearance that minus ends of MTs was moving faster than plus ends (32). This suggested that ScKar3 might be directly destabilizing MTs, preferably from the minus ends. The MTs used in this assay were weakly stabilized by paclitaxel (1 paclitaxel molecule per 5 tubulin dimers). Increasing the paclitaxel concentration inhibited the ScKar3-mediated MT minus-end destabilization (32). It was suggested that ScKar3 causes MT minus-end instability by binding between two adjacent protofilaments, which results in weakening MT protofilament lateral connections at the MT minus ends (36). The inhibition of ScKar3-mediated MT destabilization by paclitaxel is consistent with this idea, since paclitaxel stabilizes MTs by strengthening lateral interactions between MT protofilaments (37). Comparison of the crystal structure of the ScKar3 motor domain with those of both conventional Kin N kinesin and also the Kin C kinesin, DmNCD, revealed that ScKar3 has a significantly shorter L11 loop within the core motor domain (36). The L11 loop is thought to bind in the groove between MT protofilaments (38). The shorter L11 loop may force the Kar3 motor to bind deeper into the groove, triggering the lateral separation of protofilaments at the MT ends and thus initiating an MT catastrophe event (36).

The microtubule destabilizing activity of ScKar3 kinesin has also been documented *in vivo*. Mutations of ScKar3 resulted in both increased number and length of cytoplasmic MTs in budding yeast (39). Experiments *in vivo* implicate only

one other member of the Kin C subfamily, the fission yeast SpKlp2 kinesin, as an MT destabilizer (40). Further analysis of MT destabilizing activity of ScKar3 and SpKlp2 could provide important information regarding the molecular basis of this activity. Combining motility and MT depolymerizing activity may be unique to these two yeast Kin C motors. This could be one mechanism by which yeast make do with fewer kinesins than other eukaryotic cells.

While conventional Kin N kinesins and the well-characterized minus-end directed motor, DmNCD (Kin C), operate as homodimers, ScKar3 functions as a monomeric motor *in vivo* (41,42). The monomeric ScKar3 motor domain has recently been shown to associate as a heterodimer with one of two nonmotor polypeptides (Cik1 or Vik1) through corresponding coiled-coil domains. The two ScKar3 heterodimers have different cellular localizations and possibly functions. The ScKar3/Cik1 heterodimer localizes along cytoplasmic MTs during mating and along spindle MTs during mitosis, where it acts as an MT cross-linking and sliding motor (41,42). In contrast, the ScKar3/Vik1 heterodimer localizes to the mitotic spindle poles, where it organizes MT ends into spindle poles and may also destabilize cytoplasmic MTs (39,42).

These data suggest several important questions: Do any other Kin C kinesins form single motor heterodimers? How are the activities of ScKar3 heterodimeric complexes regulated? Is the MT destabilization activity of ScKar3 unique among Kin C kinesins? An *in vitro* analysis of MT motile, cross-linking and destabilizing activities of ScKar3/Vik1 and ScKar3/Cik1 heterodimers would help to elucidate the molecular mechanism of these activities.

Kin I Kinesins are MT Depolymerases

Despite the presence of the conserved core motor domain, Kin Is do not generate movement but function as MT depolymerases that disassemble MTs in an ATP-dependent fashion *in vitro* or *in vivo* (4,5). Kin Is have a unique ability to target primarily MT ends, while Kin N and Kin C kinesins have a higher affinity for the MT lattice. Likewise, while the MT lattice is known to maximally stimulate the ATPase activity of Kin N and Kin C kinesins, Kin Is have a substantial MT-end stimulated ATPase activity. Non-polymeric tubulin dimers and MT lattice also stimulate the Kin I's ATPase but to a much lesser extent (4). Kin Is efficiently depolymerize both paclitaxel and GMP-CPP stabilized MTs *in vitro* (4,5,24). Kin Is accumulate predominantly at both ends of MTs in the presence of AMP-PNP (a nonhydrolyzable ATP analogue) *in vitro*. Electron microscopic analysis of MT ends after incubation with Kin I kinesins revealed curled protofilaments (5,43). Furthermore, Niederstrasser et al. demonstrated that Kin Is are capable of depolymerizing zinc-induced tubulin polymers, characterized by an antiparallel MT protofilament arrangement unlike the parallel arrangement of protofilaments in cellular MTs (44). These data indicate that, unlike the proposed model for Kar3, Kin Is do not bind two adjacent protofilaments to force them apart to induce depolymerization. Instead, Kin Is induce protofilament curling by acting on a single MT protofilament. Three-dimensional EM reconstruction of a *Plasmodium* Kin I, pKinI, bound to single protofilament curls showed that the core motor domain binds both α and β tubulin subunits (43). It is thought that the binding of Kin Is either directly induces or stabilizes a conformational change in a GTP-tubulin dimer at the MT ends that reflects the GDP-tubulin state of depolymerizing microtubules without stimulating GTP hydrolysis on tubulin subunits (4,5). The stabilization of the curved GDP-like conformation of the terminal GTP-tubulin dimer results in destabilization of the lateral interactions between tubulin subunits in the MT lattice and loss of tubulin dimers from MT ends (45). The C-terminus of β-tubulin is required for the tubulin conformational change induced by Kin I kinesin binding (43,44).

Kinetic analysis suggests that CgMCAK, a hamster Kin I, is a processive MT depolymerase. One MCAK molecule is capable of removing approximately 20 tubulin dimers from the end of MT protofilament before it dissociates (4). Another important kinetic feature of CgMCAK-mediated MT depolymerization is the exceptionally rapid targeting of CgMCAK to MT ends: the on-rate of CgMCAK to MT ends exceeds by 100 times the rate at which tubulin dimers bind to MT ends during polymerization. These data led Hunter et al. to suggest that CgMCAK targets MT ends by diffusion along the MT lattice (4). MT-end targeting through one-dimensional diffusion along the MT protofilament is much faster than targeting through three-dimensional diffusion and is compatible with the on-rate for CgMCAK to MT ends.

The conserved core motor domain of Kin I kinesins is capable of stabilizing the curved protofilaments of depolymerizing microtubules (43). This is a key step in the mechanism of Kin I-induced MT depolymerization. However, under physiological conditions the core motor of CgMCAK (I253-S583) is unable to depolymerize MTs. The addition of the N-terminal neck domain (A182-R252) to the CgMCAK core motor domain restores MT depolymerizing activity to the level of the full-length CgMCAK both *in vivo* and *in vitro* (24,46). Hence, neck plus motor domain (A182-S583) constitutes the minimal MT depolymerase with MT depolymerizing activity similar to the full-length CgMCAK. The positively charged neck domain of CgMCAK may mediate diffusional motility through weak electrostatic interactions with the negatively charged MT lattice (46). These electrostatic interactions between the neck and the negatively charged tubulin C-terminus may also mediate processivity of CgMCAK-induced MT depolymerization. Thus, it is the catalytic processivity conferred by the neck domain that makes CgMCAK an active depolymerizer under physiological conditions.

Baculovirus-expressed Kin Is form homodimers (47–49). However, this dimerization is not essential for Kin I-mediated depolymerization activity since the minimal MT depolymerase, the neck plus motor, is a monomer (24). Kin Is lack an extended α-helical coiled-coil domain, which serves as a dimerization site for Kin N and Kin C kinesins. Only a small C-terminal domain of CgMCAK, ~40 C-terminal residues (A611-I648), is predicted to form a coiled-coil by the PairCoil program (50) and the prediction (< 50% probability coiled-coil) is relatively weak. Both the N-and C-terminal domains were shown to be necessary for CgMCAK kinetochore localization (13,48).

In contrast to the well-documented MT depolymerization activity of Kin I kinesins, Noda et al. reported that MmKIF2, a member of Kin I subfamily, generated plus-end directed motility (47). However, Desai et al. showed that XlKIF2 (which shares 80% identity with full-length MmKIF2 and 95% identity with the neck plus motor region of MmKIF2) is not able to move MTs but depolymerizes MTs similarly to the other Kin Is (5). Likewise, CgMCAK has not shown directed MT gliding motility in standard motility assays [our unpublished data,(4)]. The MmKif2 fraction, which was used for motility experiments by Noda et al. (47), was purified from Sf9 cells by incubating Sf9 cytoplasmic lysates with MTs in the absence of ATP and eluting MT-bound proteins with addition ATP – a process that could also extract endogenous kinesins from Sf9 cells. Thus, the possible contamination by endogenous plus-end directed kinesins cannot be excluded in the MmKIF2 motility assay by Noda et al. (47). By analogy to XlKIF2, we predict that MmKIF2 is an MT depolymerase.

The Kin I subfamily includes both MCAK-like and KIF2-like kinesin subclusters. The consensus protein sequences corresponding to either MCAK or KIF2 subclusters are highly similar but contain some differences, mostly in the N- and C-terminal tail domains (see online supplementary material for a protein sequence alignment of the Kin I subfamily kinesins). HsMCAK (accession #AAC27660) and HsKIF2 (accession #CAA69621) share 50% identity and 70% similarity within the full-length sequences and 70% identity and 90% similarity within the neck plus motor regions. In mammals, both MCAKs and KIF2s are expressed in the variety of tissues: hemopoietic cells, liver, kidney, spleen, lung, and brain tissues (22,47,49,51,52). MmKIF2 and its splice variant, MmKIF2β, are expressed at higher levels in developing brain and down-regulated in differentiated neurons and adult brain tissues (49,53). The expression of MmMCAK was detected in proliferating mouse myoblasts but was undetectable in differentiated myotubes as well as adult mouse skeletal muscles (54). Similarly, HsMCAK was found to decline to undetectable levels when proliferating monoblastoid cells were differentiated into monocytes (52). These data suggest that both mammalian KIF2s and MCAKs might be present at higher levels in proliferating tissues and at lower levels in differentiated tissues. In addition to the tissues above, mammalian MCAKs were also found to be expressed in: thymus, small intestine, colon, pancreas, ovary, testis, placenta, and mammary tissues as well as in tumor cell lines (22,23,52). HsMCAK (KNSL6) expression in colon cancer tissues and testis is at least 30–40 times the level detected in other tissues, which indicates a possible role of this kinesin in tumorgenesis and spermatogenesis (22). Testis-specific MCAK isoforms have been identified in humans and rats (55,56). Expression of the rat MCAK testis-specific isoform, KRP2, is restricted to a meiotically active region of the seminiferous epithelia in testis (56). While further experiments are needed to determine whether the testis-specific MCAK is present only in meiotic cells, the data above suggest that Kin Is may have important meiotic function(s) in addition to their role in mitosis.

It is unclear why cells require two highly similar depolymerizing kinesins: MCAKs and KIF2s. So far, both MCAK-like and KIF2-like proteins have been found in humans, rats, mice and frogs. MCAK is seen at kinetochores, centrosomes and midbodies in addition to a soluble pool present in nucleoplasm and cytoplasm. KIF2s appear not to localize to either kinetochores or centrosomes but are present in the cytoplasm (53,57). It is possible that KIF2 might primarily influence the dynamics of cytoplasmic MT ends, while MCAK influences both cytoplasmic MT ends and those that are embedded in centrosomes and kinetochores. MCAK and KIF2 tissue expression profiles largely overlap, but KIF2s are expressed at a higher level in developing brain tissues, where they are enriched in growth cones (49,57), while MCAKs are up-regulated in testis and proliferative cancer cells (22). It is not known whether MCAKs and KIF2s undergo cell-cycle specific regulation so that one is more active during mitosis while another is active during interphase.

Kin I Kinesins Regulate MT Dynamics Throughout the Cell Cycle

Kin Is play a major role in regulating MT dynamics *in vivo* [summarized in Table 2; reviewed in (58)]. Overexpression of CgMCAK in mammalian cells resulted in depolymerization of cytoplasmic and spindle MTs (24,48). *Xenopus* egg extracts depleted of XKCM1, a *Xenopus* Kin I, showed abnormally long MTs and 4-fold reduction in MT catastrophe frequency (59). In addition, a recent study demonstrated that physiological MT dynamics can be reconstituted by combination of purified MTs, XKCM1 and a MT-end stabilizing protein, XMAP215 (60). Maney et al. found that CgMCAK influences MT dynamics at mitotic kinetochores (48). CgMCAK localizes to the kinetochores in early prophase and remains there throughout mitosis. Depletion of CgMCAK from kinetochores either by antisense RNA or overexpression of a dominate-negative motorless mutant resulted in a lagging chromosome phenotype, which is likely to be the result of a deficiency in MT depolymerization activity at the lagging kinetochores during

Table 2: Diverse functions of Kin I kinesins. Representative members of Kin I subfamily are shown. The first two letters of the motor name refer to the species name: Cg, *Cricetulus griseus*; Xl, *Xenopus laevus*; Rn, *Rattus norvegicus*; Ce, *Caenorhabditis elegans*; Cf, *Cylindrotheca fusiformis*

Kin I kinesins	Subcellular localization	Mutant (deficient) phenotype	Functions
CgMCAK	spindle poles, kinetochores and mid-bodies (24,48)	lagging chromosomes during anaphase A in CHO cells (24,48)	regulation of MT dynamics throughout the cell cycle and depolymerization of kinetochore MTs during anaphase A in CHO cells(24,48)
XlKCM1	spindle poles and kinetochores (59)	abnormally long spindle MTs and metaphase chromosome misalignment in *Xenopus* egg extracts (59,61)	regulation of MT dynamics throughout the cell cycle and promoting metaphase chromosome alignment in *Xenopus* egg extracts (59,61,81)
CeMCAK	spindle poles and kinetochores (82)	loss of the spindle midzone during anaphase B in *C. elegans* embryos (83)	spindle midzone maintenance during anaphase B (83)
CfDSK1	spindles and spindle midzone (84)	inhibition of spindle elongation during anaphase B in the diatom *C. fusiformis* (84)	promoting spindle elongation during anaphase B (84)
RnKIF2	enriched in PC12 neurite growth cones and on nonsynaptic vesicle subtype(57)	retraction of NGF-induced PC12 neurites (57)	promoting growth cone extension (57)

anaphase (48). Displacement of XKCM1 from kinetochores by a dominant-negative mutant caused metaphase chromosome misalignment in the *Xenopus* egg extracts (61). In addition to kinetochore localization, CgMCAK also localizes to centrosomes and mid-bodies in cells (48). This localization pattern suggests that MCAK could also modulate MT dynamics at these locations as well. CgMCAK's centrosomal localization throughout the cell cycle suggests that it might be a candidate for a MT flux motor.

The importance of dynamic microtubules for proper spindle functioning is well established [reviewed in (31)]. However, the regulation of microtubule dynamics is likely to be essential for other motile processes such as growth cone extension. Exploration of the cytoplasm by dynamic microtubules followed by selective stabilization is an essential component of the motility mechanism of advancing growth cones [reviewed in (62)]. Drugs that inhibit MT dynamics have been shown to reduce neurite extension (63). Kin I kinesins would be hypothesized to increase microtubule dynamics in growing neurites. In agreement with this hypothesis, RnKIF2 appears to be important for PC12 neurite extension induced by NGF treatment (57). NGF significantly up-regulates the expression of RnKIF2 in PC12 cells where RnKIF2 becomes enriched in growth cones of NGF-induced neurites. Moreover, RnKIF2 antisense oligonucleotides caused neurite retractions in NGF-treated PC12 cells (57). Interestingly, another MT destabilizing stathmin-like protein is also up-regulated in PC12 cells treated with NGF (64). Similarly to the RnKIF2 study, inhibition of stathmin expression by antisense oligonucleotides blocked the NGF-induced neurite outgrowth in PC12 cells (65). These data suggest that proteins that influence microtubule dynamics such as KIF2 and stathmin are important for neurite extension.

Kin I and Kip 3 Kinesins Constitute Closely Related but Different Subfamilies

The *Schizosaccharomyces pombe* SpKlp5/6 kinesins were recently found to have similar properties to the Kin I subfamily kinesins (66–69). However, differences in primary sequence structure, activity and function have prompted researchers to give them their own closely related but distinct subfamily: the Kip 3 subfamily (70,71). SpKlp5/6 were found to localize to kinetochores and also have some features in common with CENP-E, a plus-end directed kinesin (66). Depletion of the Kip 3 subfamily kinesins from yeast cells showed MT-depolymerization deficient phenotypes (67–69,71,72). Kip 3 kinesins have N-terminally located motor and C-terminally located neck domains. The Kip 3 related kinesin from *Drosophila*, DmKlp67A, was shown to move MTs in the plus-end direction in an *in vitro* motility assay (73). Mutations in the same kinesin, DmKlp67A, were reported to produce abnormally elongated spindles, a phenotype which is consistent with the loss of MT destabilization activity (74). Therefore, it is possible that members of the Kip 3 subfamily of kinesins are capable of both motile and depolymerizing activities, as is Kar3. The weak structural and sequence correspondence between the Kin I and Kip 3 kinesin subfamilies suggests that the mechanism of MT destabilization by Kip 3 kinesins may be different from that of Kin Is. Detailed

analysis of the MT destabilizing activities of Kip 3 kinesins *in vitro* are required to elucidate the molecular mechanism of Kip 3-mediated MT depolymerization.

Conclusions

While significant progress has been made recently in elucidating Kin C and Kin I kinesin mechanism and functions in cells, many important questions remain to be answered: What are the structural differences between kinesins that translocate along MTs and kinesins that depolymerize them? What are the differences and similarities between molecular mechanisms of MT depolymerizing activities of Kar3, Kin I and Kip 3 kinesins? What are the functional differences between MCAK-like and KIF2-like kinesins? How are Kin Is regulated in cells? The answers to these questions will help us understand how the unconventional kinesins were specialized during evolution for their fundamental cellular roles.

Acknowledgments

We thank Jeremy Cooper, Marla Feinstein, Ayana Moore, Kathleen Rankin and Mike Wagenbach for valuable comments on the manuscript. L. Wordeman is supported by a National Institutes of Health grant (GM53654A) and a Department of Defense grant (DAMD17-01-1-0450).

Online supplemental material shows a protein sequence alignment of the Kin I subfamily kinesins.

References

1. Kull FJ, Sablin EP, Lau R, Fletterick RJ, Vale RD. Crystal structure of the kinesin motor domain reveals a structural similarity to myosin. Nature 1996;380:550–555.
2. Sablin EP, Kull FJ, Cooke R, Vale RD, Fletterick RJ. Crystal structure of the motor domain of the kinesin-related motor ncd. Nature 1996;380:555–559.
3. Vale RD, Reese TS, Sheetz MP. Identification of a novel force-generating protein, kinesin, involved in microtubule-based motility. Cell 1985;42: 39–50.
4. Hunter AW, Caplow M, Coy DL, Hancock WO, Diez S, Wordeman L, Howard J. The kinesin-related protein MCAK is a microtubule depolymerase that forms an ATP-hydrolyzing complex at microtubule ends. Mol Cell 2003;11:445–457.
5. Desai A, Verma S, Mitchison TJ, Walczak CE. Kin I kinesins are microtubule-destabilizing enzymes. Cell 1999;96:69–78.
6. Higuchi H, Endow SA. Directionality and processivity of molecular motors. Curr Opin Cell Biol 2002;14:50–57.
7. Endow SA. Determinants of molecular motor directionality. Nat Cell Biol 1999;1:E163–E167.
8. Vale RD, Fletterick RJ. The design plan of kinesin motors. Annu Rev Cell Dev Biol 1997;13:745–777.
9. Vale RD, Milligan RA. The way things move. looking under the hood of molecular motor proteins. Science 2000;288:88–95.
10. Kamal A, Goldstein LS. Principles of cargo attachment to cytoplasmic motor proteins. Curr Opin Cell Biol 2002;14:63–68.
11. Hackney DD, Stock MF. Kinesin's IAK tail domain inhibits initial microtubule-stimulated ADP release. Nat Cell Biol 2000;2:257–260.
12. Karabay A, Walker RA. Identification of microtubule binding sites in the Ncd tail domain. Biochemistry 1999;38:1838–1849.
13. Wordeman L, Wagenbach M, Maney T. Mutations in the ATP-binding domain affect the subcellular distribution of mitotic centromere-associated kinesin (MCAK). Cell Biol Int 1999;23:275–286.
14. Schief WR, Howard J. Conformational changes during kinesin motility. Curr Opin Cell Biol 2001;13:19–28.
15. Endow SA, Barker DS. Processive and nonprocessive models of kinesin movement. Annu Rev Physiol 2003;65:161–175.
16. Goldstein LS, Philp AV. The road less traveled. emerging principles of kinesin motor utilization. Annu Rev Cell Dev Biol 1999;15:141–183.
17. Mandelkow E, Mandelkow EM. Kinesin motors and disease. Trends Cell Biol 2002;12:585–591.
18. Hatsumi M, Endow SA. Mutants of the microtubule motor protein, nonclaret disjunctional, affect spindle structure and chromosome movement in meiosis and mitosis. J Cell Sci 1992;101:547–559.
19. Walczak CE, Verma S, Mitchison TJ. XCTK2: a kinesin-related protein that promotes mitotic spindle assembly in *Xenopus laevis* egg extracts. J Cell Biol 1997;136:859–870.
20. Mountain V, Simerly C, Howard L, Ando A, Schatten G, Compton DA. The kinesin-related protein, HSET, opposes the activity of Eg5 and cross-links microtubules in the mammalian mitotic spindle. J Cell Biol 1999;147:351–366.
21. Hassold T, Hunt P. To err (meiotically) is human: the genesis of human aneuploidy. Nat Rev Genet 2001;2:280–291.
22. Scanlan MJ, Welt S, Gordon CM, Chen YT, Gure AO, Stockert E, Jungbluth AA, Ritter G, Jager D, Jager E, Knuth A, Old LJ. Cancer-related serological recognition of human colon cancer: identification of potential diagnostic and immunotherapeutic targets. Cancer Res 2002;62:4041–4047.
23. Perou CM, Jeffrey SS, van de Rijn M, Rees CA, Eisen MB, Ross DT, Pergamenschikov A, Williams CF, Zhu SX, Lee JC, Lashkari D, Shalon D, Brown PO, Botstein D. Distinctive gene expression patterns in human mammary epithelial cells and breast cancers. Proc Natl Acad Sci USA 1999;96:9212–9217.
24. Maney T, Wagenbach M, Wordeman L. Molecular dissection of the microtubule depolymerizing activity of mitotic centromere-associated kinesin. J Biol Chem 2001;276:34753–34758.
25. Nishio K, Nakamura T, Koh Y, Kanzawa F, Tamura T, Saijo N. Oncoprotein 18 overexpression increases the sensitivity to vindesine in the human lung carcinoma cells. Cancer 2001;91:1494–1499.
26. Rowinsky EK. The development and clinical utility of the taxane class of antimicrotubule chemotherapy agents. Annu Rev Med 1997;48:353–374.
27. Matthies HJ, McDonald HB, Goldstein LS, Theurkauf WE. Anastral meiotic spindle morphogenesis: role of the non-claret disjunctional kinesin-like protein. J Cell Biol 1996;134:455–464.
28. Sharp DJ, Brown HM, Kwon M, Rogers GC, Holland G, Scholey JM. Functional coordination of three mitotic motors in *Drosophila* embryos. Mol Biol Cell 2000;11:241–253.
29. Pidoux AL, LeDizet M, Cande WZ. Fission yeast pkl1 is a kinesin-related protein involved in mitotic spindle function. Mol Biol Cell 1996;7:1639–1655.
30. Saunders WS, Hoyt MA. Kinesin-related proteins required for structural integrity of the mitotic spindle. Cell 1992;70:451–458.
31. Wittmann T, Hyman A, Desai A. The spindle: a dynamic assembly of microtubules and motors. Nat Cell Biol 2001;3:E28–E34.
32. Endow SA, Kang SJ, Satterwhite LL, Rose MD, Skeen VP, Salmon ED. Yeast Kar3 is a minus-end microtubule motor protein that destabilizes microtubules preferentially at the minus ends. EMBO J 1994;13: 2708–2713.
33. Prigozhina NL, Walker RA, Oakley CE, Oakley BR. Gamma-tubulin and the C-terminal motor domain kinesin-like protein, KLPA, function in the establishment of spindle bipolarity in *Aspergillus nidulans*. Mol Biol Cell 2001;12:3161–3174.

34. Walker RA, Salmon ED, Endow SA. The *Drosophila* claret segregation protein is a minus-end directed motor molecule. Nature 1990;347: 780–782.
35. Meluh PB, Rose MD. KAR3, a kinesin-related gene required for yeast nuclear fusion. Cell 1990;60:1029–1041.
36. Gulick AM, Song H, Endow SA, Rayment I. X-ray crystal structure of the yeast Kar3 motor domain complexed with Mg.ADP 2.3 A resolution. Biochemistry 1998;37:1769– 76.
37. Keskin O, Durell SR, Bahar I, Jernigan RL, Covell DG. Relating molecular flexibility to function: a case study of tubulin. Biophys J 2002;83: 663–680.
38. Sosa H, Dias DP, Hoenger A, Whittaker M, Wilson-Kubalek E, Sablin E, Fletterick RJ, Vale RD, Milligan RA. A model for the microtubule-Ncd motor protein complex obtained by cryo-electron microscopy and image analysis. Cell 1997;90:217–224.
39. Saunders W, Hornack D, Lengyel V, Deng C. The *Saccharomyces cerevisiae* kinesin-related motor Kar3p acts at preanaphase spindle poles to limit the number and length of cytoplasmic microtubules. J Cell Biol 1997;137:417–431.
40. Troxell CL, Sweezy MA, West RR, Reed KD, Carson BD, Pidoux AL, Cande WZ, McIntosh JR. pkl1 (+) and klp2 (+): two kinesins of the Kar3 subfamily in fission yeast perform different functions in both mitosis and meiosis. Mol Biol Cell 2001;12:3476–3488.
41. Barrett JG, Manning BD, Snyder M. The Kar3p kinesin-related protein forms a novel heterodimeric structure with its associated protein Cik1p. Mol Biol Cell 2000;11:2373–2385.
42. Manning BD, Barrett JG, Wallace JA, Granok H, Snyder M. Differential regulation of the Kar3p kinesin-related protein by two associated proteins, Cik1p and Vik1p. J Cell Biol 1999;144:1219–1233.
43. Moores CAYuM, Guo J, Beraud C, Sakowicz R, Milligan RA. A mechanism for microtubule depolymerization by Kinl kinesins. Mol Cell 2002;9:903–909.
44. Niederstrasser H, Salehi-Had H, Gan EC, Walczak C, Nogales E. XKCM1 acts on a single protofilament and requires the C terminus of tubulin. J Mol Biol 2002;316:817–828.
45. Muller-Reichert T, Chretien D, Severin F, Hyman AA. Structural changes at microtubule ends accompanying GTP hydrolysis: information from a slowly hydrolyzable analogue of GTP, guanylyl (alpha,beta) methylenediphosphonate. Proc Natl Acad Sci USA 1998;95: 3661–3666.
46. Ovechkina Y, Wagenbach M, Wordeman L. K-loop insertion restores microtubule depolymerizing activity of a 'neckless' MCAK mutant. J Cell Biol 2002;159:557–562.
47. Noda Y, Sato-Yoshitake R, Kondo S, Nangaku M, Hirokawa N. KIF2 is a new microtubule-based anterograde motor that transports membranous organelles distinct from those carried by kinesin heavy chain or KIF3A/B. J Cell Biol 1995;129:157–167.
48. Maney T, Hunter AW, Wagenbach M, Wordeman L. Mitotic centromere-associated kinesin is important for anaphase chromosome segregation. J Cell Biol 1998;142:787–801.
49. Aizawa H, Sekine Y, Takemura R, Zhang Z, Nangaku M, Hirokawa N. Kinesin family in murine central nervous system. J Cell Biol 1992;119:1287–1296.
50. Berger B, Wilson DB, Wolf E, Tonchev T, Milla M, Kim PS. Predicting coiled coils by use of pairwise residue correlations. Proc Natl Acad Sci USA 1995;92:8259–8263.
51. Debernardi S, Fontanella E, De Gregorio L, Pierotti MA, Delia D. Identification of a novel human kinesin-related gene (HK2) by the cDNA differential display technique. Genomics 1997;42:67–73.
52. Kim IG, June DY, Sohn U, Kim YH. Cloning and expression of human mitotic centromere-associated kinesin gene. Biochim Biophys Acta 1997;1359:181–186.
53. Santama N, Krijnse-Locker J, Griffiths G, Noda Y, Hirokawa N, Dotti CG. KIF2beta, a new kinesin superfamily protein in non-neuronal cells, is associated with lysosomes and may be implicated in their centrifugal translocation. EMBO J 1998;17:5855–5867.
54. Ginkel LM, Wordeman L. Expression and partial characterization of kinesin-related proteins in differentiating and adult skeletal muscle. Mol Biol Cell 2000;11:4143–4158.
55. Cheng LJ, Zhou ZM, Li JM, Zhu H, Zhou YD, Wang LR, Lin M, Sha JH. Expression of a novel HsMCAK mRNA splice variant, tsMCAK gene, in human testis. Life Sci 2002;71:2741–2757.
56. Sperry AO, Zhao LP. Kinesin-related proteins in the mammalian testes: candidate motors for meiosis and morphogenesis. Mol Biol Cell 1996;7:289–305.
57. Morfini G, Quiroga S, Rosa A, Kosik K, Caceres A. Suppression of KIF2 in PC12 cells alters the distribution of a growth cone nonsynaptic membrane receptor and inhibits neurite extension. J Cell Biol 1997;138:657–669.
58. Cassimeris L. Accessory protein regulation of microtubule dynamics throughout the cell cycle. Curr Opin Cell Biol 1999;11:134–141.
59. Walczak CE, Mitchison TJ, Desai A. XKCM1: a Xenopus kinesin-related protein that regulates microtubule dynamics during mitotic spindle assembly. Cell 1996;84:37–47.
60. Kinoshita K, Arnal I, Desai A, Drechsel DN, Hyman AA. Reconstitution of physiological microtubule dynamics using purified components. Science 2001;294:1340–1343.
61. Walczak CE, Gan EC, Desai A, Mitchison TJ, Kline-Smith SL. The microtubule-destabilizing kinesin XKCM1 is required for chromosome positioning during spindle assembly. Curr Biol 2002;12:1885–1889.
62. Suter DM, Forscher P. Substrate-cytoskeletal coupling as a mechanism for the regulation of growth cone motility and guidance. J Neurobiol 2000;44:97–113.
63. Tanaka E, Ho T, Kirschner MW. The role of microtubule dynamics in growth cone motility and axonal growth. J Cell Biol 1995;128:139–155.
64. Stein R, Orit S, Anderson DJ. The induction of a neural-specific gene, SCG10, by nerve growth factor in PC12 cells is transcriptional, protein synthesis dependent, and glucocorticoid inhibitable. Dev Biol 1988;127:316–325.
65. Di Paolo G, Pellier V, Catsicas M, Antonsson B, Catsicas S, Grenningloh G. The phosphoprotein stathmin is essential for nerve growth factor-stimulated differentiation. J Cell Biol 1996;133:1383–1390.
66. West RR, Malmstrom T, McIntosh JR. Kinesins klp5 (+) and klp6 (+) are required for normal chromosome movement in mitosis. J Cell Sci 2002;115:931–940.
67. West RR, Malmstrom T, Troxell CL, McIntosh JR. Two related kinesins, klp5+ and klp6+, foster microtubule disassembly and are required for meiosis in fission yeast. Mol Biol Cell 2001;12:3919–3932.
68. Garcia MA, Koonrugsa N, Toda T. Spindle-kinetochore attachment requires the combined action of Kin I-like Klp5/6 and Alp14/Dis1-MAPs in fission yeast. EMBO J 2002;21:6015–6024.
69. Garcia MA, Koonrugsa N, Toda T. Two kinesin-like Kin I family proteins in fission yeast regulate the establishment of metaphase and the onset of anaphase A. Curr Biol 2002;12:610–621.
70. Lawrence CJ, Malmberg RL, Muszynski MG, Dawe RK. Maximum likelihood methods reveal conservation of function among closely related kinesin families. J Mol Evol 2002;54:42–53.
71. Severin F, Habermann B, Huffaker T, Hyman T. Stu2 promotes mitotic spindle elongation in anaphase. J Cell Biol 2001;153 (2):435–442.
72. Straight AF, Sedat JW, Murray AW. Time-lapse microscopy reveals unique roles for kinesins during anaphase in budding yeast. J Cell Biol 1998;143:687–694.
73. Pereira AJ, Dalby B, Stewart RJ, Doxsey SJ, Goldstein LS. Mitochondrial association of a plus end-directed microtubule motor expressed during mitosis in *Drosophila*. J Cell Biol 1997;136:1081–1090.
74. Gandhi R, Bonaccorsi S, Wentworth DB, Gatti M, Pereira AJ. The KLP67A astral microtubule motor is required for proper spindle assembly during mitosis and male meiosis. Mol Biol Cell 2002;13 S(1815):322a.

75. Bascom-Slack CA, Dawson DS. The yeast motor protein, Kar3p, is essential for meiosis I. J Cell Biol 1997;139:459–467.
76. Cottingham FR, Gheber L, Miller DL, Hoyt MA. Novel roles for *Saccharomyces cerevisiae* mitotic spindle motors. J Cell Biol 1999;147: 335–350.
77. Hanlon DW, Yang Z, Goldstein LS. Characterization of KIFC2, a neuronal kinesin superfamily member in mouse. Neuron 1997;18: 439–451.
78. Yang Z, Roberts EA, Goldstein LS. Functional analysis of mouse C-terminal kinesin motor KifC2. Mol Cell Biol 2001;21:2463–2466.
79. Xu Y, Takeda S, Nakata T, Noda Y, Tanaka Y, Hirokawa N. Role of KIFC3 motor protein in Golgi positioning and integration. J Cell Biol 2002;158:293–303.
80. Noda Y, Okada Y, Saito N, Setou M, Xu Y, Zhang Z, Hirokawa N. KIFC3, a microtubule minus end-directed motor for the apical transport of annexin XIIIb-associated Triton-insoluble membranes. J Cell Biol 2001;155:77–88.
81. Kline-Smith SL, Walczak CE. The microtubule-destabilizing kinesin XKCM1 regulates microtubule dynamic instability in cells. Mol Biol Cell 2002;13:2718–2731.
82. Oegema K, Desai A, Rybina S, Kirkham M, Hyman AA. Functional analysis of kinetochore assembly in *Caenorhabditis elegans*. J Cell Biol 2001;153:1209–1226.
83. Grill SW, Gonczy P, Stelzer EH, Hyman AA. Polarity controls forces governing asymmetric spindle positioning in the *Caenorhabditis elegans* embryo. Nature 2001;409:630–633.
84. Wein H, Foss M, Brady B, Cande WZ. DSK1, a novel kinesin-related protein from the diatom *Cylindrotheca fusiformis* that is involved in anaphase spindle elongation. J Cell Biol 1996;133:595–604.

SCIENCE IN MEDICINE

The School of Medicine Presents a
Science in Medicine Lecturer

Linda Wordeman, Ph.D.

Associate Professor
Department of Physiology and Biophysics
School of Medicine
University of Washington

"Order from Chaos: Microtubule Dynamics and Chromosome Segregation"

Dr. Linda Wordeman a native of San Luis Obispo, California graduated with High Honors in Molecular Biology from the University of California at Berkeley. She completed her Ph.D. work at UC Berkeley, studying cell division in marine diatoms.

Dr. Wordeman joined the UW Department of Physiology and Biophysics in 1994 as an Assistant Professor and became Associate professor in 1999. She was the recipient of a Shannon award in 1995 and a Congressionally Directed Medical Research Program (CDMRP) Breast Cancer Idea award in 2000.

This lecture is open to all faculty, staff and students. For more information contact Vee White at veewhite@u.washington.edu

Thursday, February 6, 2003, 12:00 Noon to 1:00 p.m.
Hogness Auditorium, A-420, Health Science Building

MCAK's C-terminus Inhibits Its Lattice Stimulated ATPase Activity

A. Moore and Linda Wordeman*
University of Washington School of Medicine, Department of Physiology and Biophysics, Seattle, WA

*Corresponding author:
Dr. Linda Wordeman
Department of Physiology and Biophysics
1959 NE Pacific St.
Box 357290
Seattle WA 98195
(206) 543-4135 (office)
(206) 685-0619 (fax)
worde@u.washington.edu

Condensed title: MCAK's Cterm Inhibits Lattice ATPase Activity

Key words: MCAK, XKCM1, Kin I, kinesin, mitosis, microtubules, depolymerization

Word Count: 46,859

Abstract:

Mitotic Centromere Associated Kinesin (MCAK) is a microtubule (MT) destabilizing molecular motor. Here we show that the final eight amino acids of MCAK's carboxyl-terminus (C-term) contribute to inhibition of MT depolymerization. Overexpression of a C-term truncation of MCAK (MCAK-Q710) results in enhanced MT depolymerization in paclitaxel treated cells when compared to overexpression of full-length MCAK (wt-MCAK). Furthermore, *in vitro* depolymerization of paclitaxel-stabilized MTs was increased with purified MCAK-Q710 when compared to wt-MCAK. *In vitro* ATPase assays revealed that MCAK-Q710 has a significantly higher rate of ATP hydrolysis in the presence of paclitaxel-stabilized MTs as compared to wt-MCAK. This ATPase difference was most pronounced with longer MTs and by extension, with prolonged exposure to the MT lattice. Interestingly, wt-MCAK and MCAK-Q710 display comparable ATP hydrolysis in the presence of free tubulin. These results suggest that MCAK's C-term may selectively inhibit ATPase activity along the MT lattice resulting in limited interactions with the lattice, thereby limiting end targeting and hence, MT depolymerization.

Introduction:

The kinesin superfamily consists of motor proteins that convert chemical energy, through ATP hydrolysis, into physical work (Brady, 1985; Goldstein and Philp, 1999; Vale and Fletterick, 1997; Vale et al., 1985). These motors are involved in a wide range of cellular functions such as vesicle transport along MT tracks, signal transduction, and MT polymer dynamics (Goldstein and Philp, 1999; Vale and Fletterick, 1997; Vale and Milligan, 2000). Mitotic Centromere Associated Kinesin (MCAK) belongs to the Kin I (I stands for internal, referring to the location of the motor domain with respect to the primary amino acid sequence) subfamily of kinesin-related proteins and shares a highly conserved ATP-hydrolyzing motor (head) domain with other members of this subfamily (Vale and Fletterick, 1997; Wordeman and Mitchison, 1995). Unlike many other kinesins, which transport cargo along the surface of MTs, MCAK and its homologues depolymerize them (Desai et al., 1999; Maney et al., 2001; Walczak et al., 1996). The activity of MCAK and its homologues is critical for cellular functions such as mitotic spindle formation in Xenopus egg extracts (Tournebize et al., 2000; Walczak et al., 1996), and proper separation of sister chromatids during anaphase in mammalian cells (Maney et al., 1998). Overexpression of MCAK causes severe loss of MTs in interphase and mitotic cells (Maney et al., 1998; Maney et al., 2001) while depletion of XKCM1 (the Xenopus homologue of MCAK) results in an increased level of MT polymer (Walczak et al., 1996). MCAK's contribution to the dynamic behavior of MTs makes its regulation an important factor in maintaining proper MT functions and may provide insight into tumorgenesis (Perou et al., 1999) and some forms of cell cycle aberration (Zhai et al., 1996).

In the presence of ATP, purified MCAK and its homologues are very efficient MT depolymerizers. Fluorescence microscopy has shown that the Xenopus homologue, XKCM1, localizes preferentially to the ends of GMP-CPP (a slowly hydrolysable form of GTP) stabilized MTs (Desai et al., 1999). One current model suggests that MCAK associates loosely with the lattice of MTs, perhaps through electrostatic interactions, and then translocates to the MT ends (where depolymerization takes place) via one-

dimensional diffusion (Desai et al., 1999; Hunter et al., 2003; Ovechkina et al., 2002). Where and when, exactly, MCAK hydrolyzes ATP is still a matter of debate. XKCM1 has been shown to target MT ends in the presence of a non-hydrolysable form of ATP (AMP-PNP) (Desai et al., 1999). In addition, MT destabilization has been shown in the presence of AMP-PNP when high molar concentrations of Kin Is were present (Moores et al., 2002). However, it has been observed that Kin I kinesins stabilize protofilament peels and rings in the presences of AMP-PNP but without removing individual tubulin dimers from the protofilament (Desai et al., 1999; Moores et al., 2002; Niederstrasser et al., 2002). Thus, the MT destabilization observed in the presence of AMP-PNP, differs from that observed in the presence of ATP. This led Hunter et al. to propose that dissociation of the terminal tubulin dimer is triggered either by ATP hydrolysis or phosphate release. In addition, they propose that MCAK remains tethered to the end of the MT protofilament for a number of cycles of tubulin dissociation before it itself dissociates. In this way, MCAK would processively depolymerize MTs.

In contrast to MCAK, conventional kinesin uses ATP hydrolysis to translocate along the MT lattice. Electron microscopy and sedimentation analysis have revealed that conventional kinesin exists in two different conformations (Hackney and Stock, 2000). At physiological ionic concentrations, the protein is folded into a compact conformation. This folding is due to an interaction between the C-term and the head/neck region. In this state, ATP hydrolysis is inhibited, presumably due to interactions of domains in the tail and head. This idea is supported by the fact that a highly conserved C-term truncation of kinesin, which is unfolded, causes a loss of ATPase inhibition (Coy et al., 1999; Hackney and Stock, 2000). Similar to conventional kinesin, we show here that when the C-term of MCAK is truncated, ATPase activity is increased. This increased activity directly correlates with the presence of intact MT polymer in solution. Furthermore, the MT depolymerization rate is increased both *in vivo* and *in vitro*. We also show, using MT pelleting assays, that the C-term truncation of MCAK (MCAK-Q710) may bind more tightly with MTs as compared to the full-length protein (wt-MCAK). These results are comparable to kinesin in that the intact protein has a weaker affinity for MTs (Hackney, 1988)). We propose that wt-MCAK may act in a manner analogous to conventional

kinesin in that the C-term may act as a selective inhibitor of ATP hydrolysis by influencing the protein's interaction with the MT lattice. This inhibition may limit MCAK's ability to diffuse along the MT lattice and therefore hamper end targeting and MT depolymerization. We propose that in the absence of the C-term, MCAK may be partially processive whereas the intact protein relies primarily on diffusion to reach the MT ends. The partial processivity of the truncated protein may allow it to achieve definitive steps toward the MT ends, therefore increasing the probability of end targeting and hence, MT depolymerization.

Materials and Methods

Constructs

MCAK constructs were made by ligating MCAK PCR products (from pOPRSVICAT-GFP-MCAK (Maney et al., 1998)) with TOPO NT-GFP fragments (Invitrogen Corp., Carlsbad, CA). Gene expression was under the control of a CMV promoter. Deletions were confirmed by DNA sequencing.

Cell culture, transfections and immunofluorescence

CHO cells were cultured in αMEM with 10% fetal bovine serum, and 1X penicillin-streptomycin-glutamine (GibcoBrl, Grand Island, NY). One day prior to fixation, cells were plated onto 12mm glass coverslips at about 50% confluency. Transfections were performed with Lipofectamine Reagent (Invitrogen, Carlsbad, CA). For transfected cells cultured in the presence of paclitaxel, 15μM paclitaxel was added 2 hours into the transfection. Culture media with 10μM paclitaxel was added back to cells after a 4-hour transfection period and was maintained until fixation as described (Maney et al., 2001). Cells were cultured for 25 hours after transfection and fixed with 1% paraformaldehyde in methanol (pre-cooled to -20 C) for 3 minutes. Cells were blocked for 20 minutes with 20% donkey serum in antibody dilution buffer (PBS plus 1% BSA, 0.02% NaAzide, 0.1% Triton X-100). Tubulin staining was done with mouse anti-tubulin DM1α (Sigma ImmunoChemicals, St. Louis, MO) at a 1:500 dilution for 1 hour and Texas Red anti-mouse (Jackson ImmunoResearch, Inc., West Grove, PA) at a 1:100 dilution for 1 hour. Cells were washed with PBS and mounted with Vectashield mounting media plus DAPI (Vector Laboratories, Inc., Burlingame, CA). Analysis was done with a Nikon FX-A microscope equipped with a 60X/1.4 NA Plan Apo oil objective. Digital images were acquired with a Sensys cooled CCD camera (Photometrics, Tucson, AZ) controlled by QED camera software (QED Imaging, Inc., Tucson, AZ).

Quantitation of microtubule depolymerization *in vivo*

Digital images of transfected cells were collected for GFP and MT fluorescence for the same exposure times, respectively. Images were saved as 8-bit TIFF files with a 256 gray

scale range. Calculations and quantification were performed using NIH Image 1.62 and Microsoft Excel. Interphase cells that were free of aggregates of overexpressed protein were chosen. Cytoplasmic GFP mean fluorescence intensities were measured for each cell and the cell-free mean fluorescence was subtracted for each image to correct for background fluorescence. 44 transfected cells were measured for each construct. To quantify MTs remaining in each cell, we determined a gray scale range within which fluorescent MT polymer fell. We counted the number of pixels in this range and divided it by the number of pixels in the entire cell. We compared the means of these ratios for each of our constructs. (See text.)

Expression and purification of recombinant MCAK

Baculovirus expression of recombinant 6x-histidine tagged wt-MCAK in Sf9 cells (Pharmingen, San Diego, CA) and its purification on a nickel-nitrilotriacetic (Ni-NTA) agarose columns (Qiagen Inc., Chatsworth, CA) were performed as previously described (Maney et al., 1998). MCAK-Q710 was constructed by ligating a PCR fragment containing the truncated C-term into pVL1393-MCAK digested with NotI and NcoI. Baculovirus purification was performed as previously described. Peak fractions in elution buffer (300 mM Imidazole, pH 7.0, 300mM KCl, 50μM $MgCl_2$, 10μM MgATP, 5mM βME, 20% glucose, 10% glycerol) were aliquoted and frozen in liquid nitrogen and stored at -70 C. The number of active nucleotide binding sites was measured radiometrically as previously described (Coy et al., 1999). Because MCAK is a dimer (Maney et al., 1998), the concentrations are always expressed as the number of active heads.

***In vitro* microtubule assembly**

Bovine brain tubulin was acquired from Cytoskeleton (Denver, CO). For *in vitro* pelleting assays, 2.2μM of tubulin was added to BRB80 (80mM Pipes, pH 6.8, 1mM EGTA, 1mM $MgCl_2$) with 6mM $MgCl_2$, 1.5mM GTP, and 1.4M DMSO and incubated for 30 minutes at 37 C. Following the incubation, MTs were diluted 1:20 in 37 C BRB80 plus 15μM paclitaxel. Microtubules were stable for one week at room temperature. Variable MT lengths were achieved by passing MTs through a 30-gauge

syringe of either 0.5 inches in length (Becton Dickinson, Franklin Lakes, NJ) or 2.0 inches in length (Hamilton Co., Reno NV). Resulting lengths were determined via immunofluorescent microscopy. For ATPase assays, 11μM of tubulin was added to BRB80 with 8mM $MgCl_2$, 2mM GTP and 1.9M DMSO, and grown at 37 C as before. MTs were then diluted with BRB80 plus paclitaxel for a final paclitaxel concentration of 7.5μM.

***In vitro* microtubule depolymerization assays**

Elution buffer containing 50nM of active motor protein was mixed with 0.8mM DTT, 1.2mM MgATP, 75mM KCl and 2.2μM paclitaxel stabilized MT polymer. Reactions were incubated at room temperature for 16 minutes and centrifuged at 30 psi for 10 minutes. Supernatants and pellets were assayed for the presence of tubulin and motor on Coomassie stained SDS-polyacrylamide gels (Invitrogen, Carlsbad, CA). Bands were quantified using NIH Image 1.62. The extent of depolymerization with the 2 constructs was compared by comparing the total amount of tubulin in the supernatant minus the supernatant of a no-motor control.

ATPase assays

Assays were performed as previously described (Hunter et al., 2003). Briefly, phosphate release was determined radiometrically. 5μl of reaction mix (BRB80 with 250μM [γ-^{32}P]ATP (NEN Research Products, Boston, MA), 75mM KCl, 1mM DTT, 200μg/ml BSA, 250μM MgATP, 50nM active motor heads, 11μM tubulin (unpolymerized or MT polymer) was quenched with 500μl cold solution containing 1M hydrochloric acid, 4% perchloric acid, 180μM P_i, and 10mM ammonium molybdate. The phosphate concentration in the quenched reactions was determined by adding 1ml organic solvent (cyclohexane, isobutyl alcohol, acetone, quench solution, mixed at a ratio of 50:50:10:1), vortexing for 50 seconds, then allowing the phases to separate for approximately 10 minutes on ice. After phase separation was complete, 63% of the organic phase containing radiolabeled P_i (complexed with molybdate) was recovered, mixed with 3ml scintillation fluid (BioSafe II, Research Products International Corp., Mount Prospect,

IL), and read in a Beckman scintillation counter. Regression analysis and curves were generated using MATLAB (The MathWorks Inc.) and Microsoft Excel.

Results

Carboxyl terminal truncations of MCAK exhibit increased microtubule depolymerization *in vivo*

Chinese Hamster Ovary (CHO) cells transfected with full-length MCAK (wt-MCAK) display a complete loss of MT polymer by 25 hours post-transfection. Only a diffuse background of tubulin staining is discernable (fig. 1a, 1b). However, when wt-MCAK transfected cells are cultured for the same time duration in the presence of 15μm paclitaxel, they exhibit only a partial loss of MT polymer. The remaining MTs appear to be organized into a few, relatively long, bundles (fig. 1c, 1d) as compared to the abundant MT bundles visible in untransfected cells in the same field. Although wt-MCAK is able to depolymerize these bundled paclitaxel-MTs, complete MT depolymerization is not achieved within 25 hours. Partial abrogation of MCAK activity with paclitaxel allowed us to differentiate between MCAK constructs with slightly dissimilar rates of MT depolymerization.

Maney et al. (Maney et al., 2001) observed that wt-MCAK exhibited slightly lower MT depolymerization activity than a construct of MCAK missing the entire C-term (the region immediately following the motor domain). In order to establish which regions within the C-term inhibit MT depolymerization activity, we prepared successively smaller C-term deletions of MCAK and transfected these constructs into CHO cells cultured in the presence of 15μM paclitaxel (fig. 2a). By inspection, cells transfected with C-term deletions between S583 and Q710 exhibited equally enhanced MT depolymerization when compared to wt-MCAK. The deletion ending at H715 appears to have exhibited partially restored inhibition of MT depolymerization (data not shown). The qualitative similarity in the extent of MT depolymerization between the serial C-term

Figure 1:

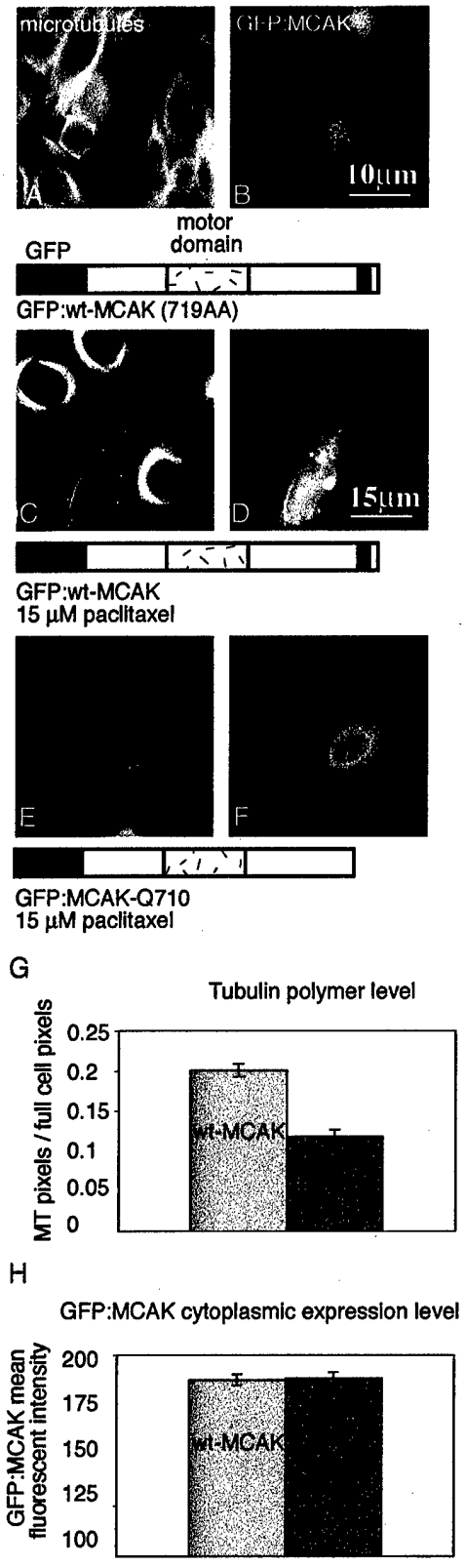

Figure 1: **C-term truncation increases MCAK's depolymerization activity.** Illustration of MT depolymerization in CHO cells transfected with GFP-tagged wt-MCAK and MCAK-Q710. The first column (A, C, D) shows MTs, antibody labeled against α-tubulin. The second column (B, D, F) shows fluorescent expression of GFP-tagged motor protein. (A) and (B) A cell transfected with GFP-tagged wt-MCAK. (C) and (D) A cell transfected with GFP-tagged wt-MCAK, cultured in the presence of 15μM paclitaxel. (E) and (F) A cell transfected with GFP-tagged MCAK-Q710 in the presence of 15μM paclitaxel. (G) is a comparison of the cytoplasmic GFP expression levels between GFP-tagged wt-MCAK and MCAK-Q710. Fluorescent intensity levels are measured over 256 gray scale values. (H) shows the difference in tubulin polymer levels for the same populations of cells.

deletions suggests that it is the extreme C-term that is responsible for auto-inhibition of MT depolymerization activity of full length MCAK.

Quantitation of *in vivo* microtubule depolymerization

To compare the relative extent of MT depolymerization between constructs *in vivo*, we devised a method whereby we could measure the amount of MT polymer in cells. GFP:MCAK fusion

constructs were transfected into CHO cells and cultured in the presence of 15μM paclitaxel for 25 hours. Cells were then fixed and labeled with a monoclonal antibody against α-tubulin. Digital images were acquired using a cooled CCD camera. Interphase cells chosen for quantitation displayed similar levels of cytoplasmic GFP expression. The average pixel intensity (mean gray value) of GFP in the cytoplasm was measured for both constructs (Fig. 1h) to control for variations in the extent of nuclear sequestration. Using a gray scale image of MTs, where MTs appear in intensity between white and light gray (grayscale value between 0 and 120) on a nearly black (grayscale value near 256) background (Fig. 1a,c and e), we recorded the pixels present within the grayscale range of 0 and 120. This number was divided by the total pixels in the cell (Fig. 1g). The resulting number gave us a normalized value representing the amount of tubulin polymer per cell.

The extreme C-term of MCAK is an inhibitor of microtubule depolymerization *in vivo*

Because of the apparent similarity of enhanced depolymerization between the C-term deletion constructs, MCAK-Q710 was chosen for quantitative comparison with wt-MCAK as it was the longest truncation construct with maximally enhanced MT depolymerization. Figure 1e shows the MTs of a cell transfected with MCAK-Q710, cultured in the presence of paclitaxel. MCAK-Q710 is able to depolymerize bundled MTs to a significantly greater extent than wt-MCAK. Note that there is only a speckling of MT polymer remaining in these cell, as compared to the longer intact bundles in cells transfected with wt-MCAK for the same amount of time.

Using the method described above, we measured the relative amount of tubulin polymer remaining in a population of transfected cells (Fig. 1g). wt-MCAK and MCAK-Q710 transfected cells exhibited a significant difference in the extent of polymer loss according to a paired t-Test with 95% confidence.

The C-term of MCAK contains a highly conserved KKR amino acid sequence (Fig. 2b, 2c). PSORT (Nakai and Kanehisa, 1992) predicts that this region is one of three potential nuclear localization sequences (NLS) found in the protein. To ensure that the difference in cytoplasmic MT depolymerization was not due to a difference in MCAK's cytoplasmic expression level resulting from differential sequestration via the NLS, we measure the relative levels of cytoplasmic expression for the same population of cells. We found that these two populations of cells exhibited statistically indistinguishable levels of protein expression (Fig. 1h). This suggests that given the same level of cytoplasmic expression, MCAK-Q710 serves as a more potent depolymerizer in comparison to wt-MCAK *in vivo*.

Figure 2:

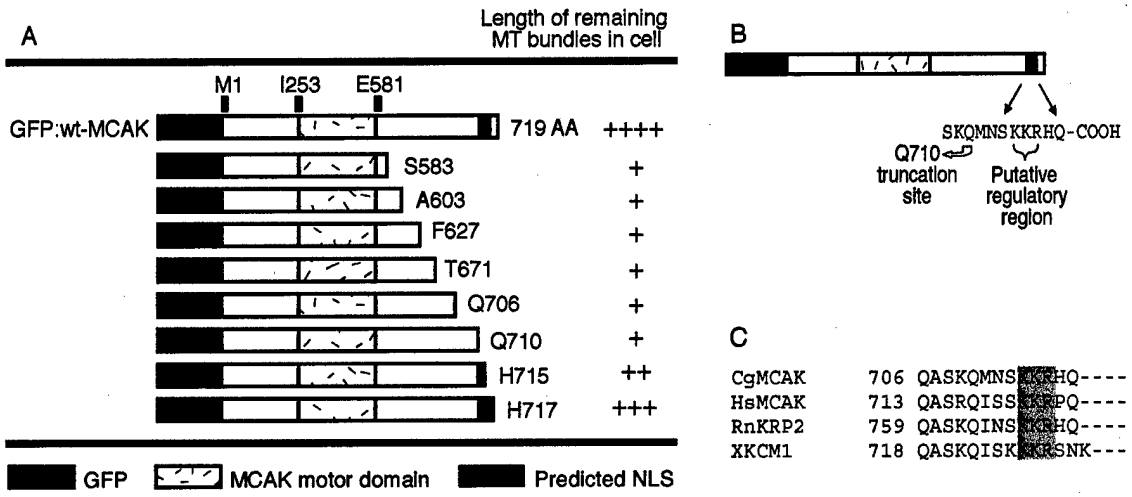

Figure 2: **Map of C-term truncations of MCAK.** C-term truncations of GFP-tagged MCAK are illustrated in conjunction with their amino acid truncation sites. Each construct was transiently transfected into CHO cells cultured in the presence of 15μM paclitaxel. Cells were fixed 16 hours post transfection and antibody labeled against α-tubulin. The extent of MT depolymerization was scored for each of the constructs. + represented the shortest MT bundles which were found in the transfectants exhibiting the highest depolymerization activity. ++++ represented the longest MT bundles, which corresponded to the lowest levels of MT depolymerization activity. (B) illustrates the region of the highly conserved KKR sequence relative to the MCAK-Q710 truncation site. (C) shows a sequence alignment of MCAK's C-term

from four different species: CgMCAK, *Cricetulus griseus,* (GenBank accession number: U11790); HsMCAK, *Homo sapiens* (U63743); *Rattus norvegicus*, (U44979); XKCMI, *Xenopus laevis* (U36485). The highly conserved KKR sequence is shaded in gray.

MT depolymerization *in vitro* is enhanced by C-term truncation of MCAK

To confirm that the difference in MT depolymerization seen *in vivo* was intrinsic to the motor and not the result of interactions with other cellular proteins, we performed a series of *in vitro* depolymerization assays. Both wt-MCAK and MCAK-Q710 were expressed and purified from baculovirus-infected SF9 cells. The purified motors were mixed with paclitaxel-stabilized microtubules (about 15μm in length, on average), and 1mM MgATP. This reaction was incubated for 16 minutes at room temperature and subsequently centrifuged to separate free tubulin dimers from larger polymer. The supernatant and pellet were then run on an SDS-gel. The amount of tubulin released into the supernatant was measured as an indication of the extent of MT depolymerization. The amount remaining in the pellet indicated the concentration of remaining MT polymer. Quantitation of these gels revealed that MCAK-Q710 is a more potent MT depolymerizer *in vitro* as well as *in vivo* (Fig. 3) when compared to wt-MCAK. There was an approximate 25% increase in the extent of MT depolymerization with MCAK-Q710 over wt-MCAK. In addition, more MCAK-Q710 was found in the MT pellet as compared to wt-MCAK suggesting that the deletion construct may have a higher affinity for MT polymer.

It has been shown that the rate at which wt-MCAK is able to depolymerize MTs is dependent upon the concentration of MT ends (Hunter et al., 2003). We sought to determine if this relationship held true for MCAK-Q710 as well. By passaging the MTs through needles of different lengths, we were able to shear them to different lengths. The resulting lengths were 5μm and 15μm. (Unsheared MTs can extend to ~40μm in length but may retain bundled MT structures and have a less consistent distribution as compared to the sheared polymer) We performed MT depolymerization

Figure 3:

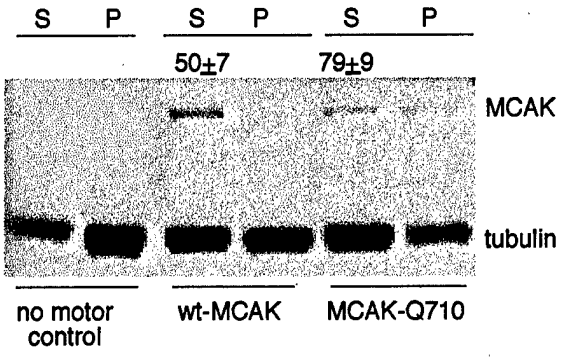

Figure 3: **MCAK-Q710 depolymerizes paclitaxel-stabilized MTs faster than wt-MCAK.** SDS-PAGE illustrates the difference in depolymerization activity between wt-MCAK and MCAK-Q710. (**S**)upernatant lanes show the amount of free tubulin dimer and unbound protein left in solution after the reaction was centrifuged. (**P**)ellet lanes illustrate the amount of larger polymer and any bound motor protein after centrifugation. The upper bands in the gel are MCAK motor and the lower bands are tubulin. In each experiment, 50nM of active motor is added to 2200nM paclitaxel stabilized MTs and 1mM MgATP. MTs were sheared to a length of 15μm on average. The depolymerization reactions went for 16 minutes at room temperature.

assays as described above using the 3 different lengths of MTs (5μm,15μm and unsheared) while holding the total MT polymer concentration constant. We found that the rate of MT depolymerization with MCAK-Q710 was higher in the presence of more MT ends (i.e. shorter MTs) similar to wt-MCAK (Fig 4). In addition, MCAK-Q710 was a more potent depolymerizer than wt-MCAK for the unsheared and 15μm MTs. (This statement could not be extended to the 5μm MTs because depolymerization was complete for both in the time frame of this experiment.)

Increasing the concentration of MT lattice significantly enhances ATPase activity of MCAK-Q710

MCAK has been shown to exhibit both free tubulin-stimulated and MT-stimulated ATP hydrolysis (Hunter et al., 2003). One possible model suggests that ATP hydrolysis or

Figure 4:

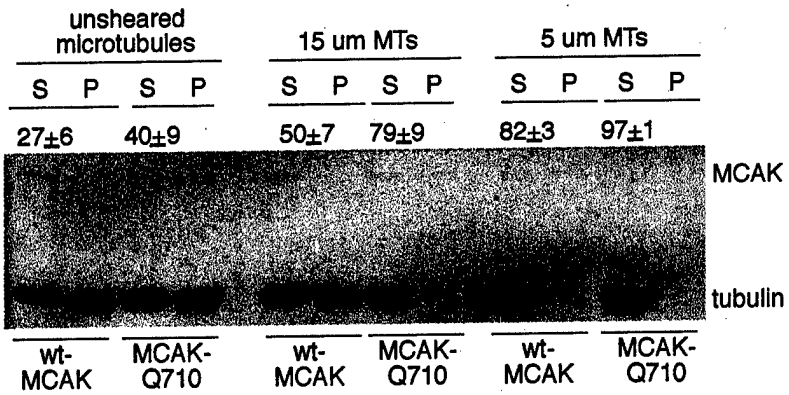

Figure 4: **Increasing the ratio of MT ends to lattice facilitates MCAK-dependent MT depolymerization.** The extent of MT depolymerization is compared for MTs of 3 different lengths by SDS-PAGE. Lanes are marked for (**S**)upernatant and (**P**)ellet. The numbers above the lanes indicate the percentage of tubulin released into the supernatant. Molar concentrations of polymerized tubulin were held constant for each trial (2200nM) as well as the concentration of active motor (50nM). Upper bands are motor protein. Lower bands are tubulin. Depolymerization reactions went for 16 minutes at room temperature.

phosphate release may serve to dissociate the terminal tubulin dimer from the MT protofilament (Hunter et al., 2003). That being the case, we wanted to determine if MCAK-Q710 had a higher depolymerization rate because it was able to more quickly promote the dissociation of the terminal tubulin dimers from the protofilament ends. Moreover, the motor must also dissociate from the terminal tubulin dimer for the dimer to be released from the MT protofilament. To determine if this process was enhanced with MCAK-Q710, we investigated whether MCAK-Q710 exhibited a higher rate of tubulin-stimulated ATPase activity than wt-MCAK. Using [γ-^{32}P]-ATP, we conducted ATPase assays in the presence of free tubulin (Fig. 5c and d). We observed that MCAK-Q710 and wt-MCAK had nearly identical tubulin-stimulated phosphate release rates, suggesting

that the enhanced MT depolymerization of MCAK-Q710 is not due to an enhanced rate of tubulin dissociation.

We performed the same assay using unsheared paclitaxel-stabilized MTs. MCAK-Q710 exhibited a significantly higher rate of ATPase activity in the presence of long MTs as compared to wt-MCAK (Fig. 5c). We repeated the assay using the same concentration of MT polymer but of shorter length (~5 and 15μm in length)(Fig. 5c and d). We found that increasing the ratio of MT ends to lattice significantly decreased ATP hydrolysis for both proteins. However, MCAK-Q710 still maintained a consistently higher rate of ATPase activity as compared to wt-MCAK.

To further characterize the differences in activity between the two proteins, we fit our ATPase data (the phosphate released in the experiments) to a growth curve. We chose the Janoschek growth curve (Equation 1) and determined the constants

$$W(t) = A - (A - W(0)) \times e^{-kt^p} \qquad \textit{Equation 1}$$

W(t) = Janoschek Growth Curve
A = asymptotic value
Point of inflection:

$$\left(\left(\frac{p-1}{pk} \right)^{\frac{1}{p}}, A - (A - W(0)) \times e^{-\frac{p-1}{p}} \right)$$

p<1 models simple exponential growth
p>1 models sigmoidal growth

based on a non-linear least squares fit. Janoschek's growth curve is a convenient model to use because it describes both exponential and sigmoidal growth (Janoschek, 1957). For values of p less than 1, growth is exponential. For values of p greater than 1, growth is sigmoidal. Sigmoidal growth suggests that there may be a delay in the reaction of the system. Note that there are three components contributing to the ATPase activity of this

system: free-tubulin stimulation, MT lattice-stimulation and MT end-stimulation. What our data suggests is that there may be a delay in maximal ATPase activity with longer MTs. wt-MCAK shows sigmoidal growth with MTs that are 15μm and unsheared whereas MCAK-Q710 only shows sigmoidal growth for MTs that are unsheared (Table 1).

Table 1:

	5μm MTs	15μm MTs	unsheared MTs	
k	3.70×10^{-3}	1.10×10^{-3}	2.12×10^{-4}	**MCAK-Q710**
p	0.6919	0.8959	1.1160	
POI	n/a	n/a	(257.31, 7.18)	
k	6.10×10^{-4}	5.53×10^{-5}	4.06×10^{-5}	
p	0.7906	1.2894	1.3564	**wt-MCAK**
POI	n/a	(628.68, 2.73)	(645.57, 5.84)	

Table 1: **Coefficients for Janoschek growth curve.** The coefficients *k* and *p* are given for each MT length as well as the point of inflection (POI) for sigmoidal curves. *k* is the reaction constant and indicates the speed at which a curve reaches an asymptotic value. *p* dictates whether a curve models simple exponential association or sigmoidal growth. Sigmoidal growth is usually indicative of a delay in cooperativity between an enzyme and a substrate. The POI indicates the point in time for which the shape of a curve changes from concave to convex.

The values of *k* (Table 1) indicate reaction constants, which describe the relative speeds at which the curves reach asymptotic levels. The values of *k* in Table 1 show a trend implying that depolymerization with shorter MTs reaches this level faster than depolymerization with longer MTs. In addition, MCAK-Q710 reaches asymptotic levels faster than wt-MCAK, consistent will all other experiments.

Model predicts that MCAK C-term truncation may enhance MT end targeting

A recent study suggests that ATP-dependent diffusional motility along the MT lattice contributes to MT depolymerization by facilitating targeting of MCAK to MT ends (Hunter et al., 2003). Enhanced ATPase stimulation of the C-term

Figure 5:

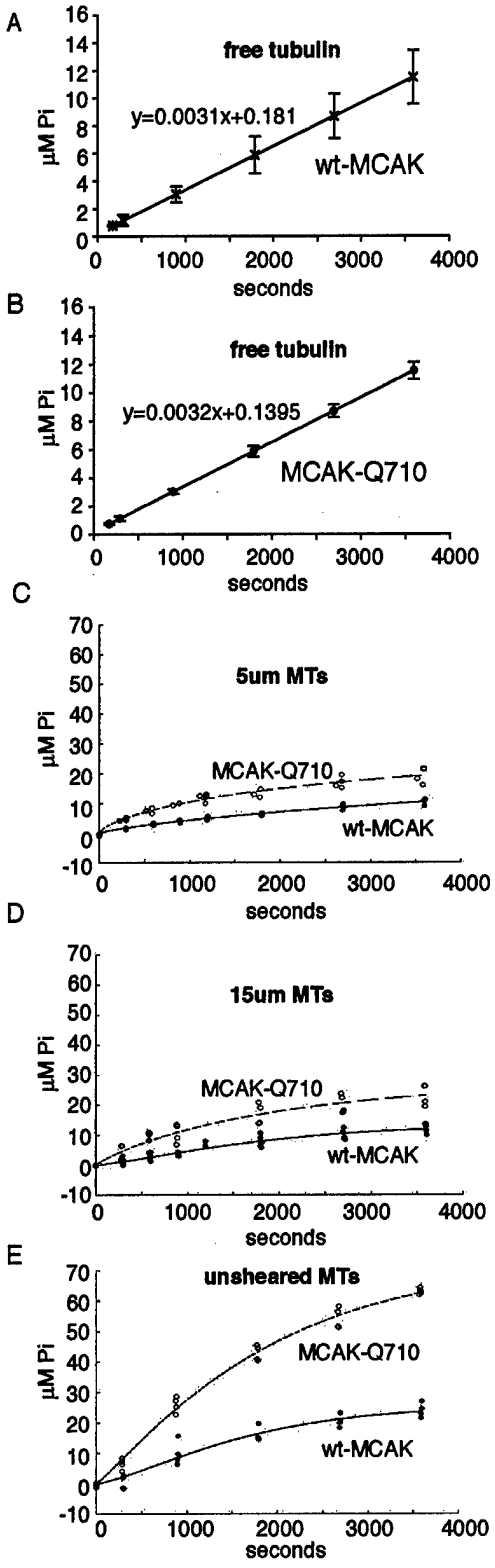

Figure 5: **Longer MTs increase MCAK's MT stimulated ATPase activity.** 50 nM active motor was incubated in the presence of 11µM tubulin, 250µM [γ-^{32}P]-ATP and 250µM cold MgATP. All figures display inorganic phosphate release (µM) over time (seconds). Linear curve fits (A, B) were generated by Microsoft Excel. All others (C, D, E) were generated with MATLAB (The MathWorks Inc.) The curves fit to the data in (C), (D), and (E) are Janoschek growth curves, fit via non-linear least square regression. (A) shows free tubulin-stimulated ATPase activity with wt-MCAK and (B) is with MCAK-Q710. (C) shows ATPase stimulation in the presence of paclitaxel-stabilized MTs, 5µm in length. (D) shows ATPase stimulation in the presence of MTs, 15µm in length. (D) shows ATPase stimulation in the presence of unsheared MTs.

truncation suggests that MCAK constructs lacking the C-term may confer more efficient mobility of the motor along the MT lattice, thereby increasing the rate at which motors reach the MT ends. This in turn may result in an increased rate of MT depolymerization.

It was also suggested by Hunter et al., that MCAK may be a processive depolymerizer. In this case, MCAK would bind to the MT end, and then 'step' backwards along the MT as it

dissociated the terminal tubulin dimers. In this case, 'step' does not necessarily imply a hand over hand model as suggested for conventional kinesin (Schief and Howard, 2001). It only implies that a cycling between weak and strong binding states results in a definitive movement in one particular direction. This ability to 'step' along the MT may be inhibited when MCAK is associated with the lattice due to it being in an 'inactive' conformation. This conformation may result from an interaction between the C-term tail region and another region of the protein (analogous to conventional kinesin (Coy et al., 1999; Hackney and Stock, 2000)). We propose that clipping the C-term from MCAK allows the motor to take periodic 'steps' or perform a periodic 'power stroke' in a particular direction along the MT lattice. If MCAK diffuses along the MT lattice via simple Brownian motion, this 'stepping' may allow the motor to definitively travel in a particular direction along the MT which results in a biased distribution of the motor. The model does not suggest that MCAK targets one end of the MT preferentially over the other, just that biased diffusion in either direction is more likely with the C-term truncation.

In order to test this proposed mechanistic difference, that may allow MCAK-Q710 to reach the ends of MTs more quickly than wt-MCAK, we employed a mathematical model based on our data from the 2 shorter MT lengths. To obtain the most accurate solution we chose the most consistent MT lengths. The 5 and 15μm MTs exhibited the most uniform MT length with greater certainty that MT bundles were eliminated (data not shown). Since our purpose was to compare the results of the mathematical model based on our ATPase assays to the results of the MT pelleting assays, we focused on the first 16 minutes of our ATPase assays.

We chose to begin by looking purely at the rates of phosphate release. By doing this, we were able to eliminate any errors in comparison resulting from slight shifts in the curves due to background noise. We fit our same ATPase data to polynomials, again using least squares analysis (Fig. 6a and b). To identify the rates at which ATPase activity was occurring, we differentiated these equations with respect to time and then examined the differences in these rates of depolymerization. Thesé and the following values are shown

Figure 6:

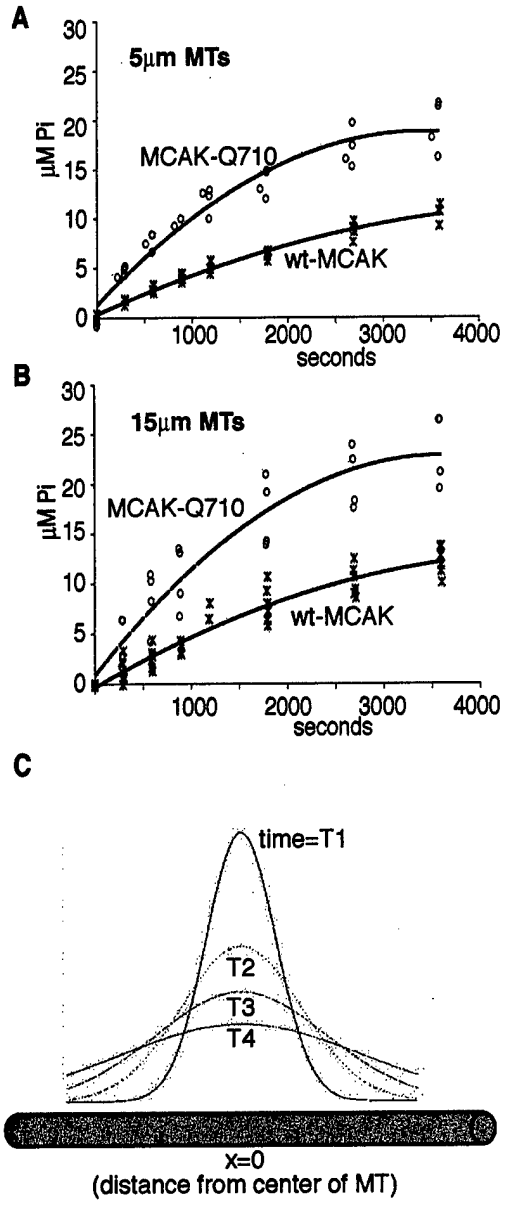

Figure 6: **Influence of differences in the ATPase rate on movement via Brownian motion.** (A) and (B) illustrate the ATPase values for 5 and 15µm MTs fit to polynomials. These equations were differentiated to evaluate the rate differences between wt-MCAK and MCAK-Q710. (C) is a plot of the equation describing the probability distribution associated with one-dimensional movement via Brownian motion for various times and over a distance traveled along the MT. At time=0, the probability of finding the particle at a location x=0 is 1. As time progresses, the particle begins to oscillate back and forth. The probability of finding the particle at some particular location along the MT is illustrated by these curves. As time increases, the bell shaped curves becomes more flat yet remains symmetrical since Brownian motion dictates that a particle has an equal chance of moving in either direction.

in Table 2. The total difference in ATPase activity (between wt-MCAK and MCAK-Q710) was determined by integrating this equation and evaluating it from t=0 to t=960 (16min). This integrated value was then divided by 960 to give an average value of ATP hydrolysis (per seconds) over a 16-minute period. Given that these assays were performed with 50nM active motor, we divided 50 by the ATPase average. This gave an estimated

frequency of how often a single motor hydrolyzes a molecule of ATP (or takes a 'step', assuming that ATP hydrolysis corresponds 1:1 to taking a 'step'). Dividing 960 seconds by this frequency, gave an approximate number of steps that a single motor would take in 16 minutes. Assuming an 8nm step size (the length of a tubulin dimer), we achieved an approximate distance traveled in one direction via periodic 'stepping'. Hunter et al. showed that MCAK was able to hydrolyze ATP at a maximal rate of 5 s^{-1}. In order to subtract the time taken to take a number of 'steps' along the lattice, we divided the approximate number of steps by five.

Table 2:

MT length	motor	$y(t)$ nM Pi/s	$\frac{dy(t)}{dt}$	$\frac{dy_{Q710}(t)}{dt} - \frac{dy_{wt}(t)}{dt}$	$\int_0^{960} \Delta \frac{dy(t)}{dt}$	ATPase average nM Pi/s
5μm	wt-MCAK	$-4\ 10^{-4}t^2+4.4t+246$	$-8\ 10^{-4}t+4.4$	$-32\ 10^{-4}t+5.9$	4189.44	4.36
	MCAK-Q710	$-20\ 10^{-4}t^2+10.3t+1169.8$	$-40\ 10^{-4}t+10.3$			
15μm	wt-MCAK	$-6\ 10^{-4}t^2+5.6t-407.9$	$-12\ 10^{-4}t+5.6$	$-28\ 10^{-4}t+6.6$	5045.76	5.26
	MCAK-Q710	$-20\ 10^{-4}t^2+12.2t+775.9$	$-40\ 10^{-4}t+12.2$			

MT length	avg. frequency of steps for single motor (in seconds)	steps taken in 16 min. by single motor	distance traveled with 8nm step (in nm)	time spent to take steps (in seconds)
5μm	11.47	83	664	16
15μm	9.5	101	808	20

Table 2: **Linear rate comparisons for wt-MCAK and MCAK-Q710.** The equations for the linear rates of phosphate release are derived from quadratic polynomials, fit to the ATPase data. The average difference (between wt-MCAK and MCAK-Q710) in phosphate release is translated into a potential number of 'steps' taken by a single motor over a 16 minute time period. The distance traveled with this particular number of 'steps' and the time taken to for these 'steps' to occur, is also illustrated.

So how does this all fit together? It has been demonstrated that MCAK is able to target MT ends in the absence of hydrolysable ATP (Desai et al., 1999). Hunter et al. proposed that MCAK may glide in a one-dimensional fashion to target MT ends in either the ATP bound state or the ADP.Pi bound state. This would account for the targeting of MCAK to MT ends in the absence of hydrolysable ATP and also for the tight coupling of MCAK to

the MT lattice in the absence of nucleotide (Maney et al., 1998; Wordeman et al., 1999). With this in mind, we considered a mechanism that would account for this gliding behavior along the MT lattice in the absence of ATP hydrolysis. A small particle suspended in liquid will perform erratic movements due to collisions with molecules in the solution. This behavior was described theoretically by Einstein (Einstein, 1906). If MCAK is tethered to the MT lattice via electrostatic interactions (Ovechkina et al., 2002), the motor will be less likely to diffuse away from the MT but still able to diffuse one dimensionally along its lattice in a random walk. This movement outward from a point due to Brownian motion cannot be described definitively, but instead by a probabilistic distribution according to the following equation (Astumian, 1997; Berg, 1983):

$$f(x,t) = \frac{e^{-\frac{x^2}{4Dt}}}{\sqrt{4\pi Dt}} \qquad \textit{Equation 2}$$

where x is the location of the particle, t is time and D is the diffusion constant for the particle. An example of these distributions is illustrated in Fig. 6c for various values of t along the length of a MT. We took the diffusion constant to be 7000 nm^2s^{-1}, as was determined experimentally by Hunter et al. We considered the probability of a single motor reaching the end of the MT (starting from the center) via simple Brownian motion (at a fixed time) verses the probability of a motor reaching the end via biased Brownian motion due to periodic 'stepping' in one direction. We compared these probabilities for wt-MCAK and MCAK-Q710 respectively, as a measure of the their comparable efficiency of depolymerization since both motors appear to have end-stimulated MT depolymerization activity. The results are in Table 3 alongside a comparison of depolymerization from the pelleting assays. The respective efficiency between wt-MCAK and MCAK-Q710 predicted from our model is almost identical to that obtained experimentally from the pelleting assays. This suggests that MCAK-Q710 may in fact exhibit greater biased movement along the MT lattice toward the end, which may account for its increased rate of MT depolymerization.

Table 3:

MT length	$\int_{-\infty}^{\frac{l}{2}} f_{wt}(x)dx$	$\int_{-\infty}^{\frac{l}{2}} f_{Q710}(x)dx$	% wt/Q710 probabilities from model	% wt/Q710 free tubulin from pellets
5μm	0.2476	0.3067	80.7	84
15μm	0.0204	0.0325	62.46	63

Table 3: **Efficiency comparison between wt-MCAK and MCAK-Q710.** Efficiency in end targeting was acquired by integrating equation 2 over the range $-\infty$ to $l/2$ where l is the length of the MT. For MCAK-Q710, before integrating, the curve was shifted to account for the number of 'steps' possibly taken by the truncated motor. The time taken (in terms of the ATP hydrolysis cycle) to perform these steps was also accounted for.

Figure 7:

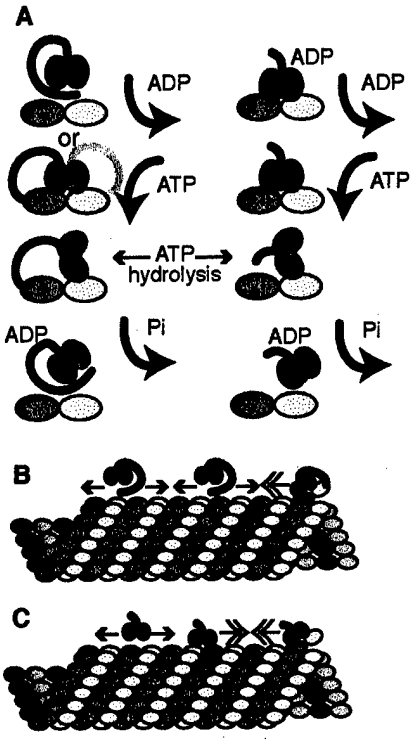

Figure 7: **Proposed model of the difference between wt-MCAK and MCAK-Q710.** (A) illustrates how free tubulin may stimulate ATPase activity with both wt-MCAK and MCAK-Q710. With wt-MCAK, the interaction between the intact C-term and the tubulin end may release its ATPase inhibition and allow association and ATPase activity in the presence of free tubulin. In the absence of the C-term, MCAK-Q710 freely associates with free tubulin, which promotes ATP hydrolysis. (B) illustrates how wt-MCAK oscillates back and forth along the MT in a weak-binding state until it finds an end, at which time the C-term associates with that end and ATPase activity is uninhibited. (C) illustrates how MCAK-Q710 may interact with the MT. While it may primarily oscillate in the loose binding state (single arrow head), similar to wt-MCAK, it may also be able to accomplish a number of steps in a definitive direction that may promote its quicker targeting to the MT end (double arrow head). This quicker end targeting may contribute to the slight increase in MT depolymerization.

Discussion

We have identified a region in the C-term of the MCAK protein that contributes to partial inhibition of its MT depolymerization activity. The specific region was mapped to the final eight of the primary amino acid sequence. Quantitative methods were used to determine that MCAK constructs lacking these final amino acids showed an ~25% increase in MT depolymerization for cells cultured in the presence of the MT stabilizing drug, paclitaxel.

These studies were all performed with MTs artificially stabilized with paclitaxel. The variation in MT depolymerization of transfected cells cultured without paclitaxel was difficult to identify. This suggests that both wt-MCAK and MCAK-Q710 are very efficient depolymerizers. However, stabilization of the MTs served to elucidate mechanistic differences between these two motors, which may in turn provide more insight as to how wt-MCAK functions in cells.

In order to determine if the difference in depolymerization was due to properties intrinsic to the protein or due to intracellular interactions, both wt-MCAK and MCAK-Q710 were purified and compared in *in vitro* depolymerization assays. It was observed that MCAK-Q710 displayed enhanced MT depolymerization *in vitro* as well as *in vivo* when compared to wt-MCAK. In addition, pelleting assays resulted in more MCAK-Q710 associated with the tubulin pellet (which corresponds to assembled tubulin polymer) where as wt-MCAK appeared to associate more with the supernatant (which consists of free tubulin dimers and unbound motor). Enhanced MT affinity of MCAK-Q710 would be consistent with conventional kinesin, which has been shown to have a higher affinity for MTs in the absence of its C-term tail domain and in the presence of ATP (Hackney and Stock, 2000).

To test if the concentration of MT ends contributed to the difference in MT depolymerization between these two motors, we performed pelleting assays using 3

different MT lengths. We observed that both motors displayed enhanced MT depolymerization with the presence of shorter MTs (in comparison to assays with longer MTs), and by extension, with the presence of more ends. This suggests that MT depolymerization is end stimulated for MCAK-Q710 as well as wt-MCAK.

To determine a mechanism that would explain the enhanced activity of MCAK-Q710, we performed ATPase assays with both motors. Hunter et al. showed that ATP hydrolysis is stimulated by free tubulin, the MT lattice and most significantly by MT ends. However, both motors exhibited nearly identical tubulin-stimulated ATPase rates. These data suggest that the enhanced activity was not due to more efficient tubulin dissociation. Interestingly, the two motors exhibited a significant difference in the ATPase activity stimulated by assembled MTs. For every MT length, MCAK-Q710 had a higher rate of ATPase activity. And this difference was increased as the length of the MTs increased. This data was fit to a growth curve that models both sigmoidal and exponential association of a molecule to a substrate (Equation 1). Longer MTs resulted in sigmoidal growth patterns according to this equation for both MCAK-Q710 and wt-MCAK (Table 1). This indicated that there was delay in at least one of the components contributing to ATP hydrolysis in the presence of long MTs. Presumably, the delay is coming from end stimulated ATP hydrolysis. This is suggested by the fact that the delay is coupled to the length of the MTs and because MCAK is believed to diffuse along the lattice to the MT ends (Hunter et al., 2003). It is also of interest to note that the point of inflection (POI) occurs further out in time for wt-MCAK as compared to MCAK-Q710 (where applicable for both). This suggests that all motor/MT interactions have not yet occurred until that point. This pattern of delayed reaction is also consistent within wt-MCAK experiments with MTs of different length (the POI for longer MTs occurs further out in time than for short). These results support the idea that there may be a diffusional component coupled to MT depolymerization and that the C-term of MCAK may contribute to the inhibition of that diffusion.

A numbers of motors (kinesin and myosin II) have been shown to exist in an inactive state (in which the tail folds in on the motor to prevent activity) and an active state

(where the protein unfolds and the tail interacts with other molecules in the system) (Alberts et al., 2002; Hackney and Stock, 2000). In the case of conventional kinesin, electron microscopy and sedimentation analysis suggest that inhibition of ATP hydrolysis is due to tail and neck/head (motor) interactions (Coy et al., 1999; Hackney and Stock, 2000). In the folded conformation, the tail mediates inhibition of ADP release (the rate limiting step in the kinesin ATP hydrolysis cycle) (Hackney, 1988; Hackney and Stock, 2000). This ADP release inhibition also promotes a weak net affinity for MTs in the presence of ATP (Hackney and Stock, 2000). Although our assays cannot resolve possible conformational differences of MCAK, our data does suggest that the C-term of MCAK may act in a manner analogous to the C-term of conventional kinesin. Absence of the MCAK C-term results in an increased rate of MT depolymerization *in vivo* and *in vitro*. *In vitro* depolymerization assays also show that MCAK-Q710 may have a higher affinity for MTs. ATPase assays demonstrate that both wt-MCAK and MCAK-Q710 have nearly identical tubulin-stimulated ATPase rates. However, the presence of MTs results in a significant increase in ATP hydrolysis with MCAK-Q710 in comparison to wt-MCAK. Moreover, as the concentration of the MT lattice increases, the difference in ATPase activity between wt-MCAK and MCAK-Q710 becomes more pronounced.

We propose that analogous to conventional kinesin, MCAK may exist in 2 conformations: folded (inactive) and unfolded (active). The C-term of MCAK may contribute to keeping the motor in the folded conformation when not at the ends of MTs to inhibit excess ATP hydrolysis along the lattice (where depolymerization does not take place). It has been suggested that MCAK may remain loosely tethered to the MT lattice via electrostatic interactions in either the ATP or ADP.Pi state (Hunter et al. 2002; Ovechkina et al. 2002). This loose tethering may prevent MCAK from diffusing away from the MT but would not interfere with its 1-dimensional diffusion along the lattice to the MT ends via simple Brownian motion. The end of the MT has been shown to be the strong binding site for MCAK. We propose that MCAK's binding to the exposed end of the terminal tubulin dimer of a MT releases its ATPase inhibition. This would explain why MCAK, unlike other kinesins, has a tubulin-stimulated ATPase activity. Whereas conventional kinesin uses cargo binding to release ATPase inhibition, MCAK may use

the binding of its C-term to the end of a tubulin dimer. Upon association with free tubulin (or the exposed end of a terminal tubulin dimer), MCAK's ATPase activity would be uninhibited, resulting in ATP hydrolysis in the presence of free tubulin. The idea of end binding and inhibition release is supported by the results of our ATPase assays for wt-MCAK and MCAK-Q710 in the presence of free tubulin. It was found that the ATPase activity for both motors was virtually equal (in the presence of free tubulin). According to our hypothesis, wt-MCAK would be able to associate with the ends of the free tubulin and release ATPase inhibition. The absence of the C-term in MCAK-Q710, would allow the truncated protein to associate freely with free tubulin because its ATPase activity is always uninhibited.

We considered the model proposed by Hunter et al. in which they explained a potential depolymerization mechanism for MCAK. Their model states, in part, that MCAK is a processive depolymerizer and that it is able to processively 'step' away from the MT end as it destabilizes the terminal tubulin dimers. The ability of MCAK to be processive can potentially explain the enhanced activity of MCAK-Q710. If MCAK's processive ability is promoted by the binding of the C-term tail to the end of the terminal tubulin dimer of a MT, then the absence of the tail (MCAK-Q710) may result in partial processivity of the motor along the lattice. By examining the differences in the rates of depolymerization between wt-MCAK and MCAK-Q710, we were able to translate the enhanced phosphate release from the experiments with MCAK-Q710 into a potential number of steps taken by a single motor in a similar assay. Evaluating the probability distribution of a particle performing Brownian movement, we were able to compare MT end-targeting efficiency based on simple Brownian motion. A comparison was made between a particle traveling from the center of a MT and one traveling from a point determined by a potential number of steps taken that corresponded to the aforementioned difference in phosphate release. These scenarios corresponded to the proposed movement of wt-MCAK and MCAK-Q710, respectively. A comparison of the efficiency of end targeting between wt-MCAK and MCAK-Q710 closely mimicked the comparison of depolymerization between the two motors based on our pelleting assays. These data taken together suggest that partial

processivity of MCAK-Q710 along the lattice may result in enhanced end targeting and hence, increased MT depolymerization.

Therefore, we propose that MCAK may exists in an active and inactive state, which is determined by the interaction between the C-term tail and another, yet determined, domain of the motor, which is presumably near the head as is seen with other motors (Alberts et al., 2002; Hackney and Stock, 2000). In this inactive state, MCAK is able to diffuse along the MT lattice via Brownian motion and target the MT ends. Strong binding to the end, via the tail, allows the motor to exist in the open conformation and processively depolymerize MTs. MCAK-Q710 may exhibit increased MT depolymerization because it is not restricted by the closed conformation caused by the tail. The open conformation of MCAK-Q710 may allow its motion along the MT lattice to be biased in a particular direction because of its ability to periodically step along the MT lattice. In this way, MCAK-Q710 may have an increased probability of reaching the MT end and therefore an increase in MT depolymerization.

Although we propose that MCAK-Q710 may take periodic steps in one direction along the MT, there remains strong evidence that this mutant, analogous to wt-MCAK, depends on loose tethering to the MT lattice to maintain efficient depolymerization. In pelleting assays where salt concentrations were markedly increased, both wt-MCAK and MCAK-Q710 were significantly diminished in their ability to depolymerize MTs (data not shown). For this reason, we believe that MCAK-Q710 has a limited ability to step along the MT and still relies on gliding, similar to wt-MCAK. This is consistent with the results from Hunter et al. in which they believe that wt-MCAK is able to processively depolymerize MTs but only up to approximately 20 dimers before the motor dissociates from the MT lattice. However, even with this limited ability to potentially step along the MT, the ability of MCAK-Q710 to take a few definitive steps in either direction may contribute to a slight increase in its efficiency in MT end targeting and ultimately, it's rate of MT destabilization.

Acknowledgements

We thank Michael Wagenbach for the wt-MCAK protein. We gratefully acknowledge Will Hancock (Department of Bioengineering, Pennsylvania State University, University Park, PA) for many suggestions and discussions pertaining to the modeling. We thank Jeremy Cooper, Henry Hess (Department of Bioengineering, University of Washington, Seattle WA), Marla Feinstein, Yulia Ovechkina, and Kathleen Rankin for many discussions and comments on the manuscript. This study was supported by National Institute of Health Grant GM53654A and Department of Defense Grant DAMD 17-01-1-0450 (to L. Wordeman) and National Institute of Health Predoctoral Fellowship 1 F31 GM65061-01 (to A.T. Moore).

References:

Alberts, B., A. Johnson, J. Lewis, M. Raff, K. Roberts, and P. Walter. 2002. Molecular Biology Of The Cell. Garland Science, New York. 1463 pp.

Astumian, R.D. 1997. Thermodynamics and kinetics of a Brownian motor. *Science.* 276:917-22.

Berg, H.C. 1983. Random Walks in Biology. Princeton University Press, Princeton. 142 pp.

Brady, S.T. 1985. A novel brain ATPase with properties expected for the fast axonal transport motor. *Nature.* 317:73-5.

Coy, D.L., W.O. Hancock, M. Wagenbach, and J. Howard. 1999. Kinesin's tail domain is an inhibitory regulator of the motor domain. *Nat Cell Biol.* 1:288-92.

Desai, A., S. Verma, T.J. Mitchison, and C.E. Walczak. 1999. Kin I kinesins are microtubule-destabilizing enzymes. *Cell.* 96:69-78.

Einstein, A. 1906. On The Theory Of The Brownian Movement. *Annalen der Physik.* 19:371-381.

Goldstein, L.S., and A.V. Philp. 1999. The road less traveled: emerging principles of kinesin motor utilization. *Annu Rev Cell Dev Biol.* 15:141-83.

Hackney, D.D. 1988. Kinesin ATPase: rate-limiting ADP release. *Proc Natl Acad Sci U S A.* 85:6314-8.

Hackney, D.D., and M.F. Stock. 2000. Kinesin's IAK tail domain inhibits initial microtubule-stimulated ADP release. *Nat Cell Biol.* 2:257-60.

Hunter, A.W., M. Caplow, D.L. Coy, W.O. Hancock, S. Diez, L. Wordeman, and J. Howard. 2003. The kinesin-related protein MCAK is a microtubule depolymerase that forms an ATP-hydrolyzing complex at microtubule ends. *Mol Cell.* 11:445-57.

Janoschek, A. 1957. Das Reaktionskinetische Grundgesetz Und Seine Beziehungen Zum Wachstums Und Ertragsgesetz. *Statistische Vierteljahresschrift.* 10:25-37.

Maney, T., A.W. Hunter, M. Wagenbach, and L. Wordeman. 1998. Mitotic centromere-associated kinesin is important for anaphase chromosome segregation. *J Cell Biol.* 142:787-801.

Maney, T., M. Wagenbach, and L. Wordeman. 2001. Molecular dissection of the microtubule depolymerizing activity of mitotic centromere-associated kinesin. *J Biol Chem.* 276:34753-8.

Moores, C.A., M. Yu, J. Guo, C. Beraud, R. Sakowicz, and R.A. Milligan. 2002. A mechanism for microtubule depolymerization by KinI kinesins. *Mol Cell.* 9:903-9.

Nakai, K., and M. Kanehisa. 1992. A knowledge base for predicting protein localization sites in eukaryotic cells. *Genomics.* 14:897-911.

Niederstrasser, H., H. Salehi-Had, E.C. Gan, C. Walczak, and E. Nogales. 2002. XKCM1 acts on a single protofilament and requires the C terminus of tubulin. *J Mol Biol.* 316:817-28.

Ovechkina, Y., M. Wagenbach, and L. Wordeman. 2002. K-loop insertion restores microtubule depolymerizing activity of a "neckless" MCAK mutant. *J Cell Biol.* 159:557-62.

Perou, C.M., S.S. Jeffrey, M. van de Rijn, C.A. Rees, M.B. Eisen, D.T. Ross, A. Pergamenschikov, C.F. Williams, S.X. Zhu, J.C. Lee, D. Lashkari, D. Shalon, P.O. Brown, and D. Botstein. 1999. Distinctive gene expression patterns in human mammary epithelial cells and breast cancers. *Proc Natl Acad Sci U S A.* 96:9212-7.

Schief, W.R., and J. Howard. 2001. Conformational changes during kinesin motility. *Curr Opin Cell Biol.* 13:19-28.

Tournebize, R., A. Popov, K. Kinoshita, A.J. Ashford, S. Rybina, A. Pozniakovsky, T.U. Mayer, C.E. Walczak, E. Karsenti, and A.A. Hyman. 2000. Control of microtubule dynamics by the antagonistic activities of XMAP215 and XKCM1 in Xenopus egg extracts. *Nat Cell Biol.* 2:13-9.

Vale, R.D., and R.J. Fletterick. 1997. The design plan of kinesin motors. *Annu Rev Cell Dev Biol.* 13:745-77.

Vale, R.D., and R.A. Milligan. 2000. The way things move: looking under the hood of molecular motor proteins. *Science.* 288:88-95.

Vale, R.D., T.S. Reese, and M.P. Sheetz. 1985. Identification of a novel force-generating protein, kinesin, involved in microtubule-based motility. *Cell.* 42:39-50.

Walczak, C.E., T.J. Mitchison, and A. Desai. 1996. XKCM1: a Xenopus kinesin-related protein that regulates microtubule dynamics during mitotic spindle assembly. *Cell.* 84:37-47.

Wordeman, L., and T.J. Mitchison. 1995. Identification and partial characterization of mitotic centromere-associated kinesin, a kinesin-related protein that associates with centromeres during mitosis. *J Cell Biol.* 128:95-104.

Wordeman, L., M. Wagenbach, and T. Maney. 1999. Mutations in the ATP-binding domain affect the subcellular distribution of mitotic centromere-associated kinesin (MCAK). ***Cell Biol Int.*** **23:275-86.**

Zhai, Y., P.J. Kronebusch, P.M. Simon, and G.G. Borisy. 1996. Microtubule dynamics at the G2/M transition: abrupt breakdown of cytoplasmic microtubules at nuclear envelope breakdown and implications for spindle morphogenesis. ***J Cell Biol.*** **135:201-14.**

Aurora B protein kinase regulates centromere targeting and the microtubule depolymerising activity of MCAK

Paul D. Andrews[1]*, Yulia Ovechkina[3], Nick Morrice[2], Michael Wagenbach[3], Linda Wordeman[3], Jason R. Swedlow[1]

[1] Division of Gene Regulation and Expression,
[2] MRC Protein Phosphorylation Unit
Wellcome Trust Biocentre
University of Dundee
Dow Street
Dundee
DD1 5EH
Scotland

[3] Department of Physiology and Biophysics
University of Washington School of Medicine
1959 N.E. Pacific Street
Seattle, Washington 98195-7290
U.S.A.

* Corresponding author:

Tel: +44 1382 348142
Fax: +44 1382 345783
E-mail: p.d.andrews@dundee.ac.uk

Words in Abstract: 145

Characters (with spaces, with references) = 49,578

Running Title: Aurora B Regulation of MCAK

Summary

We report here the mitotic regulation of the Kin I kinesin MCAK by the Aurora B kinase. Aurora B and MCAK colocalise with centromeres in mono-oriented chromosomes but are separated in bioriented chromosomes under tension. In vitro, Aurora B phosphorylates three highly conserved Ser residues in the N-terminus of MCAK. Phosphorylation by Aurora B inhibits MCAK's *in vitro* microtubule depolymerising activity. *In vivo,* an MCAK S →E mutant has reduced microtubule depolymerisation activity. Depletion of Aurora B by RNAi or expression of an Aurora B-KR dominant negative mutant prevented centromeric targeting of MCAK and inhibited MCAK phosphorylation. Aurora B depletion also decreased sister-centromere tension across mitotic centromeres and caused aberrant spindle morphology, consistent with a loss of MCAK activity at the centromere. These results suggest that Aurora B is required for MCAK targeting to centromeres and for the regulation MCAK activity in the mitotic spindle.

Introduction

Accurate chromosome segregation requires the attachment of microtubules from opposing spindle poles to kinetochores formed on sister chromatids. Bipolar attachment of chromosomes to the mitotic spindle during prometaphase requires a functioning kinetochore. The Aurora B kinase, and its associated binding partners INCENP and survivin appear to play a critical function in this process. Mutations in the yeast Aurora B homologue, Ipl1, generate stably mono-oriented chromosomes that fail to resolve (He et al., 2001; Tanaka et al., 2002). In *Drosophila* and *C. elegans*, Aurora B RNAi cells possess aberrant prometaphase-like mitotic spindles that fail to align their chromosomes on the metaphase plate and subsequently develop significant aneuploidy due to chromosome nondisjunction (Adams et al., 2001b; Giet and Glover, 2001; Kaitna et al., 2000; Oegema et al., 2001). Introduction of dominant negative mutants of the Aurora B kinase or small molecule inhibitors into mammalian cells also causes similar phenotypes (Ditchfield et al., 2003; Hauf et al., 2003; Murata-Hori and Wang, 2002). Together, these results suggest that Aurora B complex plays a critical role in establishing bipolar chromosome attachment and that this function is highly conserved.

Aurora B, INCENP, and survivin all behave as chromosome passenger proteins (Adams et al., 2001a; Wheatley et al., 2001), localizing between sister chromatid centromeres in the inner centromere from late G2 through to metaphase (Cooke et al., 1987). As chromosome segregation initiates, the complex leaves the inner centromere and concentrates on the central spindle microtubules where it has further functions in cytokinesis (Adams et al., 2001b; Giet and Glover, 2001; Kaitna et al., 2000; Oegema et al., 2001). In yeast, the Aurora B/Ipl1p complex phosphorylates a number of inner and outer kinetochore proteins (Biggins et al., 1999; Cheeseman et al., 2002). Aurora B also phosphorylates the centromere-specific histone H3 variant

CENP-A (Zeitlin et al., 2001), as well as histone H3 localized throughout the chromosome (Hsu et al., 2000; Murnion et al., 2001). The concentration of the Aurora B complex at the inner centromere and its interaction with kinetochore components suggest that it may regulate the interactions between kinetochores and microtubule ends.

One possible substrate for the Aurora B complex is the Kin I kinesin homologue MCAK/XKCM1. Unlike conventional kinesin-like proteins, Kin I family members have their motor domains in the central portion of the molecule and use the hydrolysis of ATP to depolymerise microtubule ends (Hunter et al., 2003; Hunter and Wordeman, 2000; Wittmann et al., 2001). This activity plays a critical role in the assembly and function of the mitotic spindle. In *Xenopus* egg extracts, depletion of the *Xenopus* homologue XKCM1 decreases the catastrophe rate of microtubule ends and causes chromosomes to misalign on the mitotic spindle (Desai et al., 1999; Walczak et al., 2002). In mammalian cells, depletion of MCAK by antisense DNA inhibits anaphase A (Maney et al., 1998). MCAK/XKCM1 is localized to centromeres in early prophase and remains there throughout mitosis, and thus are ideally positioned to drive chromosome movement by promoting the depolymerization of microtubule ends attached to the kinetochore (Ovechkina and Wordeman, 2003; Walczak et al., 1996; Wordeman et al., 1999). In fission yeast the Kin I-related Klp5 and Klp6 are required for both microtubule attachment and generation of tension (Garcia et al., 2002).

A critical unanswered question is how MCAK/XKCM1 activity is regulated. As a regulator of microtubule end catastrophe, soluble MCAK/XKCM1 can affect the average length of spindle microtubules in *Xenopus* egg extracts (Walczak et al., 1996). However, MCAK/XKCM1 also functions during chromosome alignment, suggesting that the activity of kinetochore-bound MCAK/XKCM1 might be tightly

regulated during the process of attachment of chromosomes to the spindle microtubules and as chromosomes undergo saltatory motion in prometaphase and metaphase (Rieder and Salmon, 1994; Skibbens et al., 1993). To explore this possibility, we have examined the interactions between the Aurora B complex and MCAK *in vivo* and *in vitro*. We find that the mitotic Aurora B complex is a critical regulator of MCAK localization and function *in vitro* and *in vivo*. When Aurora B function is inhibited in vivo, we observe a number of phenotypes that suggest that the Aurora B complex plays an essential role in centromere and kinetochore function.

Results

Dynamic colocalisation of Aurora B and MCAK

Independent immunofluorescence studies have previously shown Aurora B and MCAK localised to centromeres of mammalian chromosomes from late prophase of the cell cycle to until the metaphase-anaphase transition (Adams et al., 2001a; Maney et al., 1998). During anaphase MCAK remains centromere-associated throughout telophase while Aurora B relocalises to the spindle midzone. We re-examined the localisation of Aurora B and MCAK at pre-anaphase stages of mitosis in HeLa cells using high-resolution deconvolution microscopy. During prometaphase, Aurora B and MCAK colocalised in chromosomes not attached to the spindle or mono-oriented (attached to kinetochore fibres from one pole only; Fig. 1A). The ACA antigen, a marker for centromeres, also localised with Aurora B and MCAK. During prometaphase, biorientation of sister kinetochores results in the generation of tension across the centromere (Waters et al., 1996). We found two distinct types of Aurora B/MCAK co-localization in prometaphase cells. In centromeres under tension (as judged by the distance between ACA staining sites), Aurora B and MCAK were only partially colocalized, whereas centromeres not under tension still showed significant colocalisation. (Fig. 1B). However, in chromosomes at the metaphase plate, MCAK concentrated at two sites that partially colocalize with ACA staining but that were distinct from the strictly inner-centromeric localisation of Aurora B (Fig. 1C). MCAK and Aurora B also colocalised in cells treated with nocodozole and taxol (data not shown). The localization of MCAK is therefore dynamic, initially colocalizing with Aurora B following assembly of mitotic chromosomes, but then becoming distinct from Aurora B as tension develops across sister kinetochores.

Aurora B phosphorylates MCAK in vitro

We next tested whether the Aurora B complex might phosphorylate MCAK *in vitro*. Recombinant full length MCAK was incubated in the presence of ^{32}P-γ-ATP and mitotic Aurora B complex isolated from *Xenopus* chromosomes. We chose this strategy because we have failed to produce recombinant Aurora B complex that has the same activity and properties as the mitotic complex (Murnion et al., 2001), data not shown). Figure 2A shows that MCAK was phosphorylated *in vitro* by mitotic Aurora B complex. Kinase activity was not detected towards MCAK using interphase Aurora B or control IgG beads (Fig. 2A). These results suggested MCAK might be phosphorylated in a cell cycle–dependent manner by Aurora B.

Previously we have defined regions within the N-terminus of MCAK necessary for correct localisation and microtubule depolymerisation activity *in vitro* and *in vivo* (Maney et al., 2001; Ovechkina et al., 2002). We tested a subset of our deletion mutants and a series of site-directed mutants in a basic region close to the motor domain, that we previously defined as critical for microtubule depolymerising activity (Maney et al., 2001; Ovechkina et al., 2002) (schematically shown in Fig. 2B). We found that A182-S583 MCAK, representing the minimum MCAK construct with microtubule depolymerising activity, was the only one of the N-terminally truncated/mutated constructs to retain its ability to act as an Aurora B substrate *in vitro* (Fig. 2C). Deletion of the neck region (D218-S583 or I253-S583 MCAK) abolished detectable MCAK phosphorylation by the Aurora B complex (Fig. 2C, D). To further define the requirements for phosphorylation of MCAK, we tested an MCAK mutant in which several of the Lys and Arg residues in the neck region were mutated to Ala (A182-Ala-S583; Fig 2B-D; see Fig. 5 in ref (Ovechkina et al., 2002) for more details). These residues are essential for microtubule depolymerising activity and are postulated to be directly involved in binding the C-terminal acidic tail of

tubulin (Niederstrasser et al., 2002; Ovechkina et al., 2002). These mutations abolished detectable phosphorylation by the Aurora B complex. To determine if this result was simply due to an effect of the change in basic character of this region, we substituted this region of A182-S583 MCAK with a lysine-rich loop derived from KIF2 (A182-K-loop-D218-S583 MCAK (Ovechkina et al., 2002)). This substitution restores high levels of microtubule depolymerising activity, but not phosphorylation by the Aurora B complex.

Identification of Aurora B phosphorylation sites on MCAK

We next identified the sites in MCAK phosphorylated by the mitotic Aurora B complex. In pilot studies we incubated recombinant MCAK and ^{32}P-γ-ATP with interphase or mitotic Aurora B complex, or with recombinant yeast Ipl1p/Sli15p complex and then analysed ^{32}P-labelled tryptic peptides from MCAK by reverse-phase HPLC. Consistent with the results in Figure 2, interphase Aurora B complex produced no significant ^{32}P-labelled phosphopeptides (data not shown). The phosphopeptides generated after incubation with the mitotic Aurora B complex appeared similar to those obtained with recombinant yeast Ipl1p/Sli15p (data not shown). In all these experiments, as expected from inspection of MCAK's primary amino acid sequence, trypsin was found to generate a significant number of very short MCAK peptides, several of which were radiolabelled. To simplify the spectrum of MCAK peptides we used Lys-C for proteolytic cleavage. HPLC analysis of Lys-C-digested MCAK phosphorylated by Aurora B produced three distinct peaks of radioactivity (Fig. 3A), which were then characterized using a combination of Edman sequencing and MALDI-TOF (Fig. 3B). The identity of each of the LysC peptides is shown in Figure 3B. Peak 1 corresponded to phosphorylation at Ser 92, while Peak 2 corresponded to phosphorylation at Ser 186. Peak 3 corresponded to phosphorylation at either Ser 106, Ser 108 or Ser 112, but MALDI-TOF analysis

verified that for any one peptide, only one of these three serines residues was phosphorylated. Comparison of the integrated peak heights from the HPLC analysis indicates that Peak 3 sites are less well phosphorylated in MCAK. The Aurora B sites in MCAK conform to the loose consensus sequence derived from analysis of the limited number of *bona fide* Aurora B family substrates (Fig. 3C; (Cheeseman et al., 2002)). Alignment of MCAK and its orthologues with the closely related KIF2 kinesins within this N-terminal region reveals that the Aurora B phosphorylation site at Ser 92 is highly conserved between hamster and human MCAK and *Xenopus* XKCM1 (Fig. 3D). In addition, this site (with a threonine substituting for the serine) is found in KIF2 kinesins. In all orthologues, this site contains basic residues in the P-1, P-2 and P-3 positions and often a hydrophobic residue in the P+1 position (Fig. 3D). The residues surrounding Ser186 are similarly conserved (Fig. 3D). Significantly, mutation of the basic residues immediately N-terminal to Ser186 dramatically decreased MCAK phosphorylation by the mitotic Aurora B complex (Fig. 2C). The sequences around the alternatively phosphorylated Ser 106, Ser 108 and Ser 112 residues are also highly conserved in MCAKs (Fig. 3D). One exception is Ser 106, which is a glutamate in the equivalent position in XKCM1.

Aurora B is a major mitotic MCAK kinase

We next tested whether MCAK might be a substrate for Aurora B *in vivo* by assaying the migration of MCAK in 2D gels. Total cellular lysates from nocodozole-arrested cells treated were separated by 2D gel electrophoresis and then immunoblotted with anti-MCAK. Treatment of lysates with λ phosphatase caused a significant change in MCAK migration from a pI of ~6 to a pI of ~8, which coincides with the predicted pI of unmodified MCAK (Fig. 4A). This result suggests that most of the phosphate moieties were removed by phosphatase and that MCAK is phosphorylated *in vivo* during mitosis (Fig. 4A). We next depleted Aurora B from

HeLa cells using RNAi. Immunoblots of 2D gels of lysates probed with anti-Aurora B antibody revealed a significant depletion of the enzyme in total cell lysates (Fig. 4B, bottom panel; the effects of Aurora B RNAi are more fully characterized in Figure 7). Probing the identical immunoblots with anti-MCAK antibody showed that Aurora B RNAi caused a dramatic shift in the mobility of MCAK, again to a pI of ~8 (Figure 4B, top panel). Since the migration of MCAK on 2D gels after Aurora B depletion is similar to that observed when MCAK was dephosphorylated *in vitro*, we conclude that Aurora B is a major mitotic MCAK kinase *in vivo*.

Aurora B phosphorylation inhibits the activity of MCAK

We next assayed the microtubule depolymerising activity of MCAK phosphorylated by the mitotic Aurora B complex in an *in vitro* microtubule sedimentation assay. In the absence of MCAK, the vast majority of tubulin from the taxol-stabilized microtubules sedimented in the pellet (Fig. 5A, lanes 5-8). MCAK incubated with control beads, retained full depolymerisation activity (Fig. 5, lanes 3, 4). In contrast, the depolymerisation of MCAK phosphorylated by the Aurora B complex was significantly reduced (Fig. 5A, lanes 1, 2), suggesting that the *in vitro* phosphorylation by Aurora B inhibits the microtubule depolymerising activity of MCAK. Similarly, we show that phosphorylation of MCAK with a mixture of recombinant Ipl1p (budding yeast Aurora B) and Sli15p (budding yeast INCENP), again dramatically reduces MCAK's *in vitro* microtubule depolymerising activity (Fig. 5B, lanes 1,2).

To assess the function of MCAK phosphorylation *in vivo*, we transfected HeLa cells with GFP-MCAK constructs bearing mutations in the phosphorylation sites we identified in Figure 3 and then measured the amount of polymerized tubulin present in transfected cells (Ovechkina et al., 2002). All constructs bearing single S→A or

S→E mutations efficiently depolymerised microtubules in this *in vivo* assay (Table 1). Mutating the block of phosphorylation sites from Ser106 – Ser112 also had no effect on microtubule depolymerisation. The double mutant S92A;S186A also possessed activity in distinguishable from wild-type MCAK. However, the double mutant S92E;S186E, which mimics the phosphorylation of both of the major sites we identified *in vitro* (Fig. 3), significantly inhibits microtubule depolymerisation (Table 1). We therefore conclude that phosphorylation of MCAK *in vitro* and *in vivo* inhibits its ability to depolymerise microtubules, possibly by affecting the interaction of the enzyme with the microtubule lattice.

Aurora B targets MCAK to centromeres

We next assayed the effects of modulating Aurora B function *in vivo*. Transient expression of the "kinase-dead" KR mutant of Aurora B causes defects in chromosomal movement, spindle structure and dynein/CENP-E localisation (Murata-Hori and Wang, 2002). Cells were transfected with CFP fused to either wild type Aurora B or Aurora B-KR and co-transfected with YFP fused to full length MCAK (YFP-FL MCAK) or to a construct bearing a deletion of the MCAK motor domain (YFP-ML MCAK; (Ovechkina et al., 2002)). After transfection with wildtype CFP-Aurora B, YFP-FL MCAK localisation was indistinguishable from the endogenous protein (Fig. 6, left columns). Transfection with CFP-Aurora B-KR, caused YFP-FL MCAK to dramatically delocalise in both prometaphase and metaphase cells, relocating from the inner-centromere to the cytoplasm and to a certain degree the spindle and spindle poles (Fig. 6, right columns). A similar effect was observed on endogenous MCAK in cells that did not contain detectable YFP signal (data not shown). YFP-ML-MCAK was also delocalised by CFP-Aurora B-KR (Fig. 6). This result suggested that Aurora B kinase activity, apparently directed

towards the N-terminus of MCAK, is required for correct MCAK localization, Centromere targeting is independent of the MCAK motor domain and therefore independent of the microtubule depolymerisation activity of MCAK.

Depletion of Aurora B by RNAi delocalises MCAK and causes centromere and mitotic spindle defects

To further explore the role of Aurora B in MCAK function, we depleted Aurora B by RNAi in HeLa cells and assayed MCAK localisation. The siRNA duplex used significantly decreases Aurora B protein levels within 10 to 24 hours. Figure 7A shows representative prometaphase and metaphase cells from four independent experiments, 12-18 hours post-transfection using Aurora B siRNA or control (scrambled) siRNA duplexes. In control RNAi experiments, (Fig. 7A) both MCAK and Aurora B localisation and levels were identical to those in untransfected cells. In cells transfected with Aurora B siRNA, we found mitotic cells with Aurora B levels as low as less than 1% of control levels (Fig. 7A, lower panels). We also observed a proportion of the mitotic cell population with Aurora B levels ranging from 1% to 30% of controls, presumably due to differences in transfection efficiency. The mean depletion of Aurora B as assayed by quantifying fluorescence signal was 76.9 ± 19.6% (N = 15; also see Fig. 4B). In cells with at least 90% Aurora B depletion, we detected no significant change in total cellular MCAK (Fig. 7A). Instead, after Aurora B depletion, MCAK was no longer concentrated at its normal centromeric localisation position, but instead was now localized throughout the cytoplasm. Some MCAK appeared to decorate the mitotic spindle (Fig. 7A).

Interfering with Aurora B function by microinjection of anti-Aurora B antibodies causes elongated microtubules and spindle defects in *Xenopus* cells in culture (Kallio et al., 2002). After Aurora B RNAi, we also observed a significant effect on

microtubule morphology and the mitotic spindle. Mitotic figures were observed where chromosomes failed to completely congress to a compact, well-defined metaphase plate (Fig. 7B). Similar phenotypes have been observed in many systems after loss of Aurora B function (Adams et al., 2001b; Ditchfield et al., 2003; Giet and Glover, 2001; Hauf et al., 2003; He et al., 2001; Kaitna et al., 2000; Oegema et al., 2001; Tanaka et al., 2002) and are also remarkably similar to those observed after microinjection of anti-XKCM1 antibodies into mitotic cells (Kline-Smith and Walczak, 2002). We assayed the effect of MCAK delocalization by quantifying tubulin fluorescence in the vicinity of the kinetochore. Figure 7C shows that microtubule bundles near kinetochores are significantly denser after Aurora B RNAi cells, suggesting increased microtubule stability at the kinetochore. In budding yeast, the Aurora B homologue Ipl1p has been suggested to function in the tension-sensing mechanism at centromeres (Biggins and Murray, 2001). We therefore measured the distance between centromeres in Aurora B RNAi mitotic cells and expressed this data as a frequency distribution (Fig. 7E). Aurora B RNAi leads to a significant decrease in average centromere-centromere distances compared to control cells, most likely because loss of Aurora B inhibits the localization of MCAK, CENP-E (Murata-Hori and Wang, 2002) and possibly other factors required for force generation at the kinetochore. The decrease in tension after Aurora B depletion we observe is significant, but less than that observed when HeLa cells are treated with taxol (see Fig. 7E, legend). This partial relief of tension may be due to presence of other kinetochore factors that engage microtubules, although we cannot exclude the possibility that residual Aurora B and MCAK generate this result.

Finally, we assessed the link between aberrant mitotic spindles and the delocalization of MCAK after Aurora B RNAi. Close inspection revealed a significant decrease in the average pole-to-pole distance after Aurora B RNAi (Fig.

7C) most likely due to a significant disorganization of the microtubules in mitotic spindles, resulting in defective chromosome positioning (Fig. 7F and supplemental videos). We therefore measured the amount of tubulin in mitotic spindles, as reported by immunofluorescence, and detected no change in tubulin polymer between control RNAi and Aurora B RNAi cells. This suggests that delocalized MCAK did not significantly change bulk microtubule behavior. We also measured the proportion of MCAK localised to centromeres in normal mitotic cells by immunofluorescence and found that this fraction represented 33.5 ± 4.9% of the total cellular MCAK. It seems unlikely that this population, if released into the cytoplasm would produce a significant change in microtubule polymer levels. These data suggest that while MCAK may affect microtubules at kinetochores (Fig 7E), it may not have a major effect on non-kinetochore microtubules in HeLa cells. Therefore, we believe that the gross defects in spindle morphology observed by us and others after disruption of Aurora B may be mediated by other substrates of Aurora B.

Discussion

In this study, we present evidence that MCAK, a centromeric Kin I kinesin that depolymerises microtubules, is a substrate for the Aurora B protein kinase during mitosis. In cells depleted of Aurora B, MCAK appears to be largely dephosphorylated, suggesting that Aurora B is a major MCAK kinase. Aurora B phosphorylates MCAK in regions known to be required for centromere targeting. Disruption of Aurora B function not only decreases MCAK phosphorylation but also inhibits targeting of MCAK to the centromere. We observe a number of phenotypes consistent with the loss of centromeric MCAK function, including an increase in kinetochore microtubule density and a decrease in the amount of tension across sister centromeres. Aurora B and MCAK colocalise on mitotic centromeres before establishment of bipolar attachment, but become spatially separated when centromeres are under tension. Together, these data and the fact that Aurora B is also required for targeting of CENP-E in human cells (Murata-Hori and Wang, 2002) and the function of a number of kinetochore proteins in yeast (Biggins et al., 1999; Cheeseman et al., 2002), suggests that Aurora B plays a central role in regulating kinetochore function in all eukaryotes.

MCAK is phosphorylated in vitro and in vivo by Aurora B

Our results demonstrate, for the first time, the phosphorylation of a Kin I kinesin and identify MCAK as a critical downstream effector of the Aurora B kinase. MCAK was phosphorylated by Aurora B at two sites in the N-terminus and one in the neck region. The first of these sites (Ser92) is conserved in most Kin I's and represents a good consensus Aurora B phosphorylation site. In a second N-terminal site, one of three different serines (Ser 106, Ser 108, Ser 112) was found to be phosphorylated at any one time. To our knowledge this alternative site usage has not been reported before for Aurora B. This region is less well conserved between

members of the MCAK/KCM family, with one of the sites (Ser 108) being substituted by Glu in XKCM1. Whether this is of functional significance remains to be tested. In addition, only one of the sites (Ser 112) in this region is conserved in the KIF2s. Both N-terminal sites lie within a region shown in mammalian MCAK and *Xenopus* XKCM1 to be important for centromeric localisation (Maney et al., 2001; Walczak et al., 2002). A third site was found in the neck region of MCAK. This basic region has been postulated to form a weak electrostatic interaction with the acidic C-terminus of tubulin and may contribute to diffusional motility on the microtubule lattice (Hunter et al., 2003; Niederstrasser et al., 2002; Ovechkina et al., 2002). Phosphorylation of MCAK by Aurora B might therefore reduce the basic charge in this critical domain. Phosphorylation of MCAK by Aurora-B inhibits MCAK microtubule depolymerisation activity *in vitro* and mimicking phosphorylation with point mutants inhibits depolymerisation *in vivo* (Fig. 4, Table 1). Thus, we postulate that phosphorylation by Aurora B reduces MCAK's ability to depolymerise microtubules, most likely by disrupting key electrostatic interactions between MCAK and the carboxy-terminal tail of tubulin. The conservation of these Ser residues in other Kin I's suggests a general mechanism for regulating the function of these enzymes. Indeed, a Ser or Thr residue is often found C-terminal to the K-loop in several KIF1s, so phosphorylation may be a common mechanism for modulating K-loop function.

Loss of Aurora B results in delocalisation of MCAK and spindle microtubule defects

The phenotypes we observe after disruption of Aurora B function are most consistent with a loss of MCAK activity (Figs. 6, 7), suggesting that Aurora B positively regulates MCAK *in vivo*. Perturbation of Survivin, a protein that binds and regulates Aurora B activity increased resistance to nocodazole-induced microtubule depolymerisation, further suggesting that the Aurora B complex positively regulates

microtubule dynamics (Giodini et al., 2002). Furthermore, the Aurora B-KR mutant decreases chromosome movement in prometaphase (Murata-Hori and Wang, 2002). These data are all consistent with a role for Aurora B in regulating microtubule dynamics and force generation at the kinetochore, although MCAK may be only one of many Aurora B targets. Indeed, the Aurora B-KR mutant delocalises CENP-E, a critical kinetochore kinesin-like motor (Murata-Hori and Wang, 2002). Delocalization of MCAK from centromeres using an N-terminal dominant negative fragment of MCAK does not affect CENP-E localization (Walczak et al., 2002). Therefore Aurora B separately directs the centromere targeting, and thus the function of MCAK and CENP-E. Aurora B is required for the establishment of bipolar orientation and may be involved in resolving merotelic attachments on mitotic chromosomes (Hauf et al., 2003; Tanaka et al., 2002). As disruption of MCAK function by microinjection of anti-MCAK antibodies into mitotic cells causes similar chromosome alignment defects as interfering with Aurora B function, it seems possible that Aurora B promotes biorientation and possibly merotelic resolution through MCAK.

Paradoxically, direct Aurora B phosphorylation of MCAK inhibits its activity *in vitro*, but disruption of Aurora B function *in vivo* leads to a phenotypic reduction of MCAK activity. This is not simply a difference between *in vitro* and *in vivo* assays, as the S92E;S186E MCAK mutant also shows reduced microtubule depolymerisation activity *in vivo*. Aurora B appears to have two different effects on MCAK function. First, MCAK phosphorylation inhibits depolymerisation of microtubules. Second, Aurora B is required for MCAK localisation at centromeres and in the absence of Aurora B, MCAK function appears to be decreased. Our assays of MCAK activity address its interaction with microtubule ends, but do not fully explain the mechanism of MCAK function at centromeres. For instance, targeting of MCAK to

centromeres may require an unknown factor that is sensitive to Aurora B activity, either by phosphorylation on MCAK or on itself. In yeast at least, Aurora B is known to phosphorylate many other kinetochore proteins (Biggins et al., 1999; Cheeseman et al., 2002). The *in vitro* assays probably lack other factors, so may not fully recapitulate the *in vivo* consequences of Aurora B regulation.

It is clear that the relative localization of Aurora B and MCAK change during prometaphase (Fig. 1). Furthermore, once attached to the mitotic spindle, chromosomes display dynamic oscillatory movement, indicating rapid changes in microtubule dynamics (Rieder and Salmon, 1994; Skibbens et al., 1993). We speculate that the relative positions of Aurora B and MCAK in the inner centromere and kinetochore could allow the switching of directional movement by asymmetrically altering local microtubule dynamics. Indeed, we find that Aurora B depletion causes a partial loss of tension across metaphase centromeres (Fig. 7D) and previous work suggests that Aurora B is required for the oscillatory movements of mitotic chromosomes on the metaphase spindle (Murata-Hori and Wang, 2002). This model is especially attractive when one considers the recent discovery that protein phosphatase 1 (PP1), which antagonises Aurora B (Cheeseman et al., 2002; Hsu et al., 2000; Sassoon et al., 1999) and also regulates its activity (Murnion et al., 2001), is localised to the outer kinetochore in metaphase (Trinkle-Mulcahy et al., 2003). The dynamic balance of phosphorylation of motors such as MCAK mediated by Aurora B and PP1 might then regulate the dynamic movements of chromosomes in the mitotic spindle.

A similar mechanism might operate during the establishment of bipolar orientation where MCAK phosphorylation at the centromere might change as tension develops (Fig. 8). Since loss of Aurora B function results in the appearance of MCAK on the spindle microtubules (Figs. 6 and 7A), we therefore speculate that

centromeric MCAK is phosphorylated and localised by its proximity to Aurora B in the absence of tension. At this point, MCAK activity is inhibited, possibly to prevent reversal of the initial microtubule-kinetochore attachments. Once bipolar attachment is established, MCAK and Aurora B separate, MCAK phosphorylation decreases due to its proximity to PP1, and MCAK switches its affinity from centromeres to microtubules. Concomitantly, MCAK activity increases, allowing it to participate in force generation at the kinetochore.

Experimental Procedures

Materials and Cell Culture

General laboratory reagents were purchased from Sigma or Merck. Microcystin-LR was the generous gift of Dr. Carol MacKintosh (MRC Protein Phosphorylation Unit, University of Dundee). HeLa cells were maintained in DMEM supplemented with 10% FBS (Sigma Ltd.), 2 mM glutamate and 10 U/ml Penicillin/Streptomycin at 37°C, 5% CO_2. Sheep anti-hamster MCAK polyclonal antiserum was produced via standard immunization and bleeding protocols (Pocono Rabbit Farm & Laboratory Inc., Canadensis, PA) using baculovirus-expressed hamster MCAK that was purified as described (Maney et al., 1998) as the antigen. Antiserum was affinity purified on a column conjugated with bacterially expressed human MCAK. Bacterial expression protocol was performed as described (Ovechkina et al., 2002). Affinity purified antibodies were eluted using 100 mM glycine pH 2.5 and neutralized with 1 M Tris-HCl, pH 8.0.

Immunofluorescence Microscopy

For immunofluorescence, cells were trypsinised and plated onto 22 x 22 mm No. 1.5 coverslips, 18 hours prior to fixation. For fixation, coverslips were washed once in 37°C PBS and then immersed in 3.7% formaldehyde in PBS pH 6.8 for 5 min at 37°C with occasional gentle mixing, after which time the fixation solution was aspirated and a second bolus of fixative applied for a further 5 min at 37°C. Cells were then rinsed in PBS-Triton X-100 (0.1%) and then permeabilised in PBS-0.1%Triton X-100 for 10 min at 37°C with occasional gentle swirling. Cells were blocked in AbDil (Cramer and Desai) supplemented with 0.1% normal donkey serum for 1 hour at room temperature. Primary antibodies were diluted in AbDil.

Anti-AIM1 (human Aurora B) monoclonal antibody (BD Biosciences) was used at a 1:200 dilution. Affinity purified sheep anti-human MCAK polyclonal antibody was diluted to 1μg/ml. Rat anti-α-tubulin (Serotec) was used at a 1: 500 dilution. Human CREST autoantisera (ACA; the generous gift of Professor Bill Earnshaw, University of Edinburgh) was diluted 1:10,000. All second antibodies (labelled with either FITC, Texas-Red or Cy5) were purchased from Jackson Laboratories.

3D data sets were either acquired using a MicroMax cooled CCD camera (5MHz: Roper Scientific, USA), on a DeltaVision Restoration Microscope (Applied Precision, LLC, WA, USA), built around a Nikon TE200 Eclipse stand, fitted with a 100X/1.4N.A. PlanApo lens or using a CoolSnap HQ cooled CCD camera on a Spectris Restoration Microscope built around an Olympus IX70 stand fitted with an a 60x/1.4NA lens (Applied Precision, LLC, WA, USA). Optical sections were recorded every 0.2 μm. 3D data sets were deconvolved using the constrained iterative algorithm (Wallace et al., 2001) implemented in SoftWoRx software (Applied Precision LLC, WA, USA). Image data was quantified using SoftWoRx software. Kinetochore tubulin density was quantified in single optical sections using a 9 x 10 pixel box positioned at the plus end of kinetochore fibres, to generate an integrated pixel intensity value for over 20 individual fibres in control and Aurora B RNAi pro/metaphase cells. ACA-ACA distances were measured for clearly distinguishable metaphase centromere pairs using individual optical sections from 3D data sets from a large number of control and Aurora B RNAi cells. Data was expressed as a frequency distribution. Data was prepared for publication using Microsoft Excel, Adobe PhotoShop and Adobe Illustrator.

Aurora B Kinase isolation, in vitro phosphorylation and phosphorylation site identification

Mitotic and interphase chromatin eluates (MCE and ICE respectively) were prepared from chromatin and chromosomes assembled *in vitro* in Xenopus egg extracts (Murnion et al., 2001; Swedlow, 1999) and used as a source of cell cycle-regulated Aurora B kinase activity. Aurora B complex was immunoprecipitated from MCE or ICE using an affinity purified rabbit anti-Xaurora B polyclonal antibody raised against a peptide (CTTPSSATAAQRVLRKEP) in the N-terminus of *Xenopus* Aurora B conjugated to KLH (Field et al., 1998). This antibody recognises a single band on western blots and immunoprecipitates active Aurora B-INCENP complex from MCE and inactive Aurora B-INCENP complex from ICE (Murnion et al., 2001); data not shown). Typically, 200 µl CSF HSS or interphase HSS was used to prepare 75 µl of chromatin eluates. The Aurora B kinase complex was immunoprecipitated from 40 µl MCE or ICE using 15 µg anti-Aurora B antibody coupled to 20 µl Affiprep Protein A beads (BioRad). After incubation for 1 hour at 4°C, the beads were washed with XBE2 (Murnion et al., 2001) and used immediately in kinase reactions. Control immunoprecipitations were performed in parallel using normal rabbit IgG bound to Affiprep Protein A beads. Bacterially expressed and purified Ipl1p-GST and Sli15p-GST were the generous gifts of N. Rachidi, University of Dundee. For *in vitro* phosphorylation studies, 2-4 µl Aurora B kinase beads were incubated with 0.2 µg recombinant hamster MCAK (Maney et al., 2001), in a 20 µl reaction buffer containing 2 µl [γ-^{32}P] ATP (10 mCi/ml: specific activity > 5000 Ci/mmol), 0.2 mM cold ATP, 1 x XBE2, 5mM $MgCl_2$, 1 µM Microcystin-LR, for 1 hour at 22°C, with shaking. Kinase reaction were terminated with Laemmli sample buffer, heated to 70°C for 5 minutes and subjected to SDS-PAGE using NuPAGE 4-12% Bis-Tris gradient gels (Novex), run in MOPS running buffer under reducing conditions. After electrophoresis, gels were stained with Coomassie, destained then

either dried and subjected to autoradiography, or MCAK bands were excised. Phosphorylation site analysis was performed (Lizcano et al., 2002), except that LysC was used for enzymatic digestion. Normalised ^{32}P incorporation was measured by scanning of autoradiographs/protein gels and band intensities quantified and normalised against protein levels using Aida Software (Molecular Dynamics).

2D gel electrophoresis

To detect modification of human MCAK, HeLa cells were synchronised in metaphase with 10 μg/ml nocodazole (Sigma) for 18 hours. Whole cell extracts (Feijoo et al., 2001) were dephosphorylated *in vitro* using λ phosphatase (NEB), for 30 minutes at 30°C. Proteins were precipitated with TCA, rehydrated in sample buffer supplemented with 50 mM DTT and appropriate ampholites. Isoelectric focussing was performed overnight using a BioRad Protean IEF Cell System, employing pH 6-11 Immobiline DryStrip isoelectric focussing strips (Amersham PLC). Proteins were separated in the second dimension on NuPAGE 4-12% Bis-Tris IPG gels (Novex) run in MOPS buffer (Novex). 2D gels were blotted onto Protrans nitrocellulose membrane (Schleicher and Schuell). Human MCAK was detected using affinity purified sheep anti-human MCAK antibody, anti-sheep HRP (Diagnostics Scotland) and ECL reagents following manufacturer's recommendations (Amersham, PLC).

Microtubule depolymerisation assays

Baculovirus expressed 6His-tagged hamster MCAK (Maney et al., 1998) was phosphorylated by incubation at 22°C for 90 min in 20 ml of 8mM K-Hepes pH7.7, 65 mM KCl, 40mM Sucrose, 6 mM MgCl2, 4mM K-EGTA, pH 7.7, 60 mM Imidazole, 1 mM DTT, 0.2 mM ATP, 1 μM Microcystin-LR (Sigma), 0.03% Triton X-100 in the presence of Aurora B complexes precipitated with rabbit α-Aurora B Ab-protein A-agarose beads (or whole rabbit IgG-protein A-agarose beads as a negative control).

Microtubule depolymerisation was then performed as described previously (Maney et al., 2001; Ovechkina et al., 2002). pEGFP-CgMCAK was made by subcloning of BspE1-HindIII Cricetulus griseus MCAK cDNA into pEGFP-C1 vector (Clontech). CgMCAK mutants were made by overlapping PCR mutagenesis using PfuTurbo DNA polymerase (Stratagene) and sequenced. CHO cells were cultured and transfected as described previously (Maney et al., 2001; Ovechkina et al., 2002).

RNAi

A 21 nt siRNA (AAGAGCCUGUCACCCCAUCUG: Dharmacon Research Inc., U.S.A) corresponding to position +149 --> +169 of the human Aurora B (STK12) coding sequence was used for Aurora B RNAi, depleting Aurora B protein levels by more than 75% in less than 24 hours. A Lamin A/C siRNA duplex and a scrambled random siRNA duplex were utilised as controls (Dharmacon Research Inc., U.S.A). For RNAi, HeLa cells were seeded onto 13 mm coverslips and grown overnight in medium without antibiotics. Transfection was performed by mixing 60 pmol siRNA duplex diluted in Opti-MEM (Invitrogen, Inc.) with Oligofectamine reagent (Invitrogen, Inc.). Coverslips were removed at intervals between 5 and 48 hours post-transfection and processed for immunofluorescence. Images for Aurora B RNAi and control RNAi cells were acquired and processed under identical conditions. For analysis of protein levels, the RNAi treatment was scaled up to 6-well plate format using 900 pmol siRNA duplexes.

Acknowledgements

We thank Bill Earnshaw for the ACA antibody, Yu-Li Wang for the kinase-dead Aurora B construct, Najma Rachidi for recombinant Ipl1p/Sli15p and useful discussions, Iain Porter and Guennadi Khodouli for assistance with 2D gel electrophoresis and past and present members of Swedlow lab for help with *Xenopus* extracts, and Tomo Tanaka for critical reading of the manuscript. Supported by grants from the Wellcome Trust and Cancer Research UK (to J. R.S) and Dept. of Defense grant (DAMD17-01-1-0450) (to L.W). J. R. S is a Wellcome Trust Senior Research Fellow.

References

Adams, R. R., Carmena, M., and Earnshaw, W. C. (2001a). Chromosomal passengers and the (aurora) ABCs of mitosis. Trends Cell Biol *11*, 49-54.

Adams, R. R., Maiato, H., Earnshaw, W. C., and Carmena, M. (2001b). Essential roles of drosophila inner centromere protein (incenp) and aurora b in histone h3 phosphorylation, metaphase chromosome alignment, kinetochore disjunction, and chromosome segregation. J Cell Biol *153*, 865-880.

Biggins, S., and Murray, A. W. (2001). The budding yeast protein kinase Ipl1/Aurora allows the absence of tension to activate the spindle checkpoint. Genes Dev *15*, 3118-3129.

Biggins, S., Severin, F. F., Bhalla, N., Sassoon, I., Hyman, A. A., and Murray, A. W. (1999). The conserved protein kinase Ipl1 regulates microtubule binding to kinetochores in budding yeast. Genes Dev *13*, 532-544.

Cheeseman, I. M., Anderson, S., Jwa, M., Green, E. M., Kang, J., Yates, J. R., 3rd, Chan, C. S., Drubin, D. G., and Barnes, G. (2002). Phospho-regulation of kinetochore-microtubule attachments by the Aurora kinase Ipl1p. Cell *111*, 163-172.

Cooke, C. A., Heck, M. M., and Earnshaw, W. C. (1987). The inner centromere protein (INCENP) antigens: movement from inner centromere to midbody during mitosis. J Cell Biol *105*, 2053-2067.

Cramer, L., and Desai, A. Immunofluorescence of the Cytoskeleton. http://mitchison.med.harvard.edu/protocols/gen1.html

Desai, A., Verma, S., Mitchison, T. J., and Walczak, C. E. (1999). Kin I kinesins are microtubule-destabilizing enzymes. Cell *96*, 69-78.

Ditchfield, C., Johnson, V. L., Tighe, A., Ellston, R., Haworth, C., Johnson, T., Mortlock, A., Keen, N., and Taylor, S. S. (2003). Aurora B couples chromosome alignment with anaphase by targeting BubR1, Mad2, and Cenp-E to kinetochores. J Cell Biol *161*, 267-280.

Feijoo, C., Hall-Jackson, C., Wu, R., Jenkins, D., Leitch, J., Gilbert, D. M., and Smythe, C. (2001). Activation of mammalian Chk1 during DNA replication arrest: a role for Chk1 in the intra-S phase checkpoint monitoring replication origin firing. J Cell Biol *154*, 913-923.

Field, C. M., Oegema, K., Zheng, Y., Mitchison, T. J., and Walczak, C. E. (1998). Purification of cytoskeletal proteins using peptide antibodies. Methods Enzymol *298*, 525-541.

Garcia, M. A., Koonrugsa, N., and Toda, T. (2002). Spindle-kinetochore attachment requires the combined action of Kin I-like Klp5/6 and Alp14/Dis1-MAPs in fission yeast. Embo J *21*, 6015-6024.

Giet, R., and Glover, D. M. (2001). Drosophila aurora B kinase is required for histone H3 phosphorylation and condensin recruitment during chromosome condensation and to organize the central spindle during cytokinesis. J Cell Biol *152*, 669-682.

Giodini, A., Kallio, M. J., Wall, N. R., Gorbsky, G. J., Tognin, S., Marchisio, P. C., Symons, M., and Altieri, D. C. (2002). Regulation of microtubule stability and mitotic progression by survivin. Cancer Res *62*, 2462-2467.

Hauf, S., Cole, R. W., LaTerra, S., Zimmer, C., Schnapp, G., Walter, R., Heckel, A., Van Meel, J., Rieder, C. L., and Peters, J. M. (2003). The small molecule Hesperadin

reveals a role for Aurora B in correcting kinetochore-microtubule attachment and in maintaining the spindle assembly checkpoint. J Cell Biol *161*, 281-294.

He, X., Rines, D. R., Espelin, C. W., and Sorger, P. K. (2001). Molecular analysis of kinetochore-microtubule attachment in budding yeast. Cell *106*, 195-206.

Hsu, J.-Y., Sun, Z.-W., Li, X., Reuben, M., Tatchell, K., Bishop, D. K., Grushcow, J. M., Brame, C. J., Caldwell, J. A., Hunt, D. F., *et al.* (2000). Mitotic phosphorylation of histone H3 is governed by Ipl1/aurora kinase and Glc7/PP1 phosphatase in budding yeast and nematodes. Cell *102*, 279-291.

Hunter, A. W., Caplow, M., Coy, D. L., Hancock, W. O., Diez, S., Wordeman, L., and Howard, J. (2003). The kinesin-related protein MCAK is a microtubule depolymerase that forms an ATP-hydrolyzing complex at microtubule ends. Mol Cell *11*, 445-457.

Hunter, A. W., and Wordeman, L. (2000). How motor proteins influence microtubule polymerization dynamics. J Cell Sci *113 Pt 24*, 4379-4389.

Kaitna, S., Mendoza, M., Jantsch-Plunger, V., and Glotzer, M. (2000). Incenp and an aurora-like kinase form a complex essential for chromosome segregation and efficient completion of cytokinesis. Curr Biol *10*, 1172-1181.

Kallio, M. J., McCleland, M. L., Stukenberg, P. T., and Gorbsky, G. J. (2002). Inhibition of aurora B kinase blocks chromosome segregation, overrides the spindle checkpoint, and perturbs microtubule dynamics in mitosis. Curr Biol *12*, 900-905.

Kline-Smith, S. L., and Walczak, C. E. (2002). The microtubule-destabilizing kinesin XKCM1 regulates microtubule dynamic instability in cells. Mol Biol Cell *13*, 2718-2731.

Lizcano, J. M., Deak, M., Morrice, N., Kieloch, A., Hastie, C. J., Dong, L., Schutkowski, M., Reimer, U., and Alessi, D. R. (2002). Molecular basis for the substrate specificity of NIMA-related kinase-6 (NEK6). Evidence that NEK6 does not phosphorylate the hydrophobic motif of ribosomal S6 protein kinase and serum- and glucocorticoid-induced protein kinase in vivo. J Biol Chem *277*, 27839-27849.

Maney, T., Hunter, A. W., Wagenbach, M., and Wordeman, L. (1998). Mitotic centromere-associated kinesin is important for anaphase chromosome segregation. J Cell Biol *142*, 787-801.

Maney, T., Wagenbach, M., and Wordeman, L. (2001). Molecular dissection of the microtubule depolymerizing activity of mitotic centromere-associated kinesin. J Biol Chem *276*, 34753-34758.

Murata-Hori, M., and Wang, Y. L. (2002). The kinase activity of aurora B is required for kinetochore-microtubule interactions during mitosis. Curr Biol *12*, 894-899.

Murnion, M. E., Adams, R. A., Callister, D. M., Allis, C. D., Earnshaw, W. C., and Swedlow, J. R. (2001). Chromatin-associated protein phosphatase 1 regulates aurora-B and histone H3 phosphorylation. J Biol Chem *276*, 26656-26665.

Niederstrasser, H., Salehi-Had, H., Gan, E. C., Walczak, C., and Nogales, E. (2002). XKCM1 acts on a single protofilament and requires the C terminus of tubulin. J Mol Biol *316*, 817-828.

Oegema, K., Desai, A., Rybina, S., Kirkham, M., and Hyman, A. A. (2001). Functional analysis of kinetochore assembly in Caenorhabditis elegans. J Cell Biol *153*, 1209-1226.

Ovechkina, Y., Wagenbach, M., and Wordeman, L. (2002). K-loop insertion restores microtubule depolymerizing activity of a "neckless" MCAK mutant. J Cell Biol *159*, 557-562.

Ovechkina, Y., and Wordeman, L. (2003). Unconventional motoring: An overview of the Kin C and Kin I kinesins. Traffic *4*, 1-9.

Rieder, C. L., and Salmon, E. D. (1994). Motile kinetochores and polar ejection forces dictate chromosome position on the vertebrate mitotic spindle. J Cell Biol *124*, 223-233.

Sassoon, I., Severin, F. F., Andrews, P. D., Taba, M. R., Kaplan, K. B., Ashford, A. J., Stark, M. J., Sorger, P. K., and Hyman, A. A. (1999). Regulation of Saccharomyces cerevisiae kinetochores by the type 1 phosphatase Glc7p. Genes Dev *13*, 545-555.

Skibbens, R. V., Skeen, V. P., and Salmon, E. D. (1993). Directional instability of kinetochore motility during chromosome congression and segregation in mitotic newt lung cells: a push-pull mechanism. J Cell Biol *122*, 859-875.

Swedlow, J. R. (1999). Chromosome assembly in vitro using Xenopus egg extracts. In Chromosome Structural Analysis, W. A. Bickmore, ed. (Oxford, Oxford), pp. 167-182.

Tanaka, T. U., Rachidi, N., Janke, C., Pereira, G., Galova, M., Schiebel, E., Stark, M. J. R., and Nasmyth, K. (2002). Evidence that the Ipl1-Sli15 (Aurora kinase-INCENP) complex promotes chromosome bi-orientation during mitosis by altering kinetochore-spindle pole connections. Cell *108*, 317-329.

Trinkle-Mulcahy, L., Andrews, P. D., Wickramasinghe, S., Sleeman, J., Prescott, A., Lam, Y. W., Lyon, C., Swedlow, J. R., and Lamond, A. I. (2003). Time-lapse imaging reveals dynamic relocalization of PP1gamma throughout the mammalian cell cycle. Mol Biol Cell *14*, 107-117.

Walczak, C. E., Gan, E. C., Desai, A., Mitchison, T. J., and Kline-Smith, S. L. (2002). The microtubule-destabilizing kinesin XKCM1 is required for chromosome positioning during spindle assembly. Curr Biol *12*, 1885-1889.

Walczak, C. E., Mitchison, T. J., and Desai, A. (1996). XKCM1 - A Xenopus kinesin-related protein that regulates microtubule dynamics during mitotic spindle assembly. Cell *84*, 37-47.

Wallace, W., Schaefer, L. H., and Swedlow, J. R. (2001). A workingperson's guide to deconvolution in light microscopy. Biotechniques *31*, 1076-1097.

Waters, J. C., Skibbens, R. V., and Salmon, E. D. (1996). Oscillating mitotic newt lung cell kinetochores are, on average, under tension and rarely push. J Cell Sci *109*, 2823-2831.

Wheatley, S. P., Carvalho, A., Vagnarelli, P., and Earnshaw, W. C. (2001). INCENP is required for proper targeting of Survivin to the centromeres and the anaphase spindle during mitosis. Curr Biol *11*, 886-890.

Wittmann, T., Hyman, A., and Desai, A. (2001). The spindle: a dynamic assembly of microtubules and motors. Nat Cell Biol *3*, E28-34.

Wordeman, L., Wagenbach, M., and Maney, T. (1999). Mutations in the ATP-binding domain affect the subcellular distribution of mitotic centromere-associated kinesin (MCAK). Cell Biol Int *23*, 275-286.

Zeitlin, S. G., Shelby, R. D., and Sullivan, K. F. (2001). CENP-A is phosphorylated by Aurora B kinase and plays an unexpected role in completion of cytokinesis. J Cell Biol *155*, 1147-1157.

Figure Legends

Figure 1. Aurora B and MCAK localisation in HeLa cells. **(A)** A single optical section from a 3D deconvolved dataset showing a prometaphase HeLa cells stained for human MCAK, human Aurora B, tubulin and DNA. At this phase of the cell cycle Aurora B and MCAK show complete co-localisation as shown by line profile analysis (right panel); **(B)** Prophase and prometaphase differences in MCAK and Aurora B localisation. Cells were stained for ACA (blue), for MCAK (red), Aurora B (green). Left hand panels show two prophase sister centromeres tightly paired . Right hand panel shows example of prometaphase sister centromeres slightly separate with overlapping MCAK and Aurora B staining. **(C)** A single optical section from a 3D deconvolved dataset showing a metaphase bioriented chromosomes under tension. MCAK and Aurora B are largely non-overlapping, with MCAK close to ACA staining at the centromere/kinetochore and Aurora B remaining predominantly in the inner-centromere domain. Line profiles (lower panel) show the spatial separation along the presumed spindle axis. **(D)** A single optical section from a 3D deconvolved dataset showing metaphase bioriented chromosomes under tension. MCAK and Aurora B staining are largely non-overlapping, with MCAK close to microtubule ends in the vicinity of the kinetochore and Aurora B remaining predominantly in the inner-centromere domain. Line profiles (lower panel) show the spatial separation along the spindle axis.

Figure 2. Phosphorylation of MCAK by Aurora B *in vitro*. **(A)** Autoradiograph of SDS-PAGE gel of recombinant full-length hamster MCAK phosphorylated in the presence of ^{32}P-ATP using active Aurora B immunoprecipitated from *Xenopus*

mitotic chromosomal eluate (MCE), inactive Aurora B from *Xenopus* interphase chromosomal eluate (ICE), control immunoprecipitations from MCE and ICE or crude MCE or ICE alone. As a further control, full-length MCAK alone was incubated in kinase buffer in the presence of ^{32}P-ATP. **(B)** Schematic diagram of MCAK deletion mutants and site-directed mutants used in *in vitro* phosphorylation studies, with their microtubule depolymerising activities as measured previously (Maney et al., 2001; Ovechkina et al., 2002), included for comparison. **(C)** Autoradiograph (left hand panel) of SDS gel (right hand) of various recombinant MCAK mutants (as detailed in (B)), phosphorylated *in vitro* by mitotic Aurora B complex. **(D)** Histogram of ^{32}P incorporation into different MCAK mutants normalised to protein levels.

Figure 3. Phosphorylation site analysis of MCAK. Recombinant hamster MCAK was phosphorylated with mitotic Aurora B and digested with LysC endoproteinase. **(A)** Peptides were separated by reverse-phase HPLC and the three radioactive peptides peaks isolated. **(B)** Radiolabelled phosphopeptides were identified by MALDI-TOF and the position of the phosphorylated residue(s) determined by solid-phase Edman sequencing, monitoring release of radioactivity at each cycle. Peptide #1 was found to comprise of amino acids 90 to 96 plus one phosphate moiety (with a predicted molecular mass of 928.4573 Da versus a determined molecular mass of 926.4565 Da). Edman degradation of this peptide revealed phosphorylation at Ser 92 of hamster MCAK. Analysis of peptide #2, showed it corresponded to residues 186 to 190 plus one phosphate group (with a predicted molecular mass of 734.3312 versus a determined molecular mass of 734.33 Da), Edman degradation revealing phosphorylation at position 1, corresponding to Ser 186 in hamster MCAK. The late eluting peptide # 3 correspond to a peptide corresponded to amino acids 101 to 138

plus one phosphate group (with a predicted average molecular mass of 4283.75 versus a determined molecular mass of 4284.59 Da). Cycle-burst analysis coupled with the mass determination, showed that a mixture of peptides were present with *either* the 4th, 6th or 10th serines being radiolabelled, corresponding to phosphorylation of either Ser 106, Ser 108 or Ser 112 in hamster MCAK. **(B)** Comparision of Aurora B phosphorylation sites in other known Aurora B substrates in various organisms shows that the MCAK sites fit well with the known consensus for Aurora B (Cheeseman et al., 2002). **(D)** Alignment of Aurora B phosphorylation sites in Kin I kinesins. Aurora B phosphorylates MCAK at three sites within the N-terminus of the protein, Serine 92, Serine 106/108/112 and Serine 186. Alignment of MCAK, its orthologues and other Kin I family members reveals a high degree of conservation of the phosphorylated residues, and a large proportion of the flanking residues. Note that the alignment of Xenopus XKCM1 with its mammalian orthologues in the region of Site 2 differs from that previously published (Walczak et al., 2002).

Figure 4. MCAK phosphorylation depends on Aurora B *in vivo*. **(A)** Western blot showing human MCAK species separated by 2D gel electrophoresis (focussed using pI 6-pI 11 ampholites), of total cell extracts prepared from nocodazole arrested HeLa cells. Lower panel shows mobility of MCAK species after dephosphorylation with λ-phosphatase. Upper panel shows mock treated sample. **(B)** Western blot of total cell extracts prepared from control RNAi cells and Aurora B RNAi cells separated by 2D gel electrophoresis and probed with either an anti-human MCAK antibody (top two panels) or an anti-Aurora B antibody (lower two panels). Aurora B depletion leads to a shift of MCAK mobility from an acidic pI to a more basic pI.

Figure 5. Aurora B mediated phosphorylation dramatically inhibits the microtubule depolymerisation activity of MCAK. MCAK was phosphorylated either by Aurora B complexes precipitated with rabbit α-Aurora B Ab-protein A-agarose beads or whole rabbit IgG-protein A-agarose beads as a negative control **(A)** or recombinant Ipl1p-Sli15p complex **(B)**. Taxol-stabilized microtubules (1500 nM) were added to the phosphorylation reactions containing 24 nM MCAK dimers, incubated for 10 min at RT with in the presence of 1mM ATP, and then analyzed by sedimentation assay. The numbers are percentages of tubulin released into the supernatant of the motor-containing reactions. The average of 3 experiments ± standard deviation is shown for each supernatant fraction. In each case, the upper band on the gel is MCAK and the lower band is tubulin.

Figure 6. Expression of dominant-negative Aurora B (KR) mutant delocalises centromeric MCAK. Inhibition of Aurora B activity by expression of a kinase-dead Aurora B (KR) mutant results in loss of MCAK from centromeres, which is not dependent on MCAK motor activity. CHO cells in the left panels were transfected with CFP-Aurora B and cells on the right were transfected with CFP-Aurora B (KR). Microtubules are shown in red, YFP-MCAK or YFP-motorless (ML)-MCAK are shown in green and DNA is shown in blue.. In all panels, the CFP-Aurora B channel has been omitted for clarity. Images are maximum intensity projections of deconvolved 3D data sets.

Figure 7. Aurora B RNAi causes MCAK delocalisation from the inner centromere and mitotic spindle defects. (A) Cells at 18 hours post-transfection were fixed in PBS-formaldehyde and stained for Aurora B, MCAK, DNA and tubulin. Top panels show a control RNAi-treated mitotic cell and bottom panels show Aurora B RNAi-

treated cells. Images are single optical sections of 3D deconvolved data sets acquired under identical conditions and scaled identically. **(B)** Spindle structure is aberrant in Aurora B RNAi cells. Aurora B depleted cells were stained for Aurora B (not shown), tubulin (red) and DNA (blue). Maximum-intensity volume projections were generated from 3D deconvolved data sets. Images show typical spindles for control cells (left panel) or Aurora B RNAi cells (right panel) viewed from two different angles, the lower image is rotated about the X-axis by 90°. **(C)** Aurora B RNAi increases density of microtubules at kinetochores. Graph shows average total fluorescence of kinetochore fibre thickness. Quantitation of total background-corrected fluorescence in a 9 x 10 pixel box located in the kinetochore zone, in single Z-sections was performed for approximately 30 spindle fibres from control or Aurora B RNAi cells. Errors bars indicate SD. The same volume was used in all measurements, so a change in fluorescence indicates a change in microtubule density. **(D)** Mitotic spindles are significantly shorter in Aurora B RNAi cells. Pole-to-pole distance was measured for from control and Aurora B RNAi cells (N=10 each) and averaged. Error bars indicate SD. **(E)** Aurora B RNAi causes reduced centromere tension. Control and Aurora B RNAi cells were fixed and centromeres stained using the ACA antibody and centromere-centromere distances measured using the analysis tools in SoftWoRx. Results shown were from 20 different cells resulting in over 300 centromere pair distances being measured, plotted as a frequency distribution. The mean ± σ for these measurements are control RNAi, 1.34 ± 0.60 μm (n=496) and Aurora B RNAi 0.89 ± 0.45 μm (n=270). Note that this latter value is significantly higher than that obtained in HeLa cells treated with taxol (Trinkle-Mulcahy et al., 2003), suggesting that tension is reduced, not eliminated. **(F)** Spindle morphology is aberrant in Aurora B RNAi cells. Left panel shows a typical metaphase cell from a control RNAi experiment stained for tubulin, showing normal

astral and spindle microtubules. Right panel shows a typical "prometaphase" cell after Aurora B RNAi stained for tubulin, showing highly elongated microtubules.

Figure 8. Model for the regulation of MCAK by Aurora B in mitosis. We propose a model for the role of Aurora B in regulating of MCAK activity during biorientation and throughout the process of chromosome congression. We have adapted this model from a previous suggestion (Tanaka et al., 2002). First, MCAK is targeted to the centromere by Aurora B phosphorylation. MCAK activity is inhibited by Aurora B phosphorylation, thereby increasing the probability that microtubule capture will result in stable kinetochore-microtubule interactions. After bipolar attachment initiates, the bioriented sister centromeres are under tension and the distance between them increases. MCAK is now separated from Aurora B and closer to PP1. Kinetochore-associated PP1 is known to turn over (Trinkle-Mulcahy et al., 2003), so the kinetochore may provide a locally high concentration of PP1 activity that dephosphorylates MCAK. MCAK activity then increases, causes an increase in tension across the sister centromeres.

Table 1. *In vivo* analysis of MCAK point mutants

Mutant	Depolymerisation activity *in vivo*
FL MCAK (wild type)	+ + + +
S92E	+ + + +
S92A	+ + + +
S186E	+ + + +
S186A	+ + + +
S106E/S108E/S112E	+ + + +
S106A/S108A/S112A	+ + + +
S92E; S186E	+ +
S92A; S186A	+ + ++
GFP	-

CHO cells transfected with MCAK or MCAK mutants were scored for microtubule polymer loss (Ovechkina et al., 2002). Complete loss of MTs was scored as + + + +, 40%-50% reduction of MT polymer was scored as + +, while levels of MT polymer indistinguishable from cells transfected with EGFP control were scored as -.

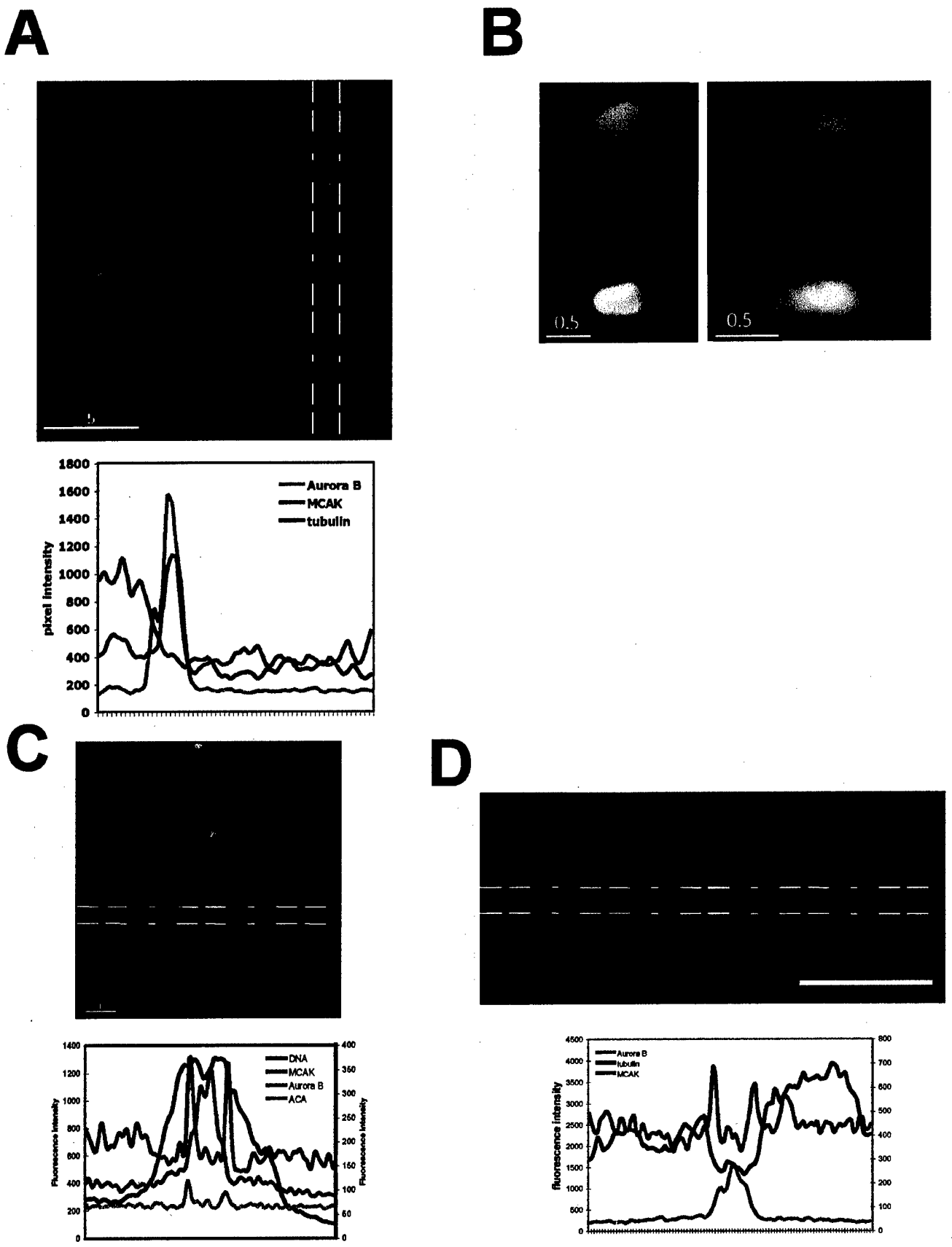

Figure 1 Andrews et al

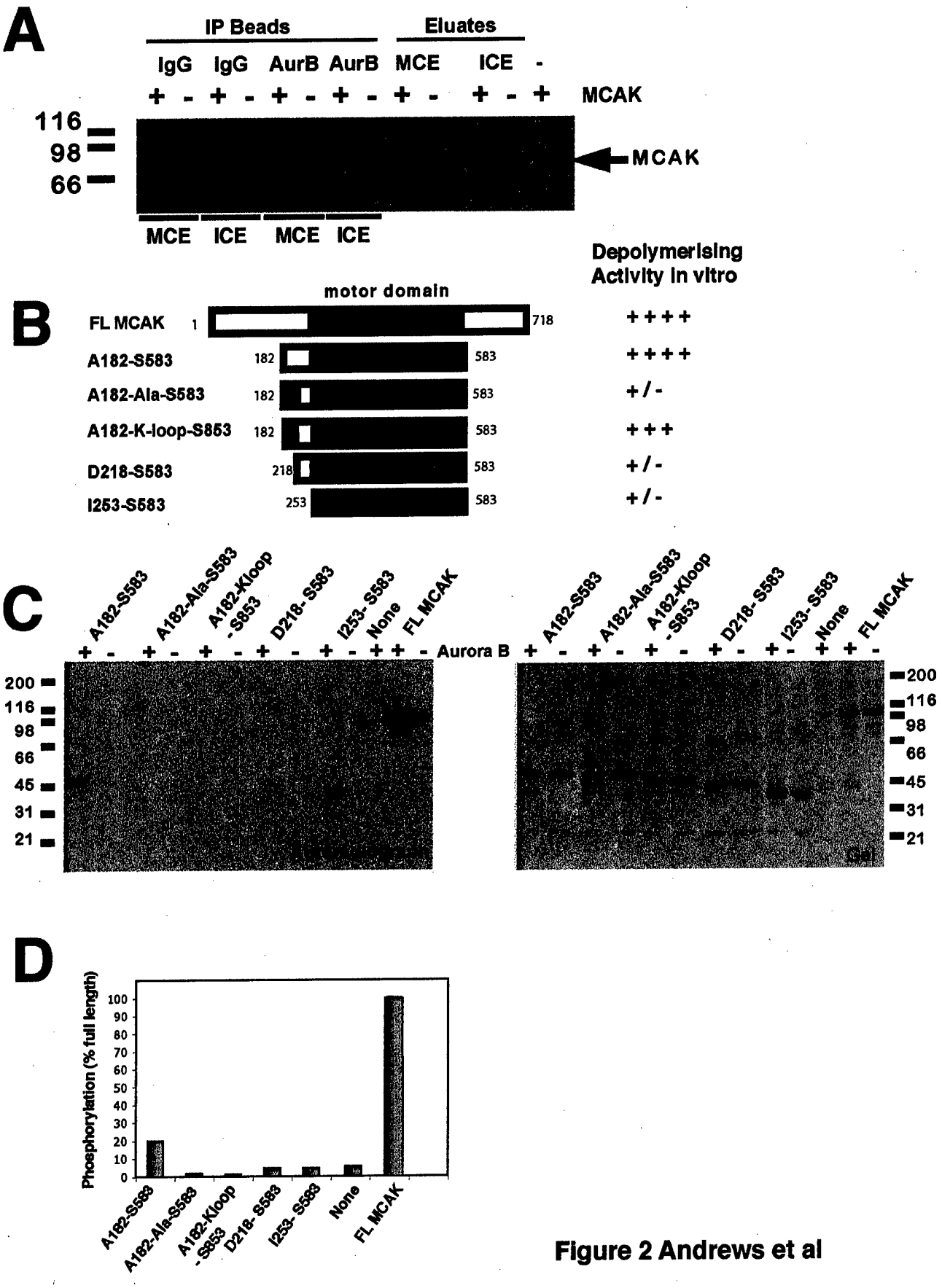

Figure 2 Andrews et al

A

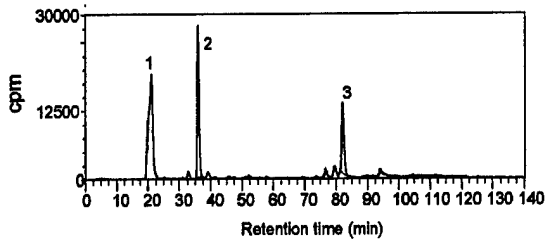

B

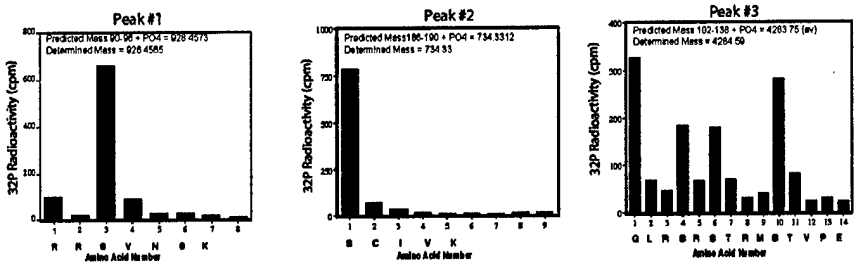

C

Hamster MCAK	87	KQKRRSVNSKI
	101	KEGLRSRSTRM
	181	PARRKSCIVKE
Histone H3	5	QTARKSTGGKA
	23	KAARKSAPATG
Human CENP-A	2	GPRRRSRKPEA
S. c. Dam1p	20	TEYRLSIGSAP
	257	KLRRKSILHTI
	267	HTIRNSIASGA
	292	PNNRISLGSGA
Spc34p	199	NQRRKTIFVED
Ndc80p	100	SVSRLSINQLG
Ask1p	200	RKRKISLLLQQ

D

```
                                    Peak 1                                  - Peak3 -
CgMCAK       77 LPLQENVTVPKQKRRSVNSKIPAPKEG--------------LRSRSTRMSTVPEVRIATQENEMEVELPV..
HsMCAK       80 LPLQENVTIQKQKRRSVNSKIPAPKES--------------LRSRSTRMSTVSELRITAQENDMEVELPA..
RnKRP2       26 --TATAGERNHPKAKTQVRQLQNSRS------------KRRPSKRSTRISTVSEVRIPAQENEMEVELPVS..
X1KCM1       79 MPPQRNVSSQNHKRKTI-SKIPAPKEVAAKNSLLSESGAQSVLRERSTRMTAIHETLPYENEMEAE-STPL..
HsKIF2       52 PASSAKVNKIVKNRRTVASIKNDPPSRDN-----------RVVGSARARPSQFPEQSSSAQQNGSVSDISPV..
MmKIF2       51 -SSSSKVNKIVKNRRTVAAVKNDPPPRDN-----------RVVGSARARPSQLPEQSSSAQQNGSVSDISPV..
MmKIF2b      51 PSSSSKVNKIVKNRRTVAARAVKNDPPPR-----------DNRVVGSARPSQLPEQSSSAQQN---------..
XKIF2        76 PAPTTKVNKIVKNRRTVAPVKNETPAKDN---------RVAAVGSARARPIQPIEQSASRQQNGSVSDISPD..

                                                                        Peak 2
CgMCAK      156 ELPLSMVSEEAEEQVHPTRSTSSAN--------PARRKSCIVKEMEKMKNKREEKRAQ
HsMCAK      159 EIPLRMVSEEMEEQVHSIRGSSSANPV-----NSVRRKSCLVKEVEKMKNKREEKKAQ
RnKRP2      105 ELPLLMISEEAEEQAHSTRSTSSANPG-----NSVRRKSCIVKEMEKMKNKREEKRAQ
X1KCM1      158 RSRSTKVSIAEEPRLQTRISEIVEESLPSGRNNQGRRKSNIVKEMEKMKNKREEQRAQ
HsKIF2      125 --------------------------------PSRRKSNCVKEVEKLQEKREKRRLQ
MmKIF2      124 --------------------------------PSRRKSNCVKEVEKLQEKREKRRLQ
MmKIF2b     106 --------------------------------ARRKSNCVKEVEKLQEKREKRRLQ
XKIF2       151 --------------------------------ASRRKSNCVKEVEKLQEKRERRRLQ
DmK1p10A    180 AAASAGPAAQGVATAATTQGAGG----------ASTRRSHALKEVERLKENREKRRAR
CfDSK        24 ------------------------------MNAANRRKSTSTVGITGRKDATRMKIEQ
```

Figure 3 Andrews et al

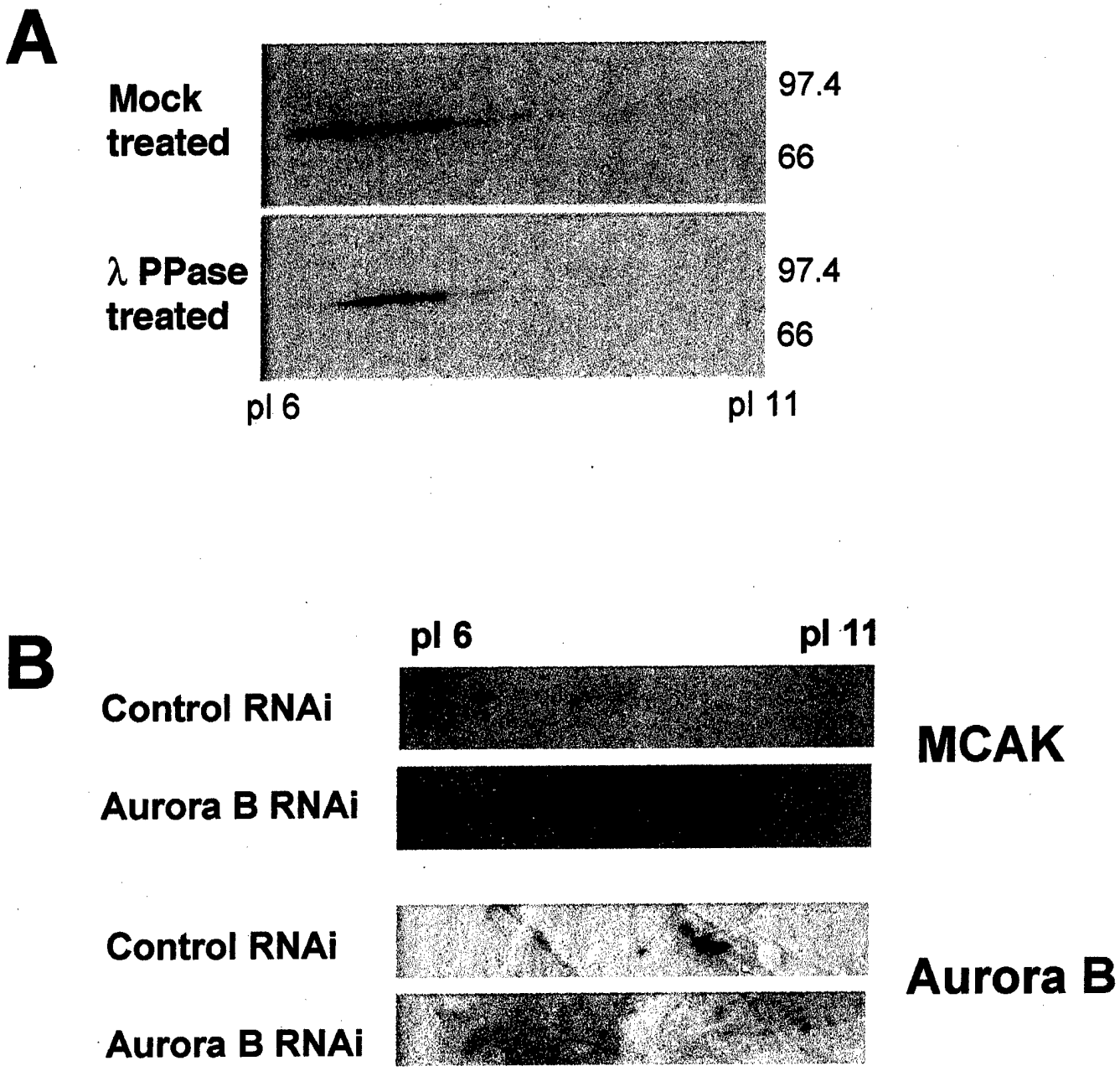

Figure 4 Andrews et al

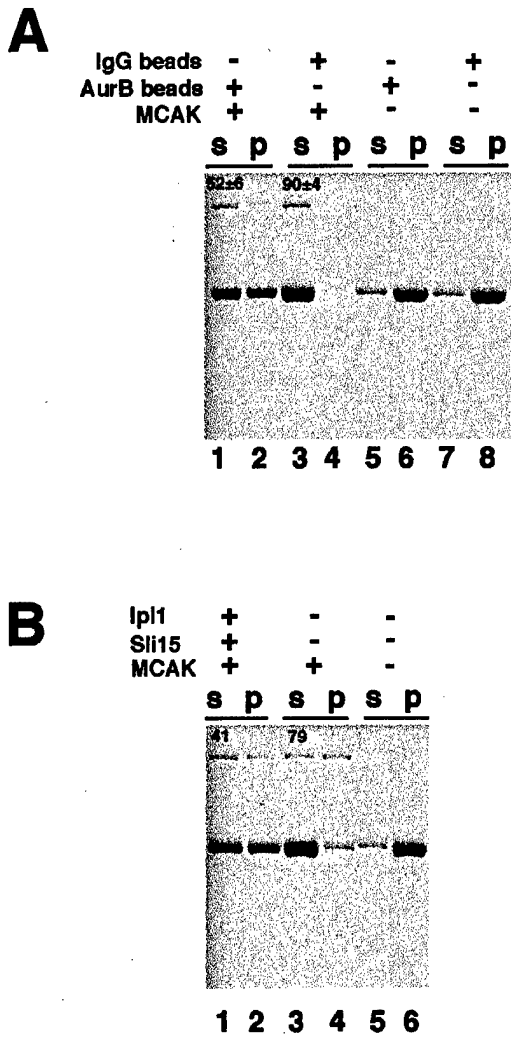

Figure 5 Andrews et al

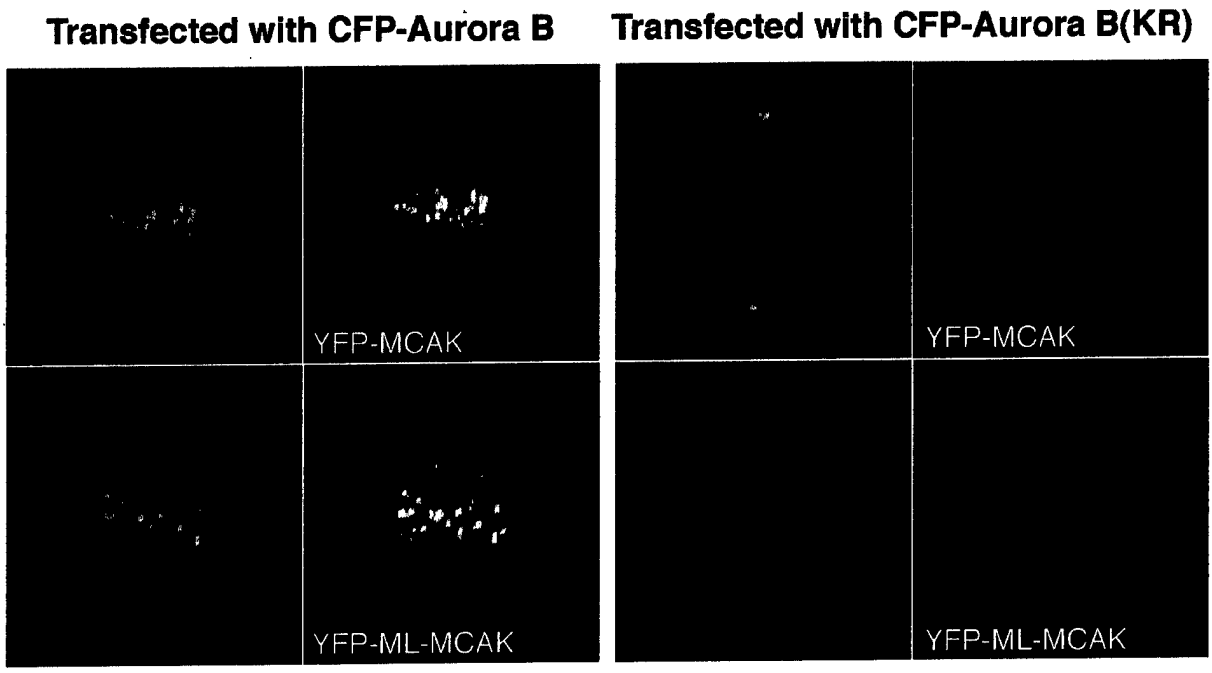

Figure 6. Andrews et al

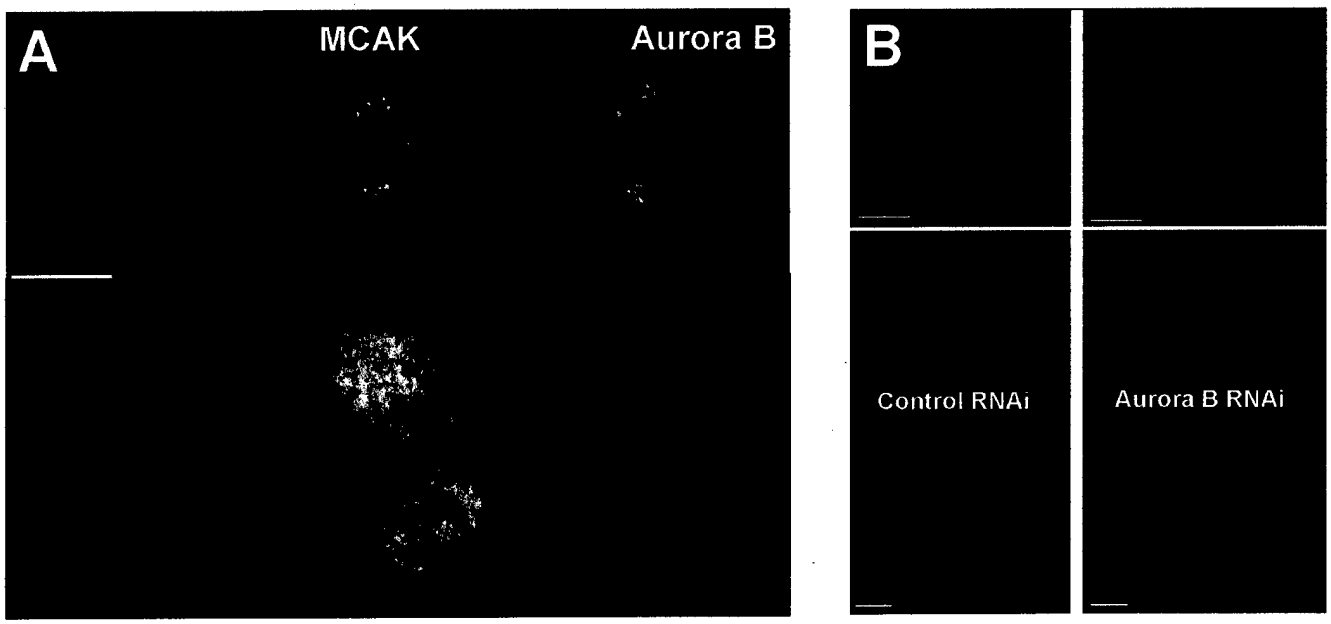

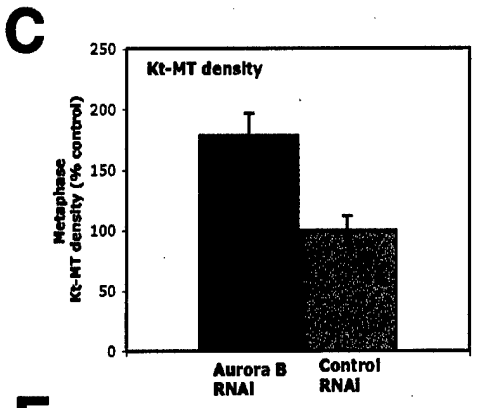

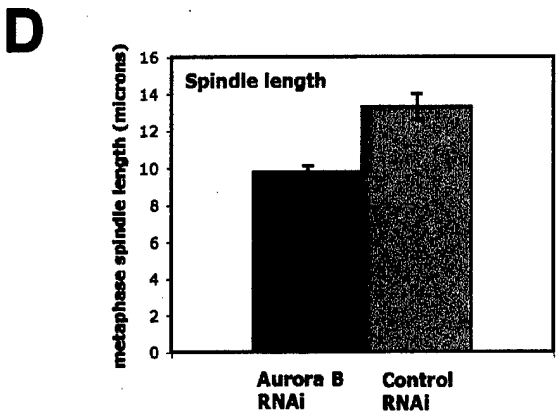

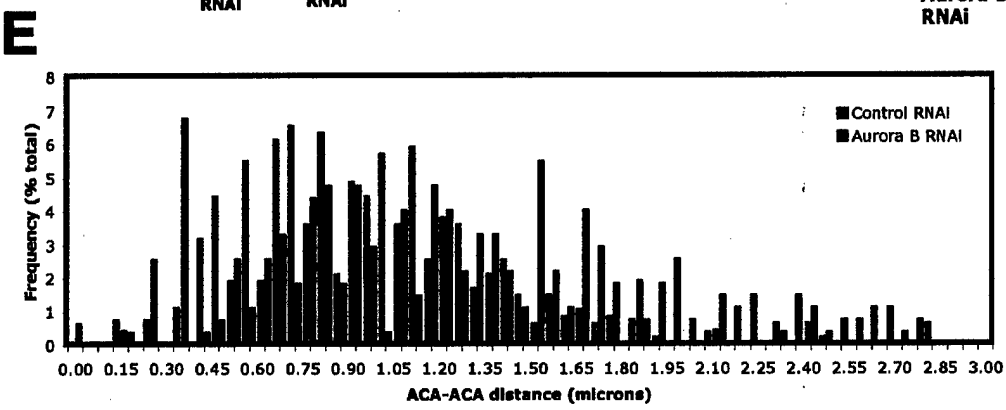

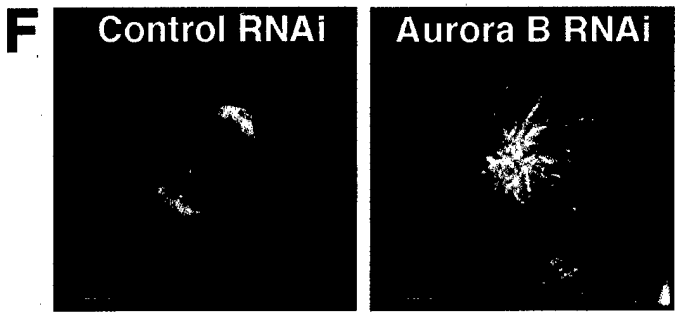

Figure-7 Andrews et al

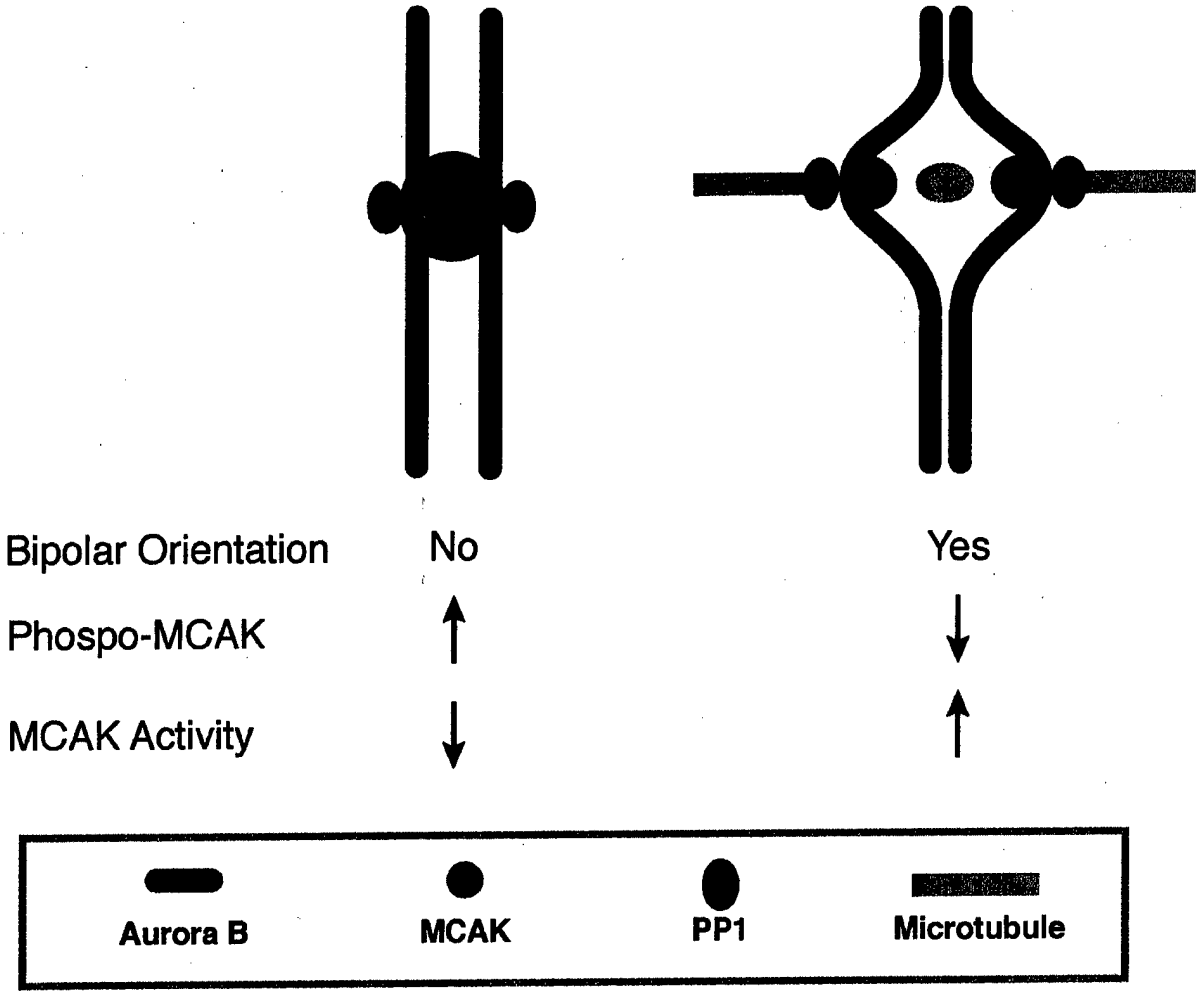

Figure 8. Andrews et al